



Small Aircrew Ejection Simulation in U. S. Navy Aircraft

Prepared by:

Jeffrey P. Nichols, John J. Quartuccio, & Thomas J. Marquette
NAWC-AD, In-Flight Escape Systems Branch, Code 4.6.2.1

Prepared for:

Naval Air Systems Command

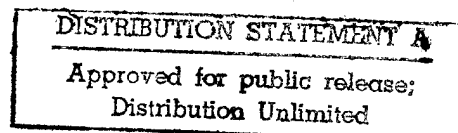
January 1996



DTIC QUALITY INSPECTED 3

Naval Air Warfare Center - Aircraft Division
P.O. Box 5152
Warminster, PA 18974-0591

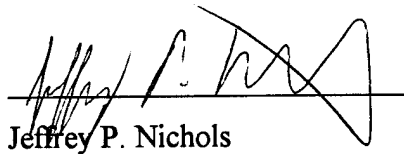
19960729 013




Small Aircrew Ejection Simulation in U. S. Navy Aircraft

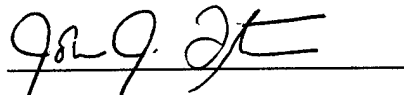
January 1996

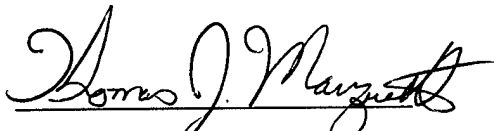
Prepared by:


Jeffrey P. Nichols

Reviewed by:


Peter Ayoub


John J. Quartuccio


Thomas J. Marquette



Naval Air Warfare Center - Aircraft Division
P.O. Box 5152
Warminster, PA 18974-0591

REPORT DOCUMENTATION PAGE

Form Approved
OMB No. 0704-0188

Public reporting burden for this collection of information is estimated to average 1 hour per response, including the time for reviewing instructions, searching existing data sources, gathering and maintaining the data need, and completing and reviewing the collection of information. Send comments regarding this burden estimate or any other aspect of this collection of information, including suggestions for reducing this burden to Washington Headquarters Services, Directorate for Information Operations and Reports, 1215 Jefferson Davis Highway, Suite 1204, Arlington, VA 22202-4302, and to the Office of Management and Budget, Paperwork Reduction Project (0704-0188), Washington, DC 20503.

1. AGENCY USE ONLY (Leave blank)		2. REPORT DATE January 1996	3. REPORT TYPE AND DATES COVERED Final	
4. TITLE AND SUBTITLE Small Aircrew Ejection Simulation in U.S. Navy Aircraft			5. FUNDING NUMBERS N001994WXCSJ8R P.E. 603208N	
6. AUTHOR(S) Jeffrey P. Nichols Thomas J. Marquette John J. Quartuccio				
7. PERFORMING ORGANIZATION NAMES(S) AND ADDRESS(ES) Naval Air Warfare Center, Aircraft Division Code (4.6.2.1) P.O. Box 5152 Warminster, PA 18974-0591			8. PERFORMING ORGANIZATION REPORT NUMBER NAWCADWAR--96-17-TR	
9. SPONSORING/MONITORING AGENCY NAMES(S) AND ADDRESS(ES) Naval Air Systems Command 1421 Jefferson Davis Highway Arlington, VA 22243			10. SPONSORING/MONITORING AGENCY REPORT NUMBER	
11. SUPPLEMENTARY NOTES NAWCADWAR P.O.C.: Jeffrey P. Nichols (Code 4.6.2.1)				
12A. DISTRIBUTION / AVAILABILITY STATEMENT Approved for Public Release. Distribution is unlimited.			12b. DISTRIBUTION CODE	
13. ABSTRACT (Maximum 200 words) With the Navy's recent expansion of the aircrew population to include a greater percentage of aviators, both male and female, the accommodation of small aircrew has become an important issue. All ejection seats currently used by the Navy were designed and test qualified for male aircrew ranging in weight from 135 lbs to 212 lbs. None of the Navy ejection seats have been test qualified for flight by aircrew smaller than a 135 lb male. It is expected that such aircrew will be subjected to higher risk of injury in the event of an ejection. Naval Air Warfare Center, Aircraft Division, Warminster has conducted simulations to predict the risk of injury in small aircrew ejections in each of the seat systems currently in the fleet. Simulations of NACES, SJU-5, SIHS, ESCAPAC IE-1, GRU-7, and LS-1A ejections with aircrew both within and below the seat design weight ranges have been completed. The calculated risks to 100 lb and 116 lb female aircrew in ejections at speeds from 0 to 600 KEAS were examined as were the calculated risks to aircrew at the limits of the design weight range in identical ejections. This paper documents the results of the simulation effort.				
14. SUBJECT TERMS Ejection, Simulation, Injury			15. NUMBER OF PAGES 76	
			16. PRICE CODE	
17. SECURITY CLASSIFICATION OF REPORT UNCLASSIFIED	18. SECURITY CLASSIFICATION OF THIS PAGE UNCLASSIFIED	19. SECURITY CLASSIFICATION OF ABSTRACT UNCLASSIFIED	20. LIMITATION OF ABSTRACT	

Table of Contents

1.0 Introduction.....	1
1.1 Background.....	1
1.2 Scope.....	1
2.0 Modeling Approach.....	2
2.1 Modeling of Aircrew Anthropometry.....	3
2.2 Ejection Simulation Program.....	5
2.2.1. Catapult Loading.....	6
2.2.2. Rocket Motor Loading.....	7
2.2.3. Aerodynamic Loading.....	7
2.2.4. Seat Stability Systems.....	8
2.2.5. Parachute Loading.....	8
2.3 Test Data Analysis.....	10
2.4 Injury Prediction.....	10
3.0 Results.....	12
3.1 Model Validation.....	12
3.2 Effect of Crew Size.....	18
4.0 Discussion.....	30
5.0 Conclusions.....	30
6.0 References.....	32
Appendix A: 6 DOF Simulation Validation	
NACES Validation.....	A1
SJU-5 Validation.....	A11

Table of Contents Continued

SIIS Validation.....	A18
ESCAPAC IE-1 Validation.....	A24
GRU-7 Validation.....	A26
LS-1A Validation.....	A26
Appendix B: Occupant Inertial Properties Analysis	
Approach.....	B1
212 lb Male.....	B5
135 lb Male.....	B6
116 lb Female.....	B7
100 lb Female.....	B8
Body Segment Definitions.....	B9
References.....	B9

List of Figures

Figure 1: Coordinate Systems for the Simulation Program.....	6
Figure 2: SJU-5 GQ 1000 Parachute Opening Load,..... 135 lb Occupant, 450 KEAS Ejection	9
Figure 3: NACES Resultant Acceleration vs. Time,..... 135 lb Occupant, 600 KEAS Ejection	13
Figure 4: NACES Resultant Acceleration vs. Time,..... 212 lb Occupant, 600 KEAS Ejection	13
Figure 5: SJU-5 Resultant Acceleration vs. Time,..... 135 lb Occupant, 600 KEAS Ejection	14
Figure 6: SJU-5 Resultant Acceleration vs. Time,..... 212 lb Occupant, 600 KEAS Ejection	14

List of Figures Continued

Figure 7: SIIS Resultant Acceleration vs. Time,.....	15
135 lb Occupant, 600 KEAS Ejection	
Figure 8: SIIS Resultant Acceleration vs. Time,.....	15
212 lb Occupant, 600 KEAS Ejection	
Figure 9: ESCAPAC IE-1 Altitude vs. Downrange Distance,.....	16
135 lb Occupant, 450 KEAS Ejection	
Figure 10: ESCAPAC IE-1 Altitude vs. Downrange Distance,.....	16
212 lb Occupant, 450 KEAS Ejection	
Figure 11: LS-1A Altitude vs. Downrange Distance,.....	17
140 lb Occupant, 30 KEAS Ejection	
Figure 12: LS-1A Altitude vs. Downrange Distance,.....	18
204 lb Occupant, 30 KEAS Ejection	
Figure 13: NACES Peak MDRC vs. Airspeed at Ejection.....	21
Figure 14: NACES Peak Radical vs. Airspeed at Ejection.....	21
Figure 15: SJU-5 Peak MDRC vs. Airspeed at Ejection.....	22
Figure 16: SJU-5 Peak Radical vs. Airspeed at Ejection.....	22
Figure 17: AV-8B SIIS Peak MDRC vs. Airspeed at Ejection.....	23
Figure 18: AV-8B SIIS Peak Radical vs. Airspeed at Ejection.....	23
Figure 19: TAV-8B SIIS Peak MDRC vs. Airspeed at Ejection.....	24
Figure 20: TAV-8B SIIS Peak Radical vs. Airspeed at Ejection.....	24
Figure 21: ESCAPAC IE-1 Peak MDRC vs. Airspeed at Ejection.....	25
Figure 22: ESCAPAC IE-1 Peak Radical vs. Airspeed at Ejection.....	25
Figure 23: GRU-7 Peak MDRC vs. Airspeed at Ejection.....	26
Figure 24: GRU-7 Peak Radical vs. Airspeed at Ejection.....	26

List of Figures Continued

Figure 25: LS-1A Peak MDRC vs. Airspeed at Ejection.....	27
Figure 26: LS-1A Peak Radical vs. Airspeed at Ejection.....	27
Figure 27: 212 lb Aircrew Normalized Acceleration..... vs. Airspeed at Ejection	29
Figure 28: 135 lb Aircrew Normalized Acceleration..... vs. Airspeed at Ejection	29

List of Tables

Table 1: Simulation Conditions.....	2
Table 2: Seat/Occupant Properties.....	5
Table 3: Values Used for MDRC Calculations.....	11
Table 4: Values Used for Radical Calculations.....	12
Table 5: GRU-7 Propulsion Validation.....	17
Table 6: GRU-7 Drogue Validation.....	17
Table 7: LS-1A Acceleration Validation.....	18

1.0 Introduction

As the Naval aircrew population expands to include a greater percentage of small aviators, both female and male, the issue of injury potential in small aircrew ejections becomes increasingly important. Because of smaller body mass and differing mass distribution, small aviators are expected to be at higher risk of injury in an ejection than larger aircrew. The In-Flight Escape Systems Branch of the Naval Air Warfare Center, Aircraft Division, Warminster (NAWCADWAR) conducted an effort to begin to quantify the risk to small aircrew. This effort included computer modeling of the NACES, SJU-5, SIIS, ESCAPAC IE-1, GRU-7, and LS-1A ejection seats with an expanded weight range. Additional analysis of the parachute opening phase was conducted using test data.

1.1 Background

In the past, Naval ejection seats have been designed and qualified to incorporate 90% to 95% of the aircrew population by weight. The minimum and maximum weights used in the qualification of the seats were based on a 1964 study¹ of Naval aircrew anthropometry. The NACES, SJU-5, SIIS, and ESCAPAC IE-1 seats were qualified using 135 lb (nude weight) and 212 lb (nude weight) occupants. These weights correspond to 3%ile by weight male and 98%ile by weight male aircrew respectfully and span 95% of the aviators in the 1964 study. The GRU-7 and LS-1A seats were qualified using 140 lb (nude weight) and 204 lb (nude weight) occupants. These weights correspond to 5%ile by weight and 95%ile by weight male aircrew respectfully and span 90% of the aviators in the 1964 study. These weight ranges were crucial specifications in the design of each of the seat systems. None of the Navy ejection seats have been qualified for flight by aircrew smaller than a 135 lb male.

1.2 Scope

The scope of this effort included computer modeling of seat system performance and loading imparted to the crew member as well as test data analysis. Modeling was done using a six degree of freedom (6DOF) escape system computer model². Computer simulations were conducted to examine the performance of each seat system for occupants both within and below the design weight ranges. Computer modeling of the seat systems does not predict component malfunctions which may result from the effects of the crew member. In addition to the modeling conducted, test data analysis was performed to evaluate recovery chute opening shock on the aircrew.

2.0 Modeling Approach

A computer model for each of the seat systems was created and validated using empirical data. The NACES, SJU-5, SIIS, and ESCAPAC IE-1 models were validated for 135 lb and 212 lb occupants; the GRU-7 and LS-1A models were validated for 140 lb and 204 lb occupants. Variations in occupant weight were then modeled and simulations were conducted for 100 lb, 116 lb occupants as well as the qualification occupant weights. Table 1 shows the conditions evaluated in this study.

Table 1: Simulation Conditions							
Seat System	Air Speed (KEAS)	Occupant Weight (lbs)					
		100	116	135	140	204	212
NACES	0	✓	✓	✓			✓
	100	✓	✓	✓			✓
	200	✓	✓	✓			✓
	300	✓	✓	✓			✓
	350	✓	✓	✓			✓
	400	✓	✓	✓			✓
	450	✓	✓	✓			✓
	500	✓	✓	✓			✓
	550	✓	✓	✓			✓
SJU-5	600	✓	✓	✓			✓
	0	✓	✓	✓			✓
	100	✓	✓	✓			✓
	200	✓	✓	✓			✓
	300	✓	✓	✓			✓
	350	✓	✓	✓			✓
	400	✓	✓	✓			✓
	450	✓	✓	✓			✓
	500	✓	✓	✓			✓
SIIS	550	✓	✓	✓			✓
	600	✓	✓	✓			✓
	0	✓	✓	✓			✓
	100	✓	✓	✓			✓
	200	✓	✓	✓			✓
	300	✓	✓	✓			✓
	350	✓	✓	✓			✓
	400	✓	✓	✓			✓
	450	✓	✓	✓			✓
ESCAPAC IE-1	500	✓	✓	✓			✓
	550	✓	✓	✓			✓
	600	✓	✓	✓			✓
	0	✓	✓	✓			✓
	100	✓	✓	✓			✓
	200	✓	✓	✓			✓
	300	✓	✓	✓			✓
	350	✓	✓	✓			✓
	400	✓	✓	✓			✓
GRU-7	450	✓	✓	✓			✓
	500	✓	✓	✓			✓
	550	✓	✓	✓			✓
	600	✓	✓	✓			✓
	0	✓	✓		✓	✓	
	100	✓	✓		✓	✓	
	200	✓	✓		✓	✓	
	300	✓	✓		✓	✓	
	350	✓	✓		✓	✓	
LS-1A	400	✓	✓		✓	✓	
	450	✓	✓		✓	✓	
	500	✓	✓		✓	✓	
	0	✓	✓		✓	✓	
	100	✓	✓		✓	✓	
	200	✓	✓		✓	✓	
	300	✓	✓		✓	✓	
	350	✓	✓		✓	✓	
	400	✓	✓		✓	✓	

In all cases the aircraft was near sea level in straight and level flight.

2.1 Modeling of Aircrew Anthropometry

The anthropometry of the aircrew was based on occupant weight and gender. To simulate worst case scenario, the computer modeling for the 100 lb, 116 lb, 135 lb, and 140 lb occupants was done with minimal (summer) gear; the modeling for the 204 lb and 212 lb occupants was done with maximal (winter) gear. The gear and seat masses used in the simulations were based on ejection test measurements.

The seat/occupant centers of gravity (cg) and moments of inertia (MOI) for the 135 lb, 140 lb, 204 lb, and 212 lb occupants were taken from test measurements. To find the seat/occupant cg and MOI for the 100 lb and 116 lb occupants, regression formulas were used³. The 135 lb and 140 lb inertial properties were used in determining the 100 lb and 116 lb properties as follows. The inertial properties for 135 lb and 140 lb occupant body segments were derived from a male data base. The occupants were considered in an approximate seated position, and the occupant cg were determined using the body segment positions, masses, and cg. The body segment moments of inertia were then rotated and translated to the occupant cg using the parallel axis theorem. The rotations of the moments of inertia were calculated using equations (1) and (2).

$$r' = \beta r \quad (1)$$

$$I' = \beta I \beta^T \quad (2)$$

where:

- r is the position vector of each body segment
- r' is the rotated position vector of each body segment
- I is the MOI of each body segment
- I' is the rotated MOI of each body segment
- β is the direction cosine matrix of each body segment
- β^T is the transpose of the direction cosine matrix of each body segment

The translations of the MOI were calculated using the parallel axis theorem as represented in the following equations:

$$\begin{aligned} I_{xx} &= (I_{xx})_{cg} + m(y^2 + z^2) \\ I_{yy} &= (I_{yy})_{cg} + m(x^2 + z^2) \\ I_{zz} &= (I_{zz})_{cg} + m(x^2 + y^2) \end{aligned}$$

$$I_{xy} = (I_{xy})_{cg} - mxy$$

$$I_{xz} = (I_{xz})_{cg} - mxz$$

$$I_{yz} = (I_{yz})_{cg} - mxy$$

The equations can be represented in general as equation (3).

$$I_{ij} = I_{cg_{ij}} - m(r_i r_j - r^2 \delta_{ij}) \quad (\text{no sum}) \quad (3)$$

where:

I_{ij} is the i th row and j th column term of the translated MOI tensor of each body segment

$I_{cg_{ij}}$ is the i th row and j th column term of the MOI tensor of each body segment about the segment cg

m is the mass of each body segment

r is the position vector of the body segment cg relative to the system cg,
 $r^2 = x^2 + y^2 + z^2$

δ_{ij} is the del operator, $\delta_{ij} = 0$ for $i \neq j$, $\delta_{ij} = 1$ for $i = j$

Knowing the properties for the 135 lb and 140 lb occupants alone in an ejection position, the effects of the occupants on the seat/occupant cg and MOI were removed leaving the cg and MOI of the ejection seats alone. The seat alone inertial properties are representative of the seats at full ejection weight combined with flight gear and clothing.

The inertial properties of the 100 lb and 116 lb occupant body segments were then calculated using regression formulas. The cg and MOI for these occupants in an ejection position were calculated as described above for the 135 lb and 140 lb occupants. The effect of the 100 lb and 116 lb occupants' cg and MOI were then added to the seat alone cg and MOI giving the seat/occupant properties for these aircrew weights. These calculations are described in detail in Appendix B. Also included in Appendix B are the values used in the calculations for the NACES seat.

Occupant gender was a factor in the determination of mass distribution. The mass distribution for the 100 lb and 116 lb occupants is representative of that of a female. The mass distribution for the 135 lb, 140 lb, 204 lb, and 212 lb occupants is representative of that of a male.

The moments of inertia and the center of gravity of each body were held constant throughout the simulations of the ejection sequence. Table 2 shows the occupant, gear, and seat masses used in the simulations as well as the moments of inertia, principle direction, and center of gravity of each of the seat/occupants modeled.

Table 2: Seat/Occupant Properties										
Seat System	Occupant Nude Weight (lbs)	Gear Weight (lbs)	Seat* Ejected Weight (lbs)	Total Ejected Weight (lbs)	Seat/ Occupant Ixx (slug-ft ²)	Seat/ Occupant Iyy (slug-ft ²)	Seat/ Occupant Izz (slug-ft ²)	Seat/Occ. Principle Direction (deg)	Seat/ Occ. xcg (ft)	Seat/ Occ. zcg (ft)
NACES	212	42.6	216	470.6	29.82	33.43	7.66	16.3	0.875	1.143
	135	35.1	216	386.1	19.05	21.43	7.06	16.8	0.775	1.434
	116	35.1	216	367.1	19.59	20.65	5.64	18.0	0.768	1.392
	100	35.1	216	351.1	19.05	20.03	5.45	17.5	0.749	1.403
SJU-5	212	48.0	194	454.0	26.04	28.50	8.20	17.3	1.021	1.272
	135	34.0	194	363.0	19.20	20.48	5.99	16.7	0.900	1.413
	116	34.0	194	344.0	18.41	19.58	5.79	18.0	0.897	1.362
	100	34.0	194	328.0	17.90	19.01	5.62	17.7	0.881	1.368
SIIS	212	37.0	169	418.0	22.00	22.00	6.30	9.0	0.882	1.038
	135	19.0	169	323.0	14.00	13.70	6.00	9.0	0.702	1.485
	116	19.0	169	304.0	13.27	12.95	4.88	10.2	0.689	1.435
	100	19.0	169	288.0	12.77	12.35	4.69	9.23	0.681	1.449
ESCAPAC IE-1	212	51.0	149	412.0	24.44	34.65	10.95	17.0	1.034	1.392
	135	31.0	149	315.0	17.20	21.25	6.25	15.0	0.959	1.276
	116	31.0	149	296.0	16.47	20.50	6.14	15.1	0.980	1.229
	100	31.0	149	280.0	15.96	19.94	5.98	14.7	0.980	1.246
GRU-7	204	50.0	220	474.0	15.0	29.00	12.40	24.0	1.071	1.518
	140	20.0	220	380.0	10.3	20.00	8.5	24.0	0.954	1.768
	116	20.0	220	356.0	9.85	18.77	7.59	34.6	0.942	1.711
	100	20.0	220	340.0	9.33	18.13	7.37	33.9	0.919	1.710
LS-1A	204	NA	NA	361.5	16.21	17.62	5.66	NA	0.942	1.075
	140	NA	NA	287.2	13.99	13.69	5.55	NA	0.825	1.033
	116	NA	NA	263.2	12.27	11.88	5.81	NA	0.796	0.928
	100	NA	NA	247.2	11.75	10.82	5.21	NA	0.743	0.894

* Seat weight includes survival kit and parachute pack

2.2 Ejection Simulation Program

The NAWCADWAR 6DOF computer model for ejection seat systems was used in this effort. The model applies forces to the seat and occupant in accordance with each of the major ejection phases. The phases of ejection include: (1) the catapult phase, (2) the rocker motor phase, (3) the aerodynamic loading / drogue deceleration phase, and (4) the recovery phase.

For each of the seat system models, the locations of the occupant and seat components were established in the Seat Coordinate System (SCS). The forces and moments applied over the seat were transformed to the center of gravity of the seat/occupant. Numerical integration was then computed about the center of gravity in the SCS to determine

deflections and rotations incrementally. Figure 1 illustrates the coordinate systems used by the model.

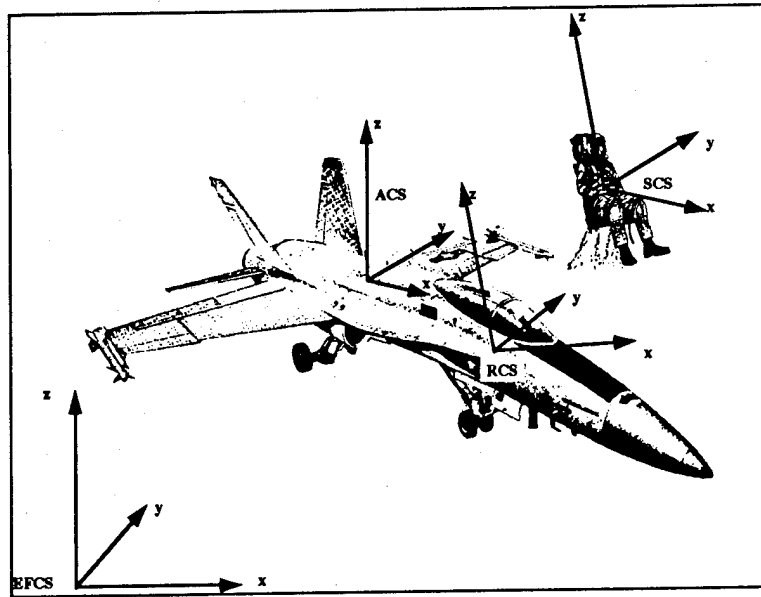


Figure 1: Coordinate Systems for the Simulation Program

2.2.1 Catapult Loading

The catapult loading was applied by the model through the use of thrust vs. time curves. For each of the seats modeled, the point of application and thrust vector of the catapult loads was determined from test measurements. The NACES and SIIS catapult models were based on catapult pressure data taken in zero knot sled tests. The SJU-5 catapult model was based on Z (vertical) acceleration data taken in zero knot sled tests. Because the SJU-5 and GRU-7 utilize functionally identical catapult tubes, the GRU-7 simulations were conducted using the SJU-5 catapult model. The ESCAPAC IE-1 and LS-1A catapult models were based on thrust data taken by the Indian Head Division, Naval Surface Warfare Center (IHD/NSWC) in thrust stand tests of the respective catapults.

Because the mass of the seat/occupant effects the pressure in the catapult tube, the mass of the occupant has an effect on the catapult thrust. At the time of this study there was no empirical catapult thrust data for 100 lb or 116 lb occupants. The only data available was taken using masses representative of the seats' design weight range upper and lower limits. Consequently, it was necessary to use the 140 lb or 135 lb occupant catapult models in the 100 lb and 116 lb simulations. This resulted in slightly higher accelerations during the catapult phase of the 100 lb and 116 lb occupants than are expected in actual ejections.

Catapult testing with light weight occupants was under way at the time of this effort. In the future 100 lb and 116 lb occupant ejection simulations will be conducted utilizing empirically determined thrust curves for the respective weights.

2.2.2 Rocket Motor Loading

The rocket motor loading was applied by the model via thrust vs. time curves knowing the point of application and thrust vector. The thrust data used in the rocket models was found for each of the seat systems using thrust stands such as those available at IHD/NSWC. Rocket thrust is not dependent upon seat/occupant weight. Because of this, for each seat, the same thrust curve is used for all ejected weights.

The NACES, SJU-5, SIIS, and GRU-7 rocket motors are located on the seat bucket. Consequently, the point of application of the rocket forces varies as the seat position is varied. For these seat systems, the rocket motor phase was modeled with the rocket nozzle positioned in the seat bucket full up position and the full down position. Simulations for the 100 lb, 116 lb, 135 lb, and 140 lb occupants were done with the seat modeled in the full up position. Simulations for the 204 lb and 212 lb occupants were done with the seat modeled in the full down position.

The ESCAPAC IE-1 and LS-1A have combined catapult and rocket motors. The entire seat system is moved when the seat position is adjusted and consequently seat position is not a factor in the modeling of the rocket phase.

2.2.3 Aerodynamic Loading

Free stream aerodynamic coefficients for ejection seat platforms were obtained through wind tunnel test facilities. This data varies with airspeed (Mach number) and seat orientation to the wind stream (angle of attack and sideslip angle). A data matrix incorporating these variables was used in the simulations to determine the forces and moments acting on the seat systems at any speed and orientation. The forces and moments, once determined, were transferred to the seat/occupant center of gravity.

At high speeds, the aerodynamics of the aircraft greatly effect the seat coefficients, particularly in pitch (angle of attack). This effect was shown to be a function of the separation distance from the aircraft. The simulation program utilized multiple aerodynamic tables to model this phase of ejection.

2.2.4 Seat Stability Systems

Aerodynamic loading and aircraft proximity effects place a great deal of demand on the seat stability systems. Immediately upon rail separation, aircraft proximity adversely effects the stability of the seat systems. The de-stabilization increases greatly with airspeed at ejection. Seat systems which utilize deployable means of stability can be ineffective at this stage.

The NACES, SJU-5, SIIS, GRU-7, and LS-1A ejection seats utilize deployable drogue chutes to provide aerodynamic stability and reduce seat velocity. The SJU-5, SIIS, GRU-7, and LS-1A seat systems utilize drogues with single attachment points. The SJU-5, GRU-7 and LS-1A drogues are attached at the top of the head box to align the seats for parachute deployment. SIIS drogue attachment point is aligned with the seat center of gravity. Test data shows that the SJU-5 and GRU-7 drogues are deployed from 0.5 seconds to 0.6 seconds after system initiation. The SIIS and LS-1A drogues are deployed at ~0.3 seconds and ~0.08 seconds respectively. In addition to a drogue, the SIIS seat system utilizes a DART for initial pitch control.

Empirical data shows that the NACES drogue is deployed between 0.18 seconds and 0.22 seconds after system initiation. The NACES drogue is attached to the seat via a three point bridle. The drogue forces are applied by the model to the seat system at the confluence point of the bridle. In unstable situations, one or more of the bridle lines can go slack and temporarily decrease the effectiveness of the drogue. To emulate this, the model applies a factor to the drogue fill times when the drogue is deployed in unstable conditions. This decreases the initial effectiveness of the drogue and results in accurate simulation of seat dynamics and loading.

The ESCAPAC IE-1 does not use a drogue; this seat system utilizes a STAPAC rocket motor to provide a margin of pitch control. The ESCAPAC IE-1 also has a deployable aerodynamic fin which induces yaw and causes the seat to diverge.

The timing and physical characteristics of each of the seat stability systems are modeled to reflect test data and measurements.

2.2.5 Parachute Loading

In each of the seat system models the forces applied to the seat/crew member during the drogue phase and forces applied to the crew member during the recovery parachute phase were based on equations (4) and (5).

$$F = (CD*S)*1/2*\rho*V^2 \quad (4)$$

where

$CD*S$ is the drag area defined as

$$CD*S = (CDo*So)*((1-\tau)*(t/to)^j + \tau) \quad (5)$$

where

CDo is the nominal drag coefficient (0.6 for the drogue, 0.75 for the recovery parachutes)

So is the nominal parachute area at the mouth of the canopy.

The coefficient j characterizes the area exposed for a given time of inflation (t/to). This relationship is based on theoretical and experimental work conducted by W. P. Ludtke⁴. For all aeroconical drogue parachutes, $j=1$ (i.e. the area increases linearly with time). For 28 foot flat canopies, such as those of the SIIS, ESCAPAC IE-1, GRU-7, and LS-1A, j is equal to 6. The 17.5 foot diameter SJU-5 parachute (GQ-1000) also has j equal to 6. For the aeroconical NACES GQ-5000 recovery parachute, however, j was found through simulation to be equal to 2; this represents quadratic opening.

The parameter τ is the ratio of the area that is pre-exposed to the air flow at the time of full line stretch to the total area of the parachute. This parameter is not necessarily a characteristic of the parachute and can account for the variations seen in parachute openings.

Figure 2 shows the validation of the parachute opening model used in the simulations.

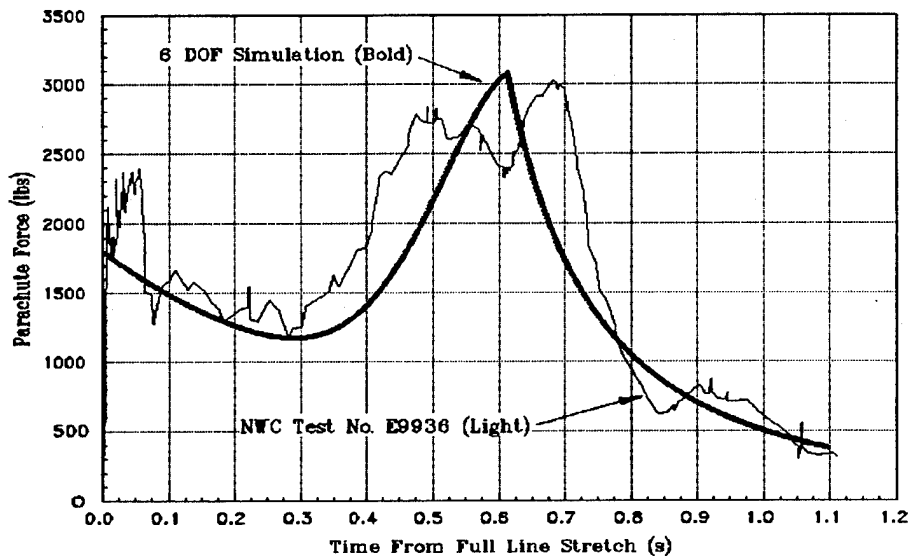


Figure 2: SJU-5 GQ 1000 Parachute Opening Load,
135 lb Occupant, 450 KEAS Ejection

2.3 Test Data Analysis

In addition to the modeling conducted, test data analysis was performed to evaluate seat system performance during the parachute recovery phase. To evaluate seat system performance during the recovery phase, thorax acceleration data recorded in ejection sled tests was analyzed. Analysis of parachute shock loads was conducted for the NACES, SJU-5, and SIHS seats with 135 lb and 212 lb occupants at speeds from 100 to 600 KEAS. Test data for the other seats and aircrew weights was not available. Though this analysis was not as extensive as the simulation analysis, it provide an indication of the type of risk small aircrew may be subjected to during recovery chute deployment.

2.4 Injury Prediction

Two methods of injury prediction were used in calculation risk of injury in the simulations: the Multiaxial Dynamic Response Criteria⁵ (MDRC) and the Radical⁶ calculation. Both methods evaluate risk of injury associated with the ejection sequence at a critical point. The critical point used in this analysis was located 3 inches forward of the seat reference point; this position corresponds roughly to the location of the base of the spine of the aircrew. Because MDRC and Radical calculations are based on an occupant restrained in an ejection seat, the implementation of these calculations is only valid through the time of seat occupant separation. The risk of injury during the recovery phase was not evaluated in the simulation analysis.

Both the MDRC and the Radical were computed as a function of time for each axis (x, y, z). The MDRC was computed as follows:

$$\delta_{tt} + 2\zeta\omega_n\delta_t + \omega_n^2\delta(t) = a_c \quad (6)$$

$$DR(t) = \frac{\omega_n^2\delta(t)}{g} \quad (7)$$

where:

δ_{tt} is the acceleration of the dynamic response model mass relative to the critical point

δ_t is the relative velocity of the model mass

$\delta(t)$ is the relative displacement of the model mass

ζ is the damping coefficient ratio

ω_n is the natural frequency of the model

- a_c is the acceleration at the critical point as determined by the seat simulation model
 g is the acceleration due to gravity

Equation (7) was computed for each of the orthogonal axes (x, y, and z). These values were then used to compute the MDRC as follows:

$$MDRC = \sqrt{\left(\frac{DRx}{DRx_L}\right)^2 + \left(\frac{DRy}{DRy_L}\right)^2 + \left(\frac{DRz}{DRz_L}\right)^2} \leq \quad (8)$$

where:

DRx, DRy, and DRz are the dynamic responses for the x, y, and z axes
 DRx_L, DRy_L, and DRz_L are the DR limit values

Table 3 lists the MDRC parameters used in this analysis

Table 3: Values Used for MDRC Calculations							
Parameter	Risk	x		y		z	
		DRx > 0	DRx < 0	DRy > 0	DRy < 0	DRz > 0	DRz < 0
DR Limit	low	35	28	14	14	15.2	13.4
DR Limit	moderate	40	35	17	17	18	16.5
DR Limit	high	46	46	22	22	22.8	20.4
ω_n (rad/s)		62.8	60.8	58.0	58.0	52.9	47.1
ζ		0.2	0.04	0.09	0.09	0.22	0.24

The method of calculation of the Radical is dependent upon the direction of the loading to the crew member. When the vertical component of the loading is in the positive Z direction (up), the Radical is calculated using equation (9).

$$Radical = \sqrt{\left(\frac{Gx}{Gx_L}\right)^2 + \left(\frac{Gy}{Gy_L}\right)^2 + \left(\frac{DRz}{DRz_L}\right)^2} \leq 1 \quad (9)$$

When the vertical component of the loading is in the negative Z direction (down), equation (10) is used. Gx, Gy, and Gz are the X (for-aft), Y (lateral), and Z (vertical) loads and Gx_L, Gy_L, and Gz_L are the limits in the respective directions.

$$Radical = \sqrt{\left(\frac{Gx}{Gx_L}\right)^2 + \left(\frac{Gy}{Gy_L}\right)^2 + \left(\frac{Gz}{Gz_L}\right)^2} \leq 1 \quad (10)$$

DRz is calculated using equations (6) and (7) as in the MDRC calculations. When the loading on the crew member is within 5 degrees of vertical, the DRz limits shown in Table 3 are used in the Radical calculations. When the loading is not within 5 degrees of vertical the limits shown in Table 4 are used.. The Gx and Gy limits used in the Radical calculation are shown in Table 4.

Table 4: Values Used for Radical Calculations							
Parameter	Risk	x		y		z	
		Gx > 0	Gx < 0	Gy > 0	Gy < 0	DRz > 0	Gz < 0
Limit	moderate	35	30	15	15	16	12

The values listed in Table 3 and Table 4 were derived from experimental methods of male subjects. The values would differ for variations in occupant gender and size. These modified values would be determined through experimental means, but are beyond the scope of this effort.

The risk of injury during recovery phase was examined by performing test data analysis. The chest accelerations measured in ejection sled tests were used to calculate normalized acceleration. Equation 10 was used in this calculation for both positive and negative accelerations. The limits shown in Table 4 were used; the DRz > 0 limit was used as the Gz > 0 limit. The normalized acceleration calculation is intended to generate risk of injury values comparable to the Radical calculation.

The results shown in the following section were based on the moderate risk level. A value of 1.0 indicates moderate risk; a value of 1.2 indicates high risk; a value of 0.8 indicates low risk. The moderate risk level corresponds to 5% major injury rate. The high risk level corresponds to 50% injury rate, and the low risk corresponds to 0.5% injury rate.

3.0 Results

Test data analysis and two series of ejection simulations were conducted. The first simulation series was used to validate each of the seat models. The second series was used to evaluate the effect of aircrew weight on risk of injury in an ejection.

3.1 Model Validation

The model for each of seat systems was validated using test data for occupants at the upper and lower limits of the design weight ranges. Simulated accelerations, seat dynamics, and

dynamics, and trajectories were matched to those of ejection tests. The validation plots and tables are shown in detail in Appendix A.

The NACES model was validated using data from 0 KEAS and 600 KEAS sled track tests. Simulated X, Y, Z, and resultant accelerations and trajectories for 135 lb and 212 lb occupants were compared to those measured in the NACES sled track test series conducted at NWC China Lake. Figures 3 and 4 show resultant acceleration in 600 KEAS ejections for 135 lb and 212 lb occupants. Additional plots are shown in Appendix A.

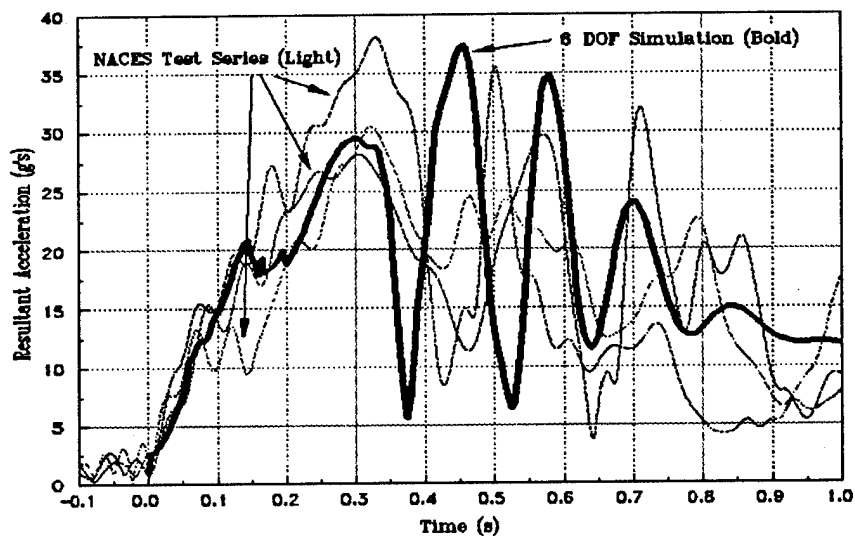


Figure 3: NACES Resultant Acceleration vs. Time, 135 lb Occupant, 600 KEAS Ejection

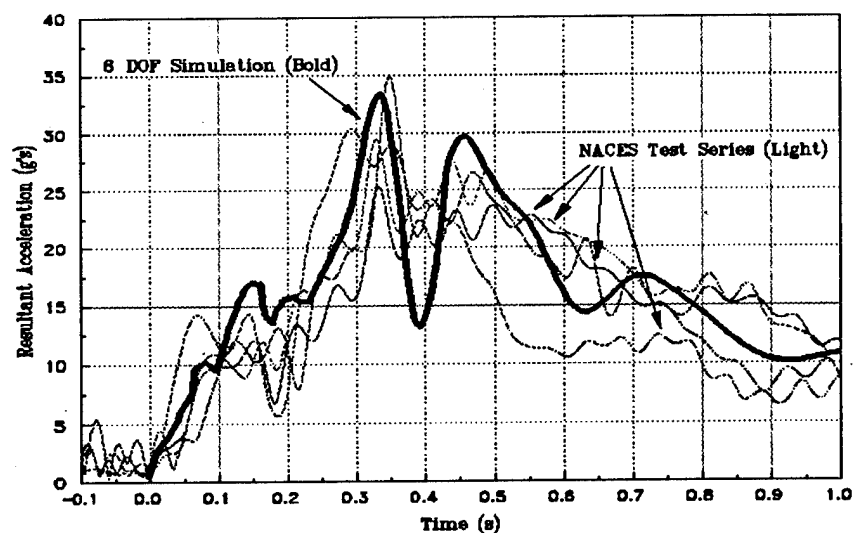


Figure 4: NACES Resultant Acceleration vs. Time, 212 lb Occupant, 600 KEAS Ejection

The SJU-5 model was also validated using data from 0 KEAS and 600 KEAS sled track tests. Simulated X, Y, Z, and resultant accelerations and trajectories for 135 lb and 212 lb

occupants were matched to those measured in the SJU-5 sled track test series conducted at NWC China Lake. Seat Z acceleration measured during the catapult phase of a 0 KEAS test was used to validate the catapult phase of the model. However, the only full sequence accelerations available at the time of analysis were dummy chest accelerations. Dummy acceleration can vary significantly from seat acceleration because of overshoot and other dynamic factors. Dummy accelerations are typically higher than seat accelerations. Because the simulation data represents seat acceleration, there are discrepancies between the test data and the simulation data. Figures 5 and 6 show resultant acceleration in 600 KEAS ejections for 135 lb and 212 lb occupants. Additional plots are shown in Appendix A.

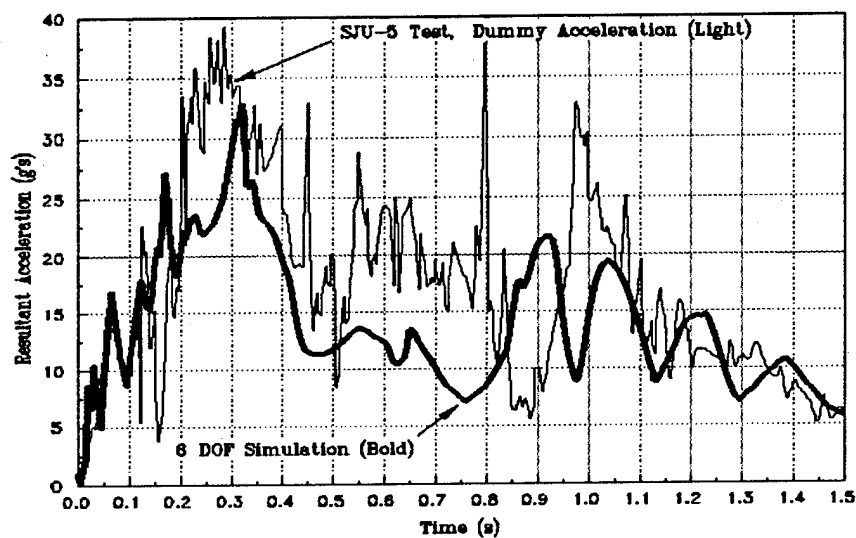


Figure 5: SJU-5 Resultant Acceleration vs. Time, 135 lb Aircrew, 600 KEAS Ejection

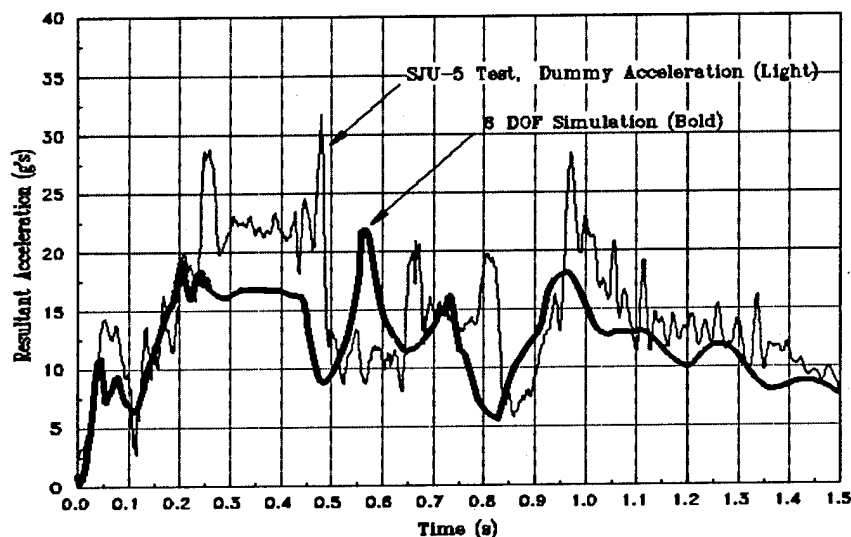


Figure 6: SJU-5 Resultant Acceleration vs. Time, 212 lb Aircrew, 600 KEAS Ejection

The SIIS model was validated using acceleration data from 0 KEAS and 600 KEAS sled track tests. Simulated X, Y, Z, and resultant accelerations for 135 lb and 212 lb occupants were matched to those measured in the SIIS AV-8B sled track test series conducted at NWC China Lake. At the time of analysis there was no seat acceleration data available from 212 lb occupant 600 KEAS tests. Consequently, it was necessary to validate the SIIS large occupant, high speed model with dummy data. All other SIIS validation was done with seat acceleration data. Figures 7 and 8 show resultant acceleration in 600 KEAS ejections for 135 lb and 212 lb occupants. Additional plots are shown in Appendix A.

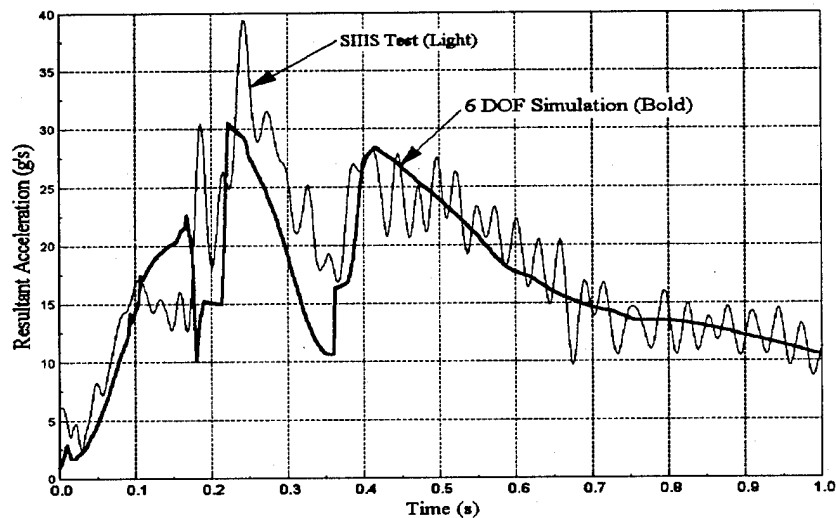


Figure 7: SIIS Resultant Acceleration vs. Time, 135 lb Aircrew, 600 KEAS Ejection

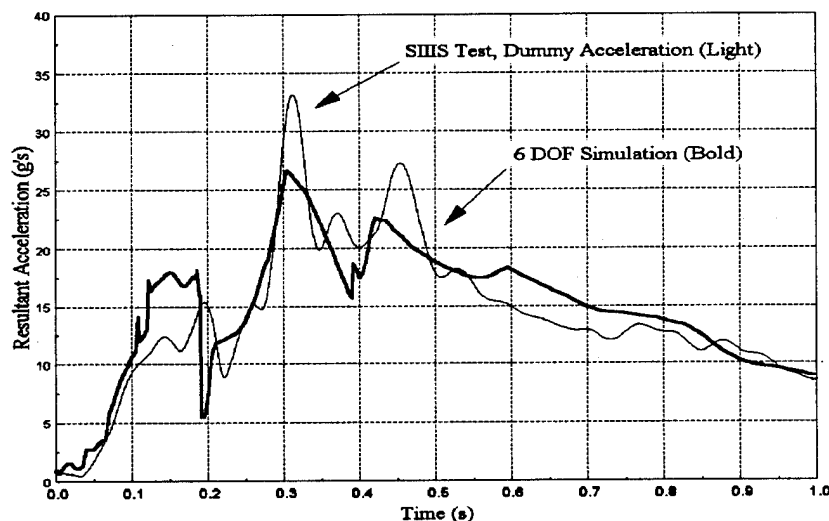
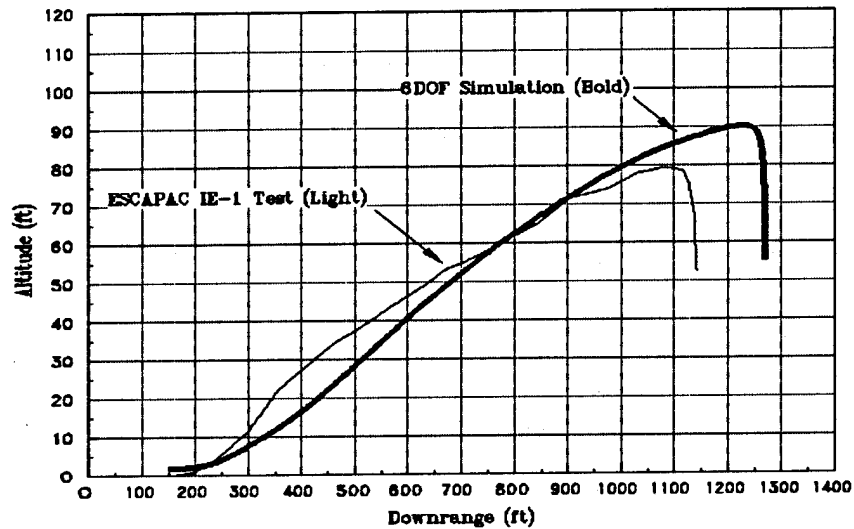


Figure 8: SIIS Resultant Acceleration vs. Time, 212 lb Aircrew, 600 KEAS Ejection

There was no ESCAPAC IE-1 acceleration test data available at the time of this effort. Consequently the ESCAPAC IE-1 model was validated using trajectories only. Simulated

trajectories for 135 lb and 212 lb occupants in 0, 120 and 450 KEAS ejections were matched to those measured in ESCAPAC IE-1 tests. Figures 9 and 10 show trajectories in 450 KEAS ejections for 135 lb and 212 lb occupants. Additional plots are shown in Appendix A.



*Figure 9: ESCAPAC IE-1 Altitude vs. Downrange Distance,
135 lb Occupant, 450 KEAS Ejection*

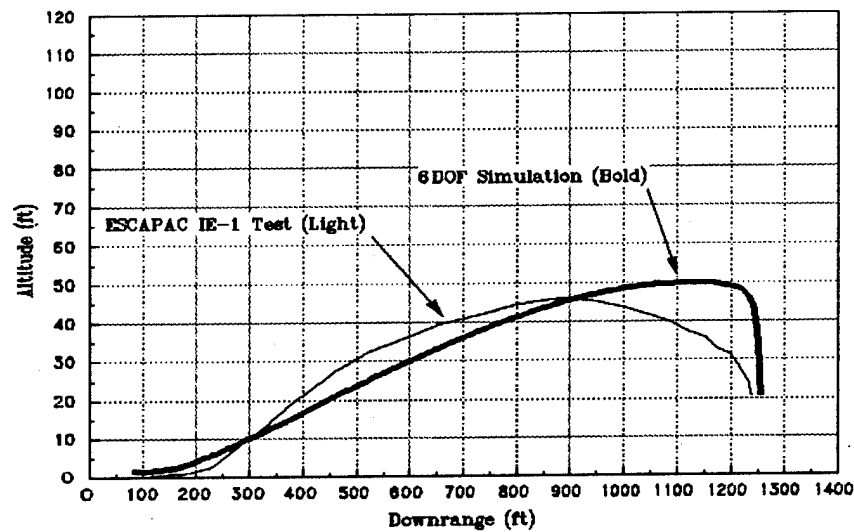


*Figure 10: ESCAPAC IE-1 Altitude vs. Downrange Distance,
212 lb Occupant, 450 KEAS Ejection*

The GRU-7 model was validated by matching simulated peak and average accelerations to those generated in GRU-7 ejection tests. Because the GRU-7 simulations utilized the validated SJU-5 catapult model, validation of the GRU-7 model concentrated on the rocket

and drogue phases. To validate the rocket phase of the model, the average Z acceleration (Gz) during rocket motor firing was examined. Table 5 shows the comparison of the rocket average Gz values for 140 lb and 204 lb occupants.

Table 5: GRU-7 Propulsion Validation				
	140 lb Occupant		204 lb Occupant	
	Test	Simulation	Test	Simulation
Rocket Ave. Gz	8.7	9.7	7.2	7.8

To validate the drogue phase of the model, the maximum decelerations during the drogue phase were examined. Table 6 shows the comparison of the drogue phase peak acceleration values for 140 lb and 204 lb occupants.

Table 6: GRU-7 Drogue Validation				
Airspeed (KEAS)	140 lb Occupant		204 lb Occupant	
	Test Peak gs	Simulation Peak gs	Test Peak gs	Simulation Peak gs
265	10.4	8.1	7.8	7.2
435	16.8	17.3	16.3	14.8
600	>25 *	25.0	24.8	23.4

* Measured acceleration level greater than 25 g accelerometer limit.

The LS-1A model was validated by matching simulated trajectories and accelerations to those measured in LS-1A ejection tests. At the time of this effort no LS-1A test data was available for ejections at speeds above 30 KEAS. Figures 11 and 12 show trajectories of 30 KEAS ejections for 140 lb and 204 lb occupants.

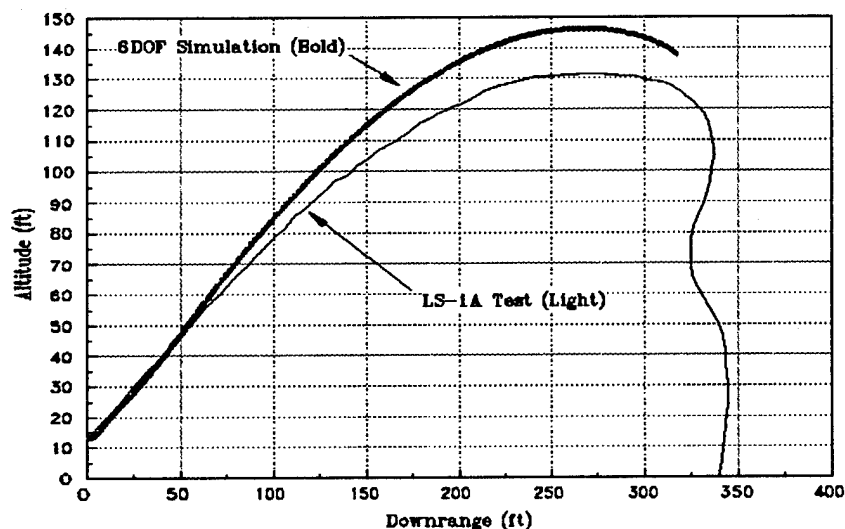


Figure 11: LS-1A Altitude vs. Downrange Distance,
140 lb Occupant, 30 KEAS Ejection

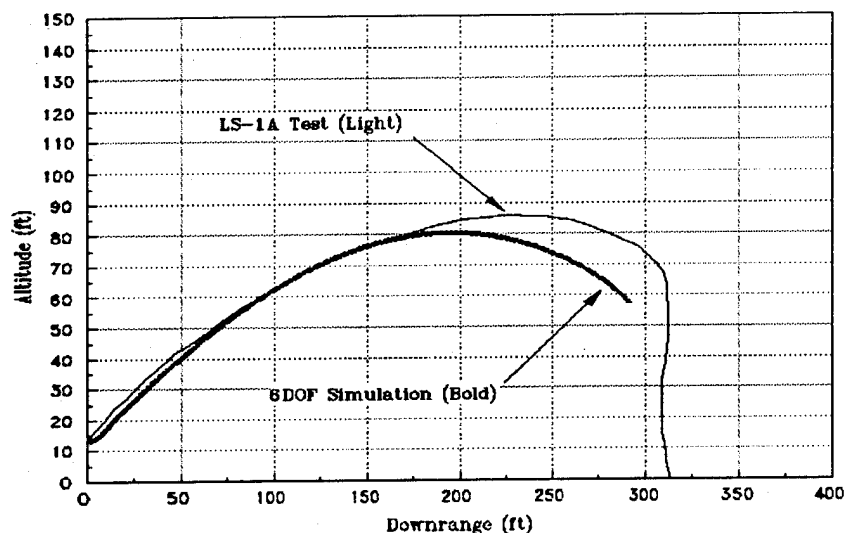


Figure 12: LS-1A Altitude vs. Downrange Distance,
204 lb Occupant, 30 KEAS Ejection

Table 7 shows a comparison of peak gs for 140 lb and 204 lb occupant ejections at speeds of 0 and 30 KEAS

Table 7: LS-1A Acceleration Validation				
	140 lb Occupant		204 lb Occupant	
Speed	Test	Simulation	Test	Simulation
(KEAS)	Peak gs	Peak gs	Peak gs	Peak gs
0	13.0	13.5	11.0	12.1
30	13.5	13.5	12.5	12.1

3.2 Effects of Crew Size

Each of the conditions shown in Table 1 was simulated throughout the full ejection sequence from system initiation to occupant impact. The injury prediction methods described in section 2.4 were used to determine the peak MDRC and Radical values in each of the simulations. Because MDRC and Radical calculations are only valid through the time of seat occupant separation, the risk of injury during the recovery phase is not illustrated in these calculations. MDRC and Radical were calculated for all occupants from catapult initiation to seat/occupant separation.

The peak MDRC and Radical values generated in each of the simulations were examined. For each of the seat systems, the peak values for each occupant at each speed were plotted and compared. Figures 13, 15, 17, 19, 21, 23, and 25 show the peak MDRC values vs. airspeed at ejection for each of the seat systems. Figures 14, 16, 18, 20, 22, 24, and 26 show the peak Radical values vs. airspeed at ejection.

In all of the seat systems evaluated, the highest risks of injury in low speed ejections were calculated to be during the catapult phase. In the NACES, SJU-5, SIIS, GRU-7, and LS-1A seat systems the highest risks of injury in high speed ejections were calculated to be from aerodynamic loading either during the initial wind blast or the drogue deployment. In the ESCAPAC IE-1 high speed simulations the highest risks of injury were calculated to be during initial wind blast for large aircrew and during the catapult phase for small aircrew.

Figures 13 and 14 show the MDRC and Radical values calculated in the NACES simulations. At all speeds the calculated risk was highest for the 100 lb aircrew followed by the 116 lb aircrew, the 135 lb aircrew, and the 212 lb aircrew with the lowest. Though a trend of increasing risk with decreasing weight is clearly evidenced, in some of the high speed simulations the risk of injury to the 116 lb aircrew was only marginally higher than the risk of injury to the 135 lb aircrew. This was a result of the seat/occupant orientations during drogue deployment. In NACES high speed ejections the peak risk of injury occurs during the drogue phase. The orientation of the seat/occupant has a significant effect on the risk to the aircrew. Because the NACES has a fast acting drogue, the seat/occupant is typically aligned with the air stream at drogue deployment and the orientation for all occupants is similar. However, there is some variation in orientation at drogue deployment, and some cases, the less favorable orientation of a larger occupant will result in a risk of injury equal to or higher than that for a smaller aircrew.

Figures 15 and 16 show the peak MDRC and Radical values calculated in the SJU-5 simulations. Figures 23 and 24 show the peak MDRC and Radical values calculated in the GRU-7 simulations. In the SJU-5 and GRU-7 low speed ejection simulations, the trend of increasing risk with decreasing weight was evidenced. However it was difficult to identify a trend in the high speed simulations. This was a result of the slow acting stabilization systems of these seats. Because of the 0.5 to 0.6 second time delay between system initiation and drogue deployment, the SJU-5 and GRU-7 seat systems have a period of unstable flight in high speed ejections. As demonstrated in testing, the seat/occupant orientations and rotation rates during this time period vary greatly from one ejection to the next and may induce significantly different dynamic responses. This was evidenced in the MDRC and Radical plots of the two seat systems. For example, in the SJU-5 550 KEAS simulations, the peak risk was calculated to be highest for the 212 lb occupant. This was a result of the drogue deployment occurring when the seat was yawed 90 degrees (sideways) to the air stream. Drogue deployment in this orientation caused in high lateral loads and high rotation rates which put the occupant at high risk. Though the other occupants had lower weights, they were in more favorable orientations during drogue deployment in these simulations and consequently had lower risk of injury. It has been demonstrated in previous work by NAWCADWAR, that when the seat orientation at drogue deployment is the same for all occupants, the risk of injury increases as weight decreases.⁷

Figures 17, 18, 19, and 20 show the peak MDRC and Radical values calculated in the SIIIS simulations. Two configurations of the SIIIS were modeled: the AV-8B (Stencel SJU-4/A) version which has no divergence, and the TAV-8B (Stencel SJU-13A) version which induces divergence with an additional rocket motor positioned near the seat headbox. As can be seen in these figures, the risk of injury in both the AV-8B and TAV-8B SIIIS did not increase significantly as speed increased. This is a result of the seat/occupant remaining aligned with the air stream. Because of this the majority of the loading was in the X (for-aft) direction, the direction in which human tolerance is greatest. Though it has been evidenced that divergence rocket motors can result in significantly higher risks of injury, the TAV-8B divergence rocket motor was shown to have little effect on the risk of injury. This is because the TAV-8B rocket motor induces divergence by rolling the seat/occupant. Divergence rocket motors which yaw the seat can result in high lateral loading and high risk of injury; rolling the seat has no effect on risk of injury as the loading remains in the for-aft direction. An additional factor which results in low risk of injury at high speeds is the drogue attachment point. Because the drogue acts through the cg, drogue deployment with the seat in adverse orientations will not result in high rotation rates and lateral loading which can be injurious. However, because the drogue acts through the cg, the orientation at recovery parachute deployment may not be optimal and may result in injury. Variations in the SIIIS orientation at drogue deployment in the 600 KEAS simulations did cause some cross over in the risk values of the smaller occupants. With these exceptions, the calculated risk was highest for the 100 lb aircrew followed by the 116 lb aircrew, the 135 lb aircrew, and the 212 lb aircrew with the lowest.

Figures 21 and 22 show the peak MDRC and Radical values calculated in the ESCAPAC IE-1 simulations. At all speeds the calculated risk was highest for the 100 lb aircrew followed by the 116 lb aircrew, the 135 lb aircrew, and the 212 lb aircrew with the lowest. Because the ESCAPAC IE-1 does not utilize a drogue chute, the risk of injury at high speeds was lesser than that seen in the other seat systems. However, because this seat system is not decelerated by a drogue, it is expected that the risk of injury will be high during the recovery parachute deployment.

Figures 25 and 26 show the peak MDRC and Radical values calculated in the LS-1A simulations. Because the LS-1A was only qualified for ejection at 485 KEAS and the T-2 aircraft is not expected to exceed speeds of 525 KEAS, the LS-1A simulations were only conducted at speeds up to 500 KEAS. At all speeds in the LS-1A simulations, the calculated risk was highest for the 100 lb aircrew followed by the 116 lb aircrew, the 140 lb aircrew, and the 204 lb aircrew with the lowest.

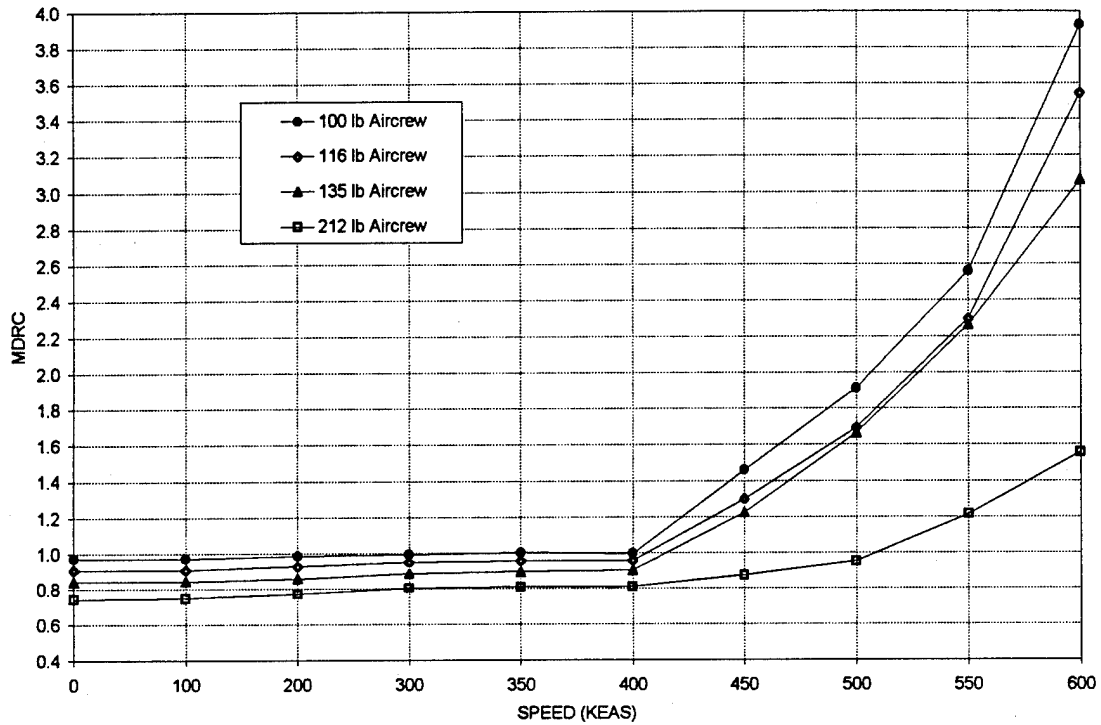


Figure 13: NACES Peak MDRC vs. Airspeed at Ejection

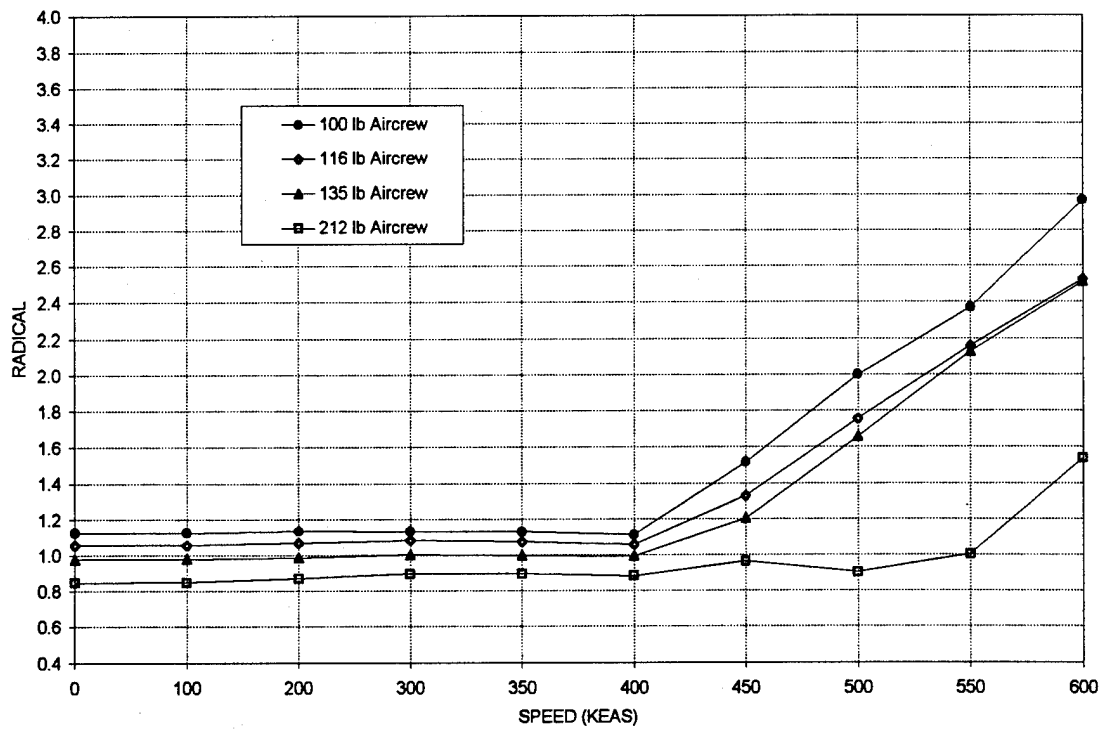


Figure 14: NACES Peak Radical vs. Airspeed at Ejection

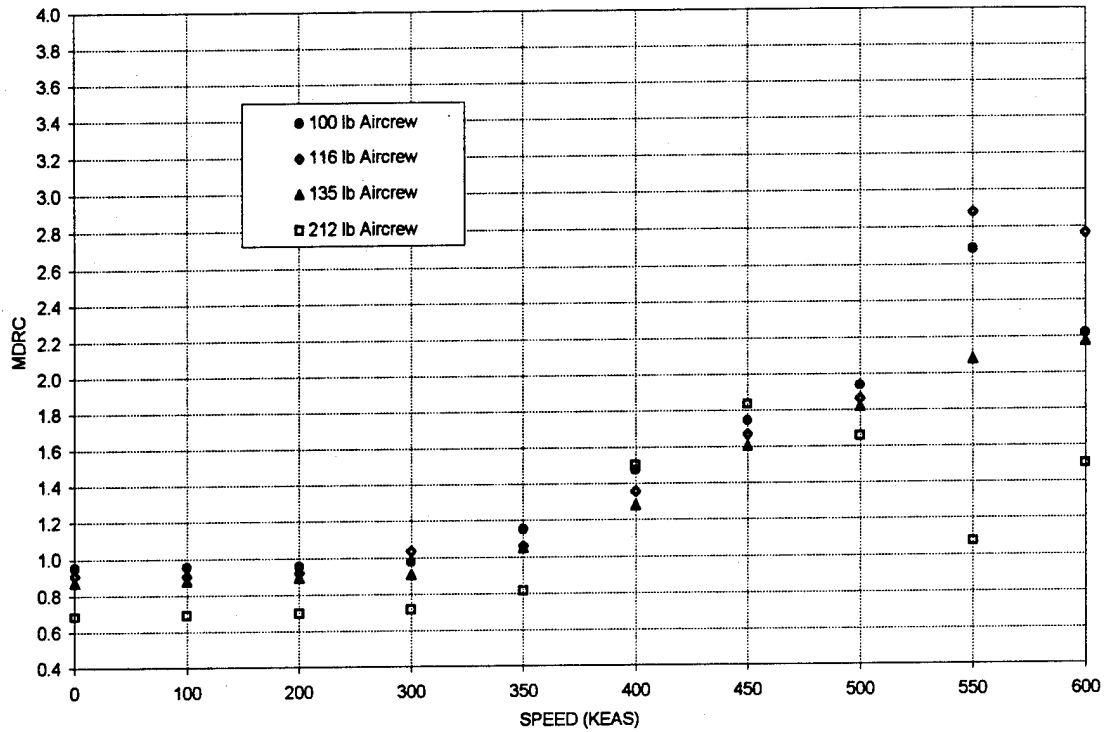


Figure 15: SJU-5 Peak MDRC vs. Airspeed at Ejection

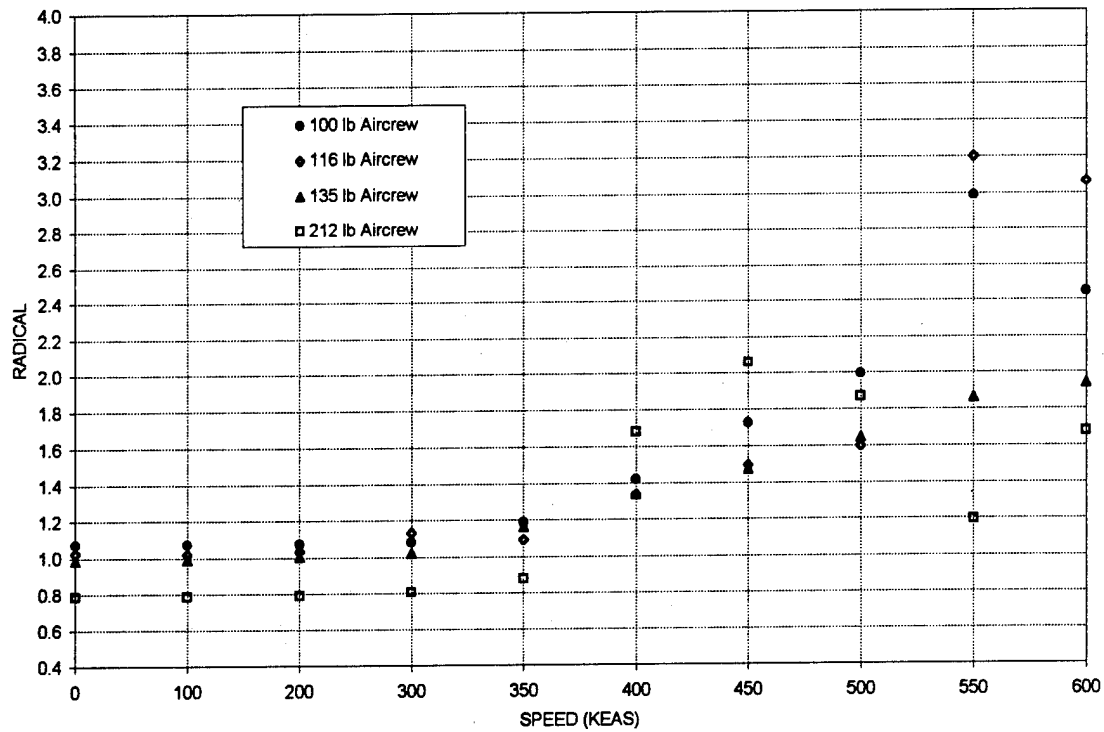


Figure 16: SJU-5 Peak Radical vs. Airspeed at Ejection

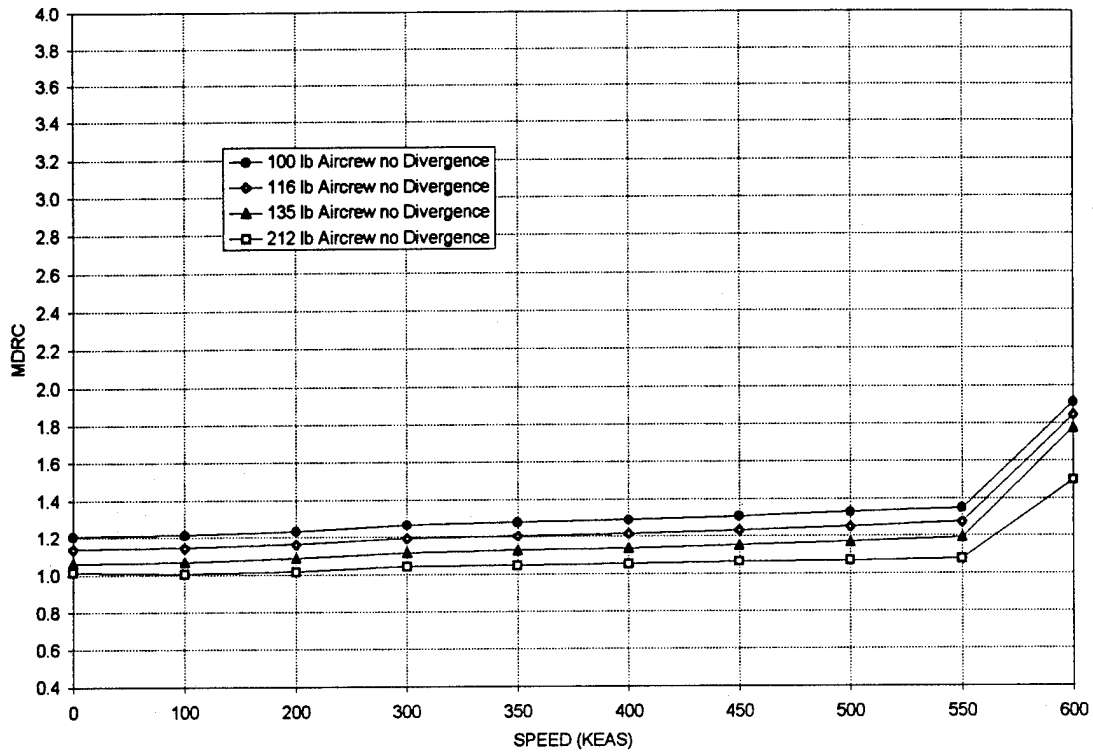


Figure 17: AV-8B SIIIS Peak MDRC vs. Airspeed at Ejection

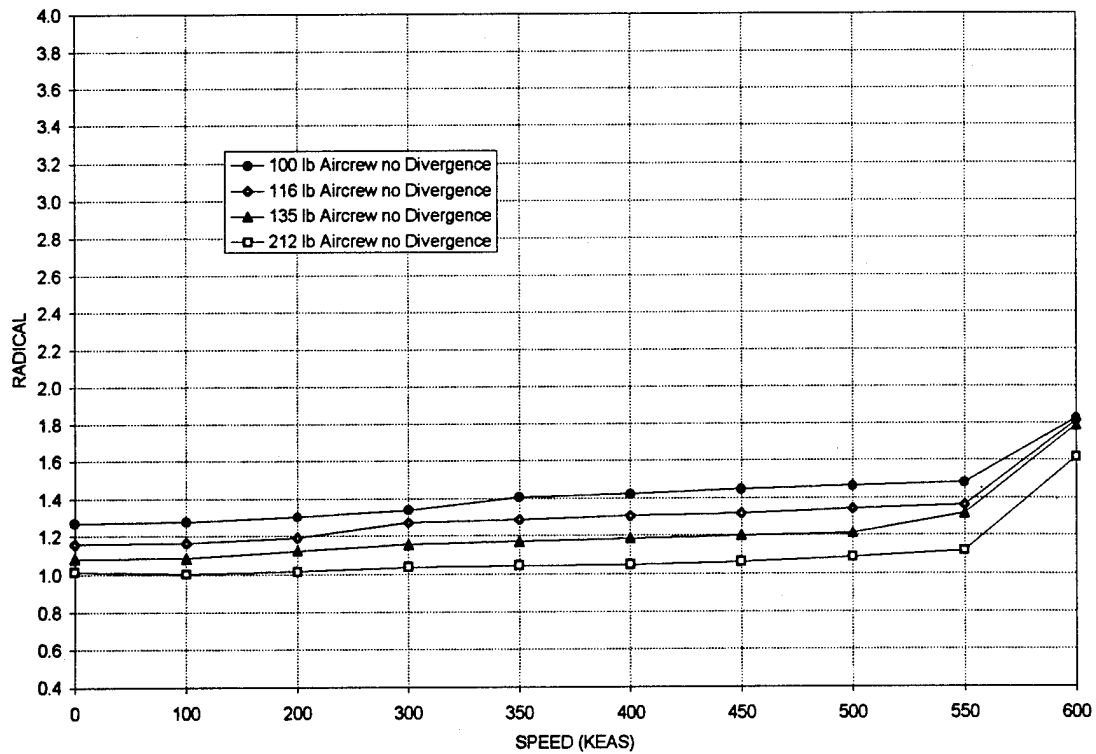


Figure 18: AV-8B SIIIS Peak Radical vs. Airspeed at Ejection

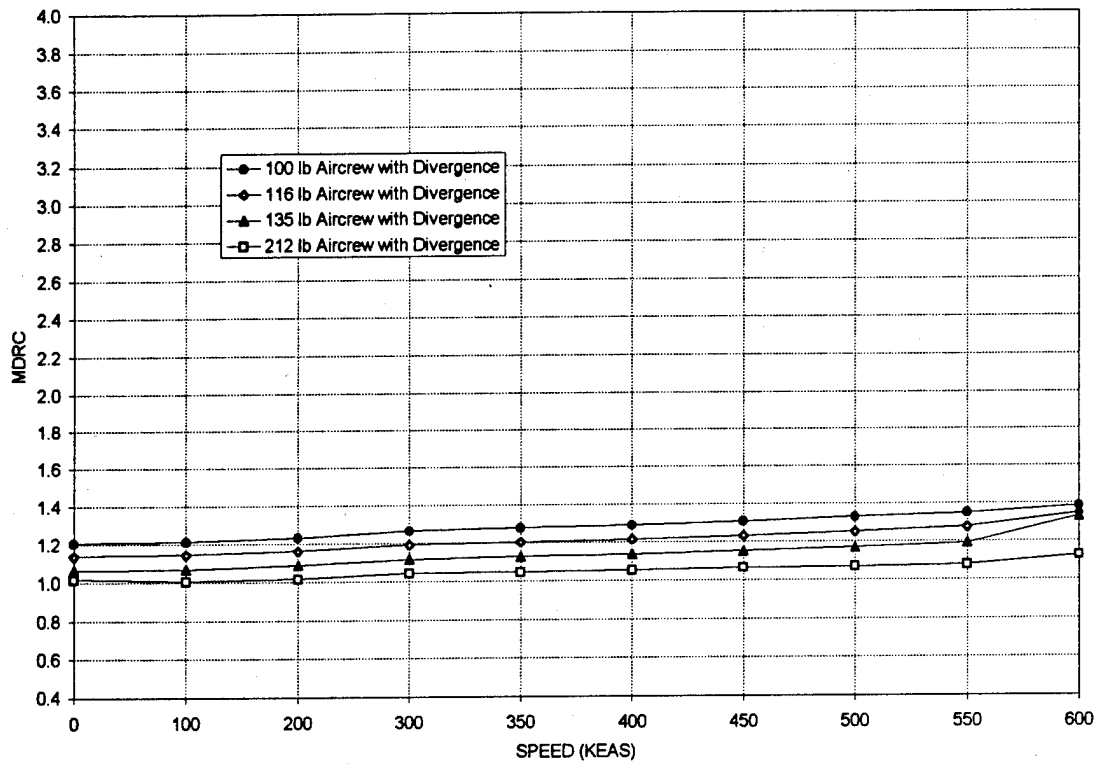


Figure 19: TAV-8B SIIS Peak MDRC vs. Airspeed at Ejection

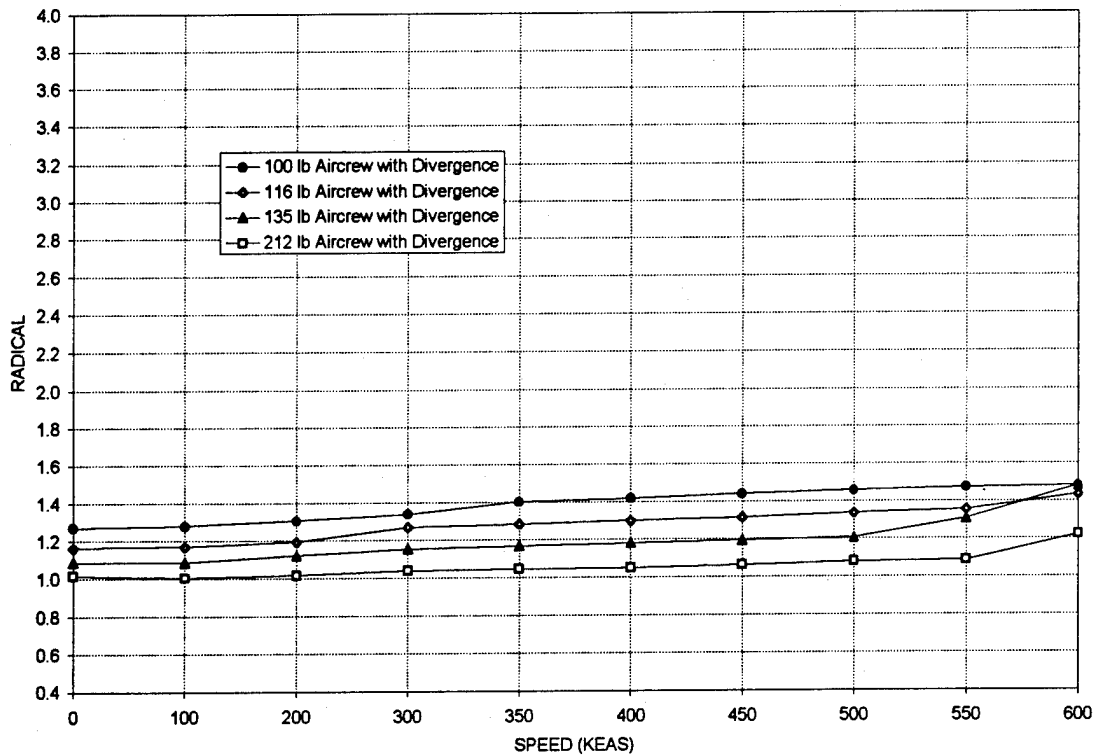


Figure 20: TAV-8B SIIS Peak Radical vs. Airspeed at Ejection

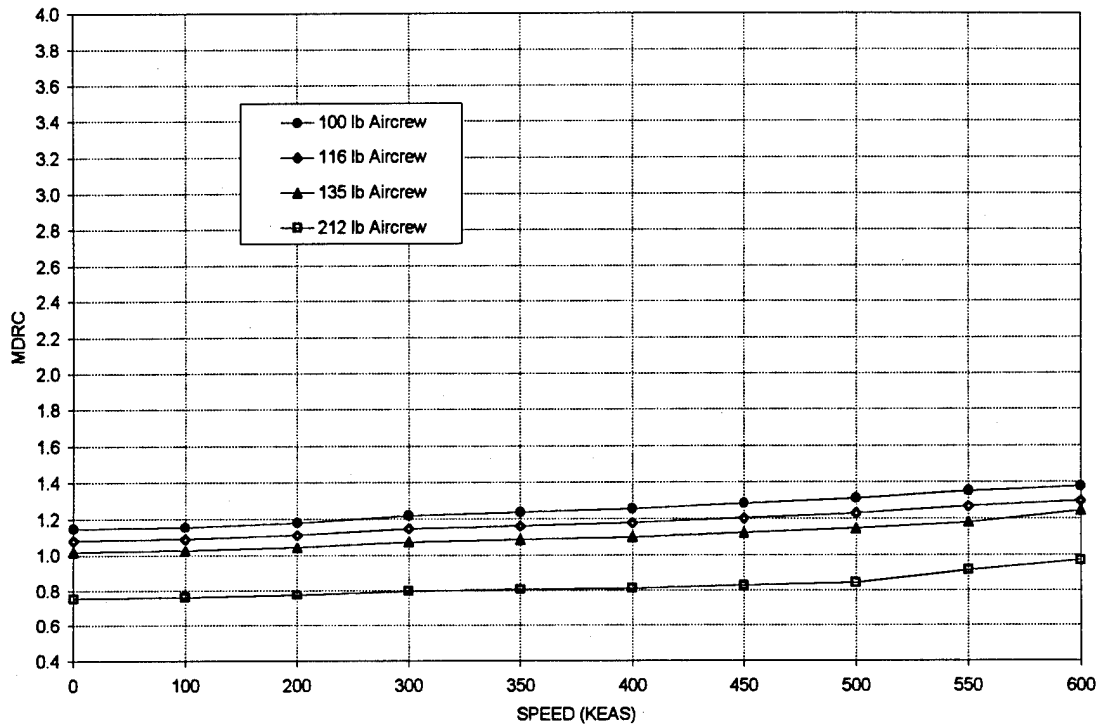


Figure 21: ESCAPAC IE-1 Peak MDRC vs. Airspeed at Ejection

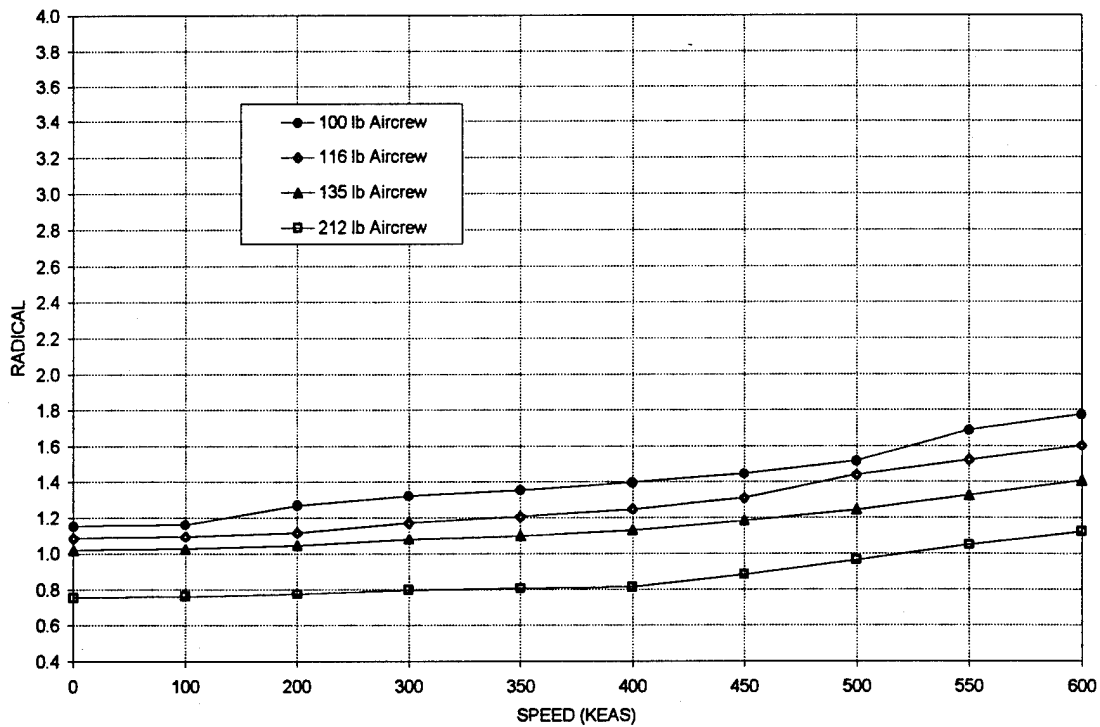


Figure 22: ESCAPAC IE-1 Peak Radical vs. Airspeed at Ejection

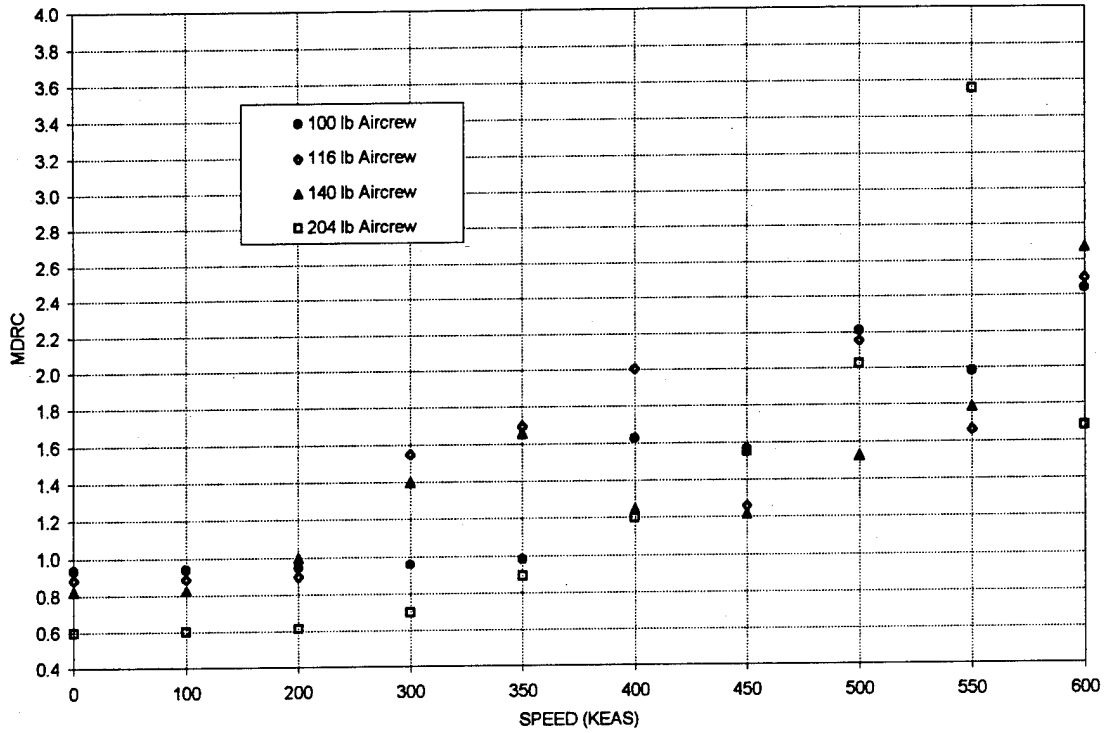


Figure 23: GRU-7 Peak MDRC vs. Airspeed at Ejection

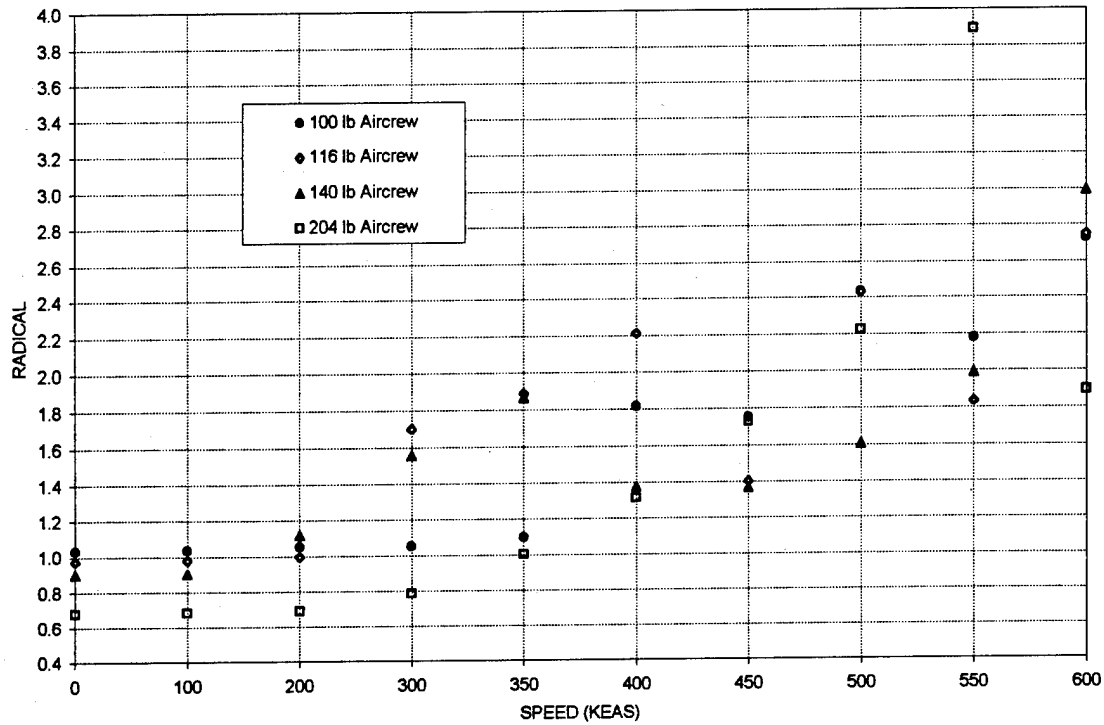


Figure 24: GRU-7 Peak Radical vs. Airspeed at Ejection

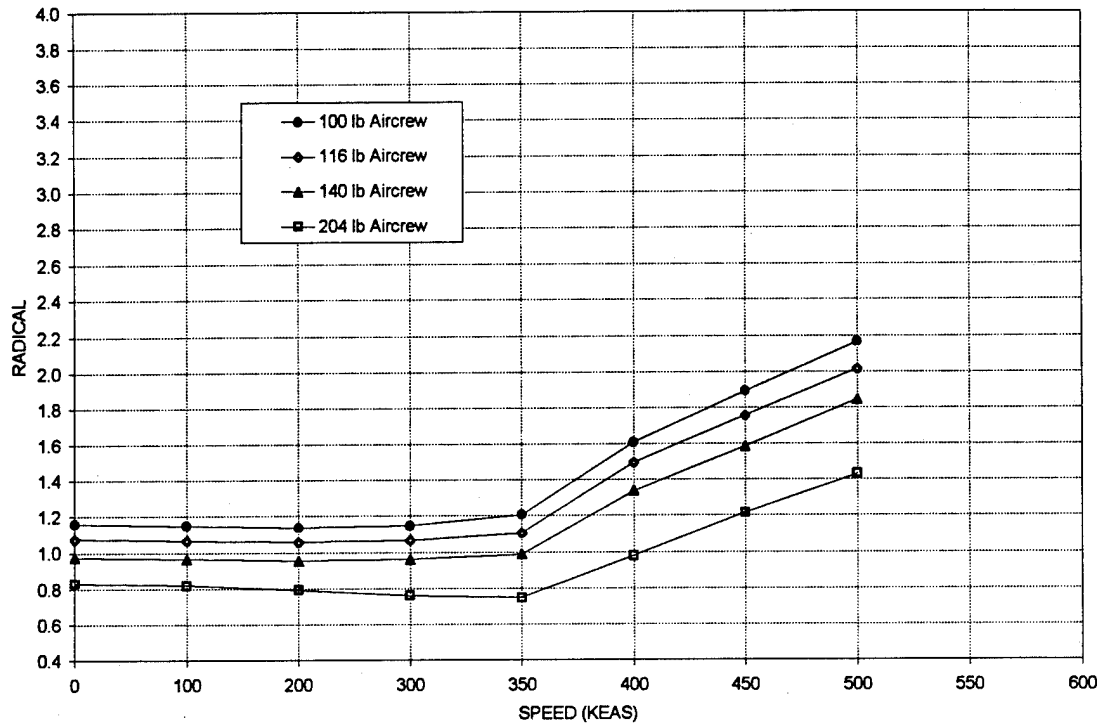


Figure 25: LS-1A Peak MDRC vs. Airspeed at Ejection

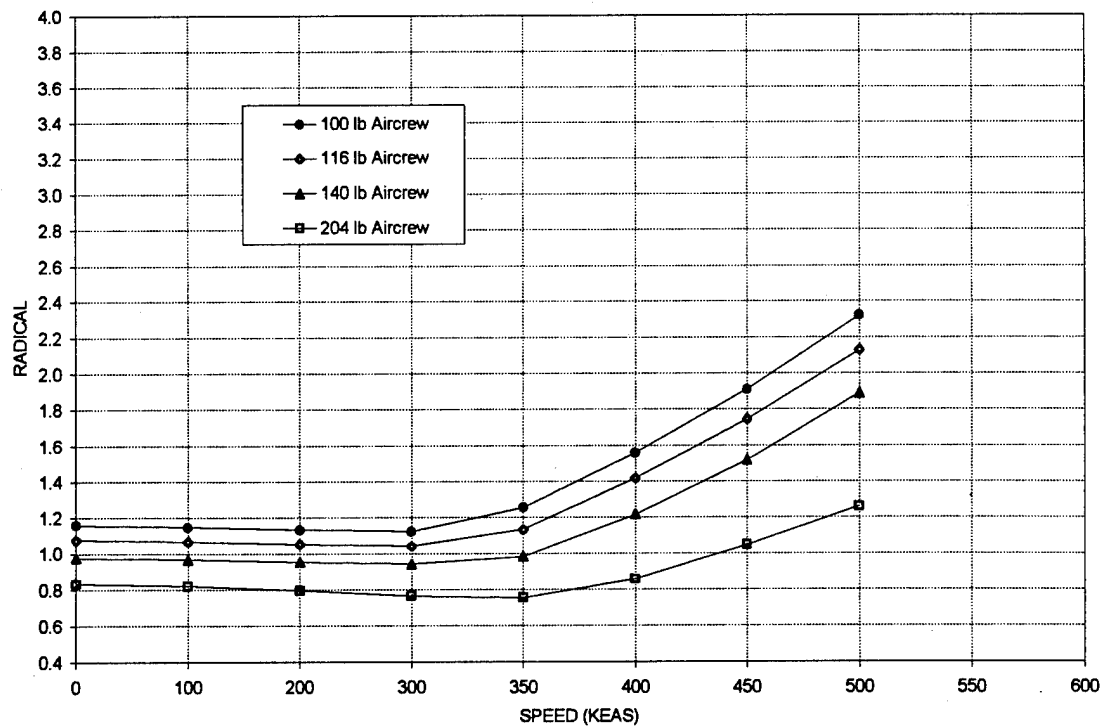


Figure 26: LS-1A Peak Radical vs. Airspeed at Ejection

To evaluate the risk of injury during the recovery phase, test data analysis was performed. Chest acceleration data from NACES, SJU-5, and SIIS sled tests was used to calculate normalized acceleration and indicate risk of injury. The normalized accelerations calculated in 212 lb, and 135 lb aircrew ejections are shown in Figure 27 and 28 respectfully.

The results of this analysis indicate that 212 lb aircrew may be at high risk of injury in ejections at speeds as low as 200 KEAS, and 135 lb occupants may be at high risk in ejections as low as 150 KEAS. The high risks of injury in the NACES and SIIS ejections at speeds around 200 KEAS are largely a result of the modes of the seat systems. NACES and SIIS seat systems operate in mode 1 in ejections at speeds from 0 to ~300 KEAS and 0 to ~225 KEAS respectively. Because mode 1 is for low speed, low altitude ejections, the time delay for recovery chute deployment is relatively short, and the recovery chute shock loads can be excessive in ejections at the upper end of the mode 1 envelope. When the seat systems operate in mode 2, the time delay is increased. The effects of modes is illustrated in Figure 27. The SIIS normalized acceleration is shown to be greater than 1.3 in the ejection at ~225 KEAS but below 0.7 in the ejection at ~250 KEAS. This is because the seat system operated in mode 2 in the second ejection and the parachute was consequently deployed at a latter time and at a lower airspeed. Another factor which contributes to the high risk of injury in the SIIS ejections is the seat systems ballistic spreaders. The ballistic spreaders result in rapid parachute inflation and consequently, high parachute shock loads.

This analysis also indicates that though the MDRC and Radical calculations indicated that risk of injury in SIIS ejections did not increase significantly in high speed ejections, the normalized acceleration can exceed 1.8 in SIIS ejections at 450 KEAS and higher.

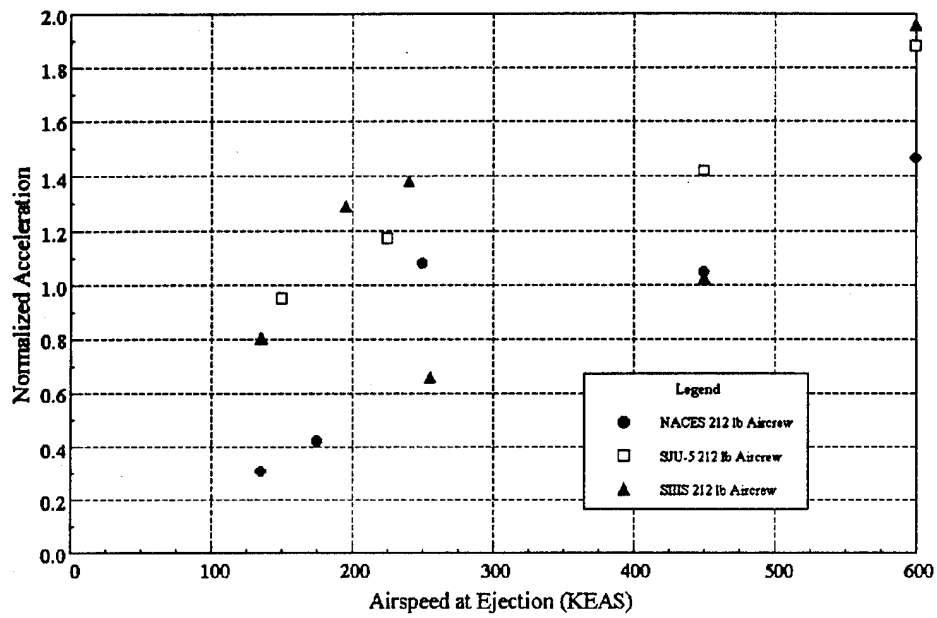


Figure 27: 212 lb Aircrew Normalized Acceleration vs. Airspeed at Ejection

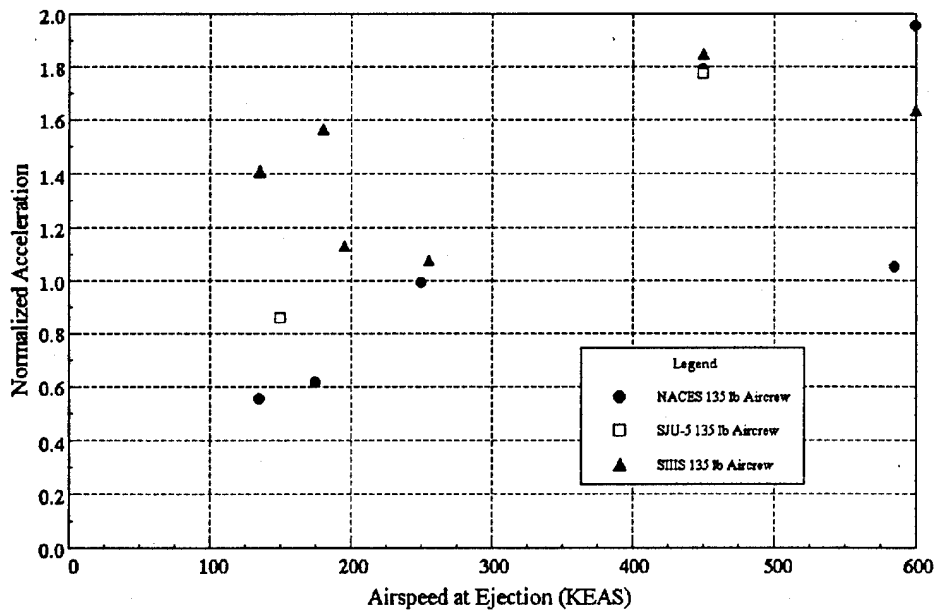


Figure 28: 135 lb Aircrew Normalized Acceleration vs. Airspeed at Ejection

4.0 Discussion

The results of this analysis establish trends in risk of injury in small aircrew ejections. The trend of increasing risk with decreasing aircrew weight is clearly evidenced in the MDRC and Radical values shown in Figures 13 through 26. The simulations indicate that a 116 lb occupant will be at higher risk of injury in an ejection than a 135 lb or 140 lb occupant and that a 100 lb occupant will be at higher risk of injury than a 116 lb occupant.

The current ejection seats were designed to limit acceleration levels for the minimum design weight aircrew (135 lb or 140 lb) to values specified in MILSPEC 18471. These acceleration limits correspond approximately to moderate (5%) risk of injury for the minimum design weight aircrew. Because of the trend of increasing risk with decreasing aircrew weight, the risk of injury to the 100 lb and 116 lb occupants exceeds 5% in most of the scenarios evaluated. In all of the seat systems evaluated the risk to the 100 lb and 116 lb occupants is greater than 50% in ejections at speeds of 450 KEAS and above.

Because MDRC and Radical calculations are only valid for a seated occupant, additional analysis of parachute shock loads was conducted to allow a more comprehensive evaluation of risk of injury. The normalized acceleration calculated from test data indicates that small aircrew may be at high risk of injury during recovery parachute deployment in ejections at speeds as low as 150 KEAS.

5.0 Conclusions

This effort predicts that small aircrew will have an increased risk of injury during ejection. In all cases where a trend was identifiable, the calculated risks to the 100 lb and 116 lb aircrew were consistently higher than those calculated for the occupants for which the seat systems were qualified. This analysis indicates that small occupants will be at high risk of injury in high speed ejections in all of the seat systems evaluated. The analysis also indicates that small aircrew may be at high risk of injury during parachute deployment in ejections at speeds as low as 150 KEAS.

Though in some cases, the seat performance for the minimum qualification weight of the seat systems (135 or 140 lbs) and the 116 lb and 100 lb aircrew was similar, the risk of injury to all of these occupants was significant at high speeds and cannot be considered safe. At the time of the development of these seat systems there were few small aviators, and the seat performance for small aircrew was not a major concern. However, with today's increasing number of small aviators, ejection seat performance with 140 lb and smaller aircrew is a significant issue.

It is important to note that the results of this effort are based on experimentally determined limits of male subjects. The effect gender on the tolerance limits is currently not known; female aviators may be at higher risk than predicted by this effort. It should also be noted that this analysis is theoretical. The computer simulations implement normal operation of all seat components. The effects seat instability and increased acceleration levels on component function is not anticipated by the model. For example, the simulations do not evaluate a drogue system's ability to deploy the recovery parachute in adverse orientations. Further efforts should include seat system testing to verify the simulation results and examine seat component functioning.

As discussed in section 2.2.1, the catapult modeling in the 100 lb and 116 lb aircrew simulations was based on thrust data from 135 lb and 140 lb aircrew. Because of this, the predicted risk of injury to the 100 lb and 116 lb aircrew in low speed ejections may be slightly higher than actual. In the future 100 lb and 116 lb simulations will be conducted using experimentally derived thrust data for the respective weights. However, it is expected that calculating risk using 100 lb and 116 lb occupant thrust curves will not alter the trends documented in this report.

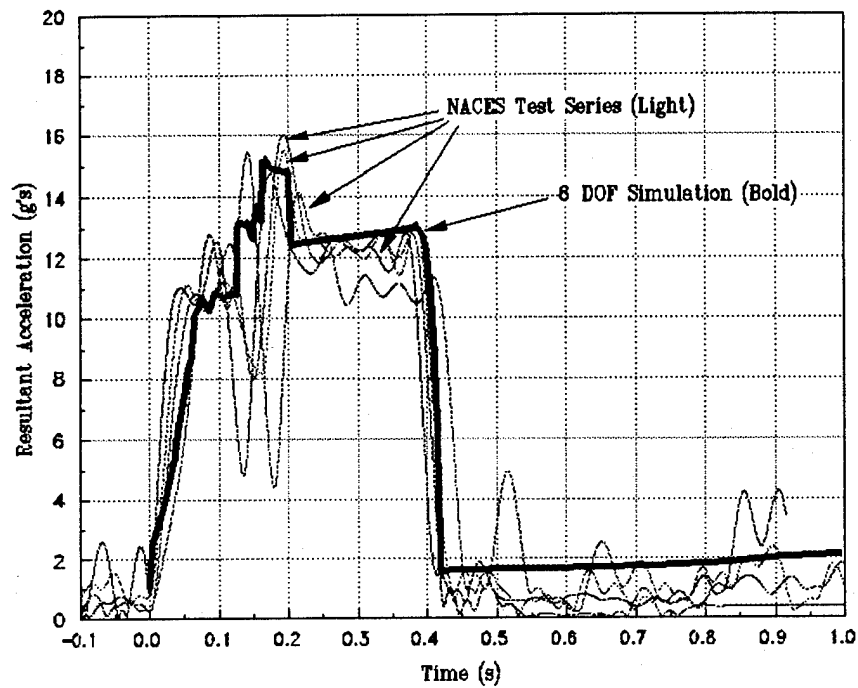
The limitations in small occupant performance can potentially be overcome through the implementation of current advances in technology. Technologies are currently under advanced development which can potentially resolve the stability deficiencies incurred with reduced occupant mass. These specific technologies include advanced propulsion, aerodynamic surfaces, and seating geometry. Technology spin off of these capabilities will provide a potential solution, enabling safe escape of the small occupant at the full aircraft speed range.

6.0 References

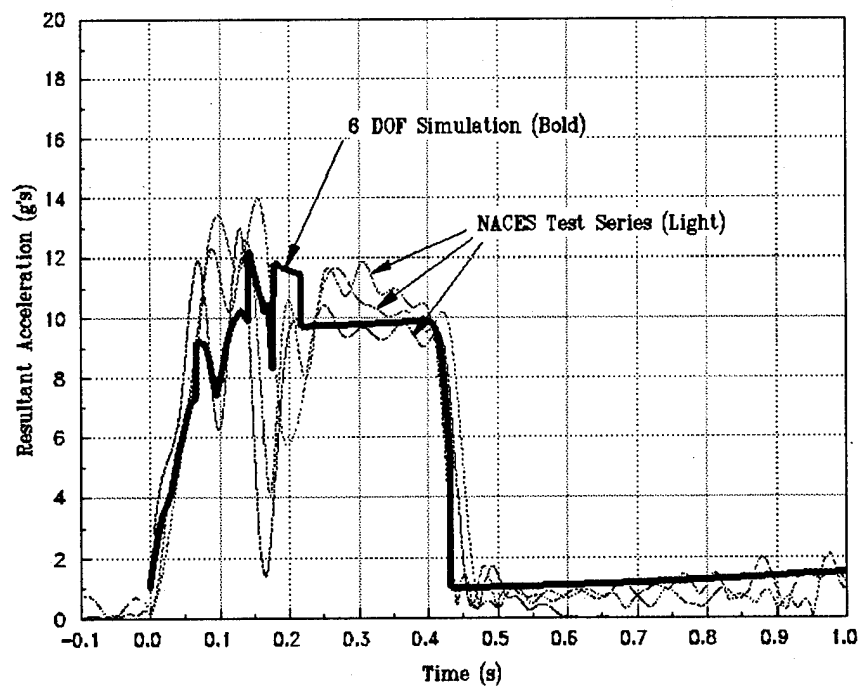
1. Gifford, E. C., Lazo, J., Provost, J. R., "Aerospace Crew Equipment Laboratory Anthropometry of Naval Aviators - 1964". NAED-ACEL-533, Oct. 8 1965
2. Yeiser, C. W., Olson, M. B., "Advanced Crew Capsule Escape System Simulation (ACCESS) Computer Program: ACCESS Users' Manual Volume 2". Dec. 1992
3. Baughman, L., Douglas, "Development of an Interactive Computer Program to Produce Body Description Data". Report No. AFAMRL-TR-83-058, July 1983
4. Ludtke, W. P., "Notes on a Generic Parachute Opening Force Analysis", AIAA-86-2440-CP, Oct. 1986
5. Brinkley, J. W., Mosher, S. E., Specker, L. J., "Development of Acceleration Exposure Limits for Advanced Escape Systems".
6. "U. S. Air Force Guide Specification, Emergency Escape, Aircraft", Report No, AFGS-87235B, Mar. 1992
7. Quartuccio, J. J., Nichols, J. P., Marquette, T. J., "Ejection Seat Performance Evaluation for Small Aircrew in the F-14A Aircraft, GRU-7A Seat System", May 1994

APPENDIX A:
6 DOF Simulation Validation

NACES ESCAPE SYSTEM VALIDATION RESULTANT ACCELERATION, 0 KEAS EJECTION

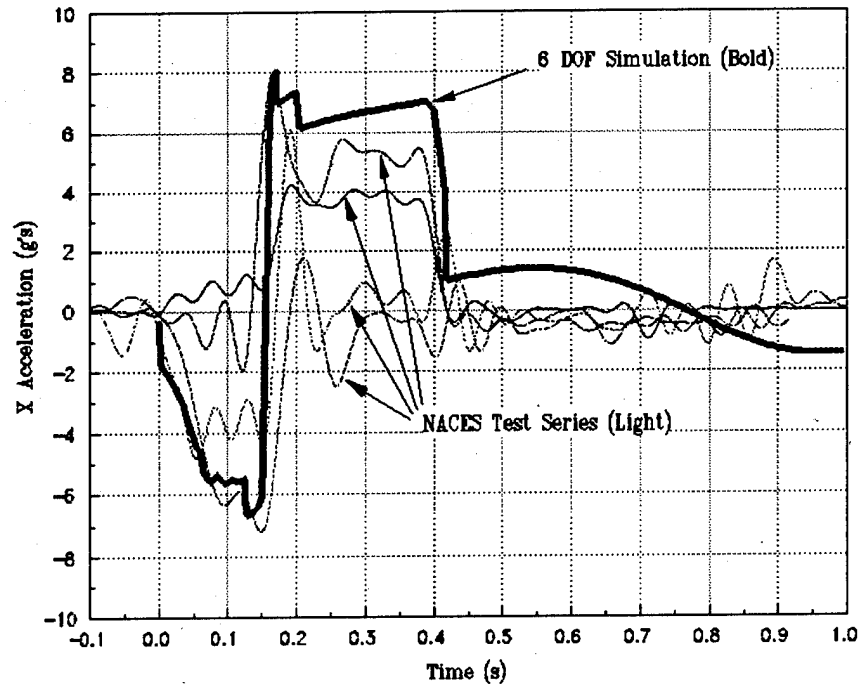


Resultant Acceleration vs. Time
135 lb Aircrew, 0 KEAS

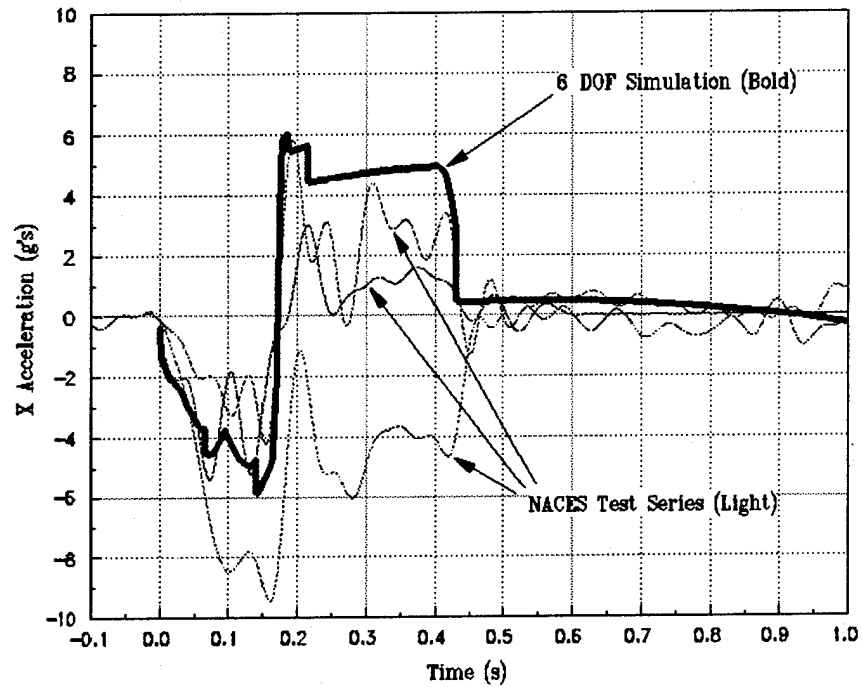


Resultant Acceleration vs. Time
212 lb Aircrew, 0 KEAS

NACES ESCAPE SYSTEM VALIDATION DOWN RANGE (X) ACCELERATION, 0 KEAS EJECTION

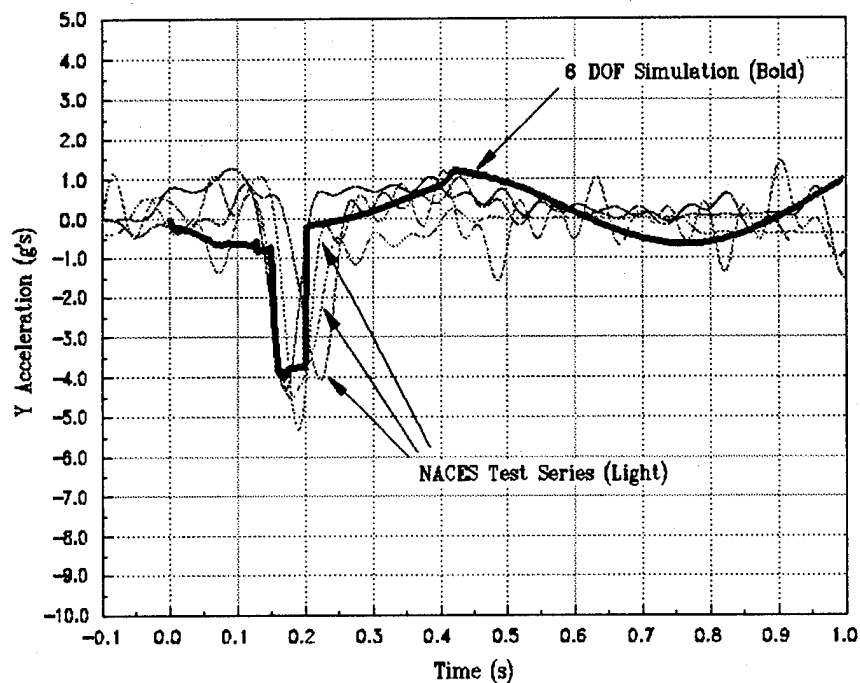


X Acceleration vs. Time
135 lb Aircrew, 0 KEAS

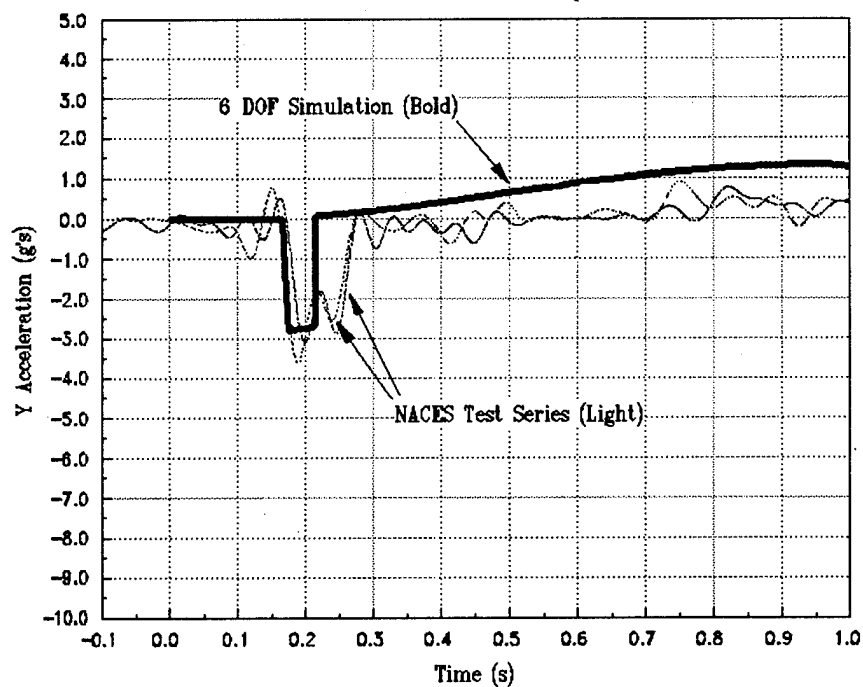


X Acceleration vs. Time
212 lb Aircrew, 0 KEAS

NACES ESCAPE SYSTEM VALIDATION LATERAL (Y) ACCELERATION, 0 KEAS EJECTION

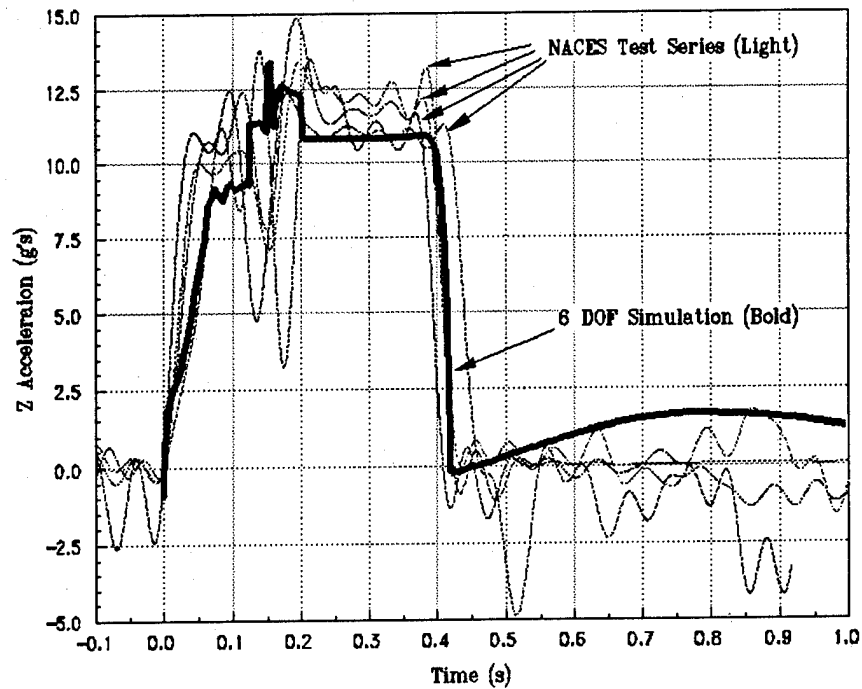


Y Acceleration vs. Time
135 lb Aircrew, 0 KEAS

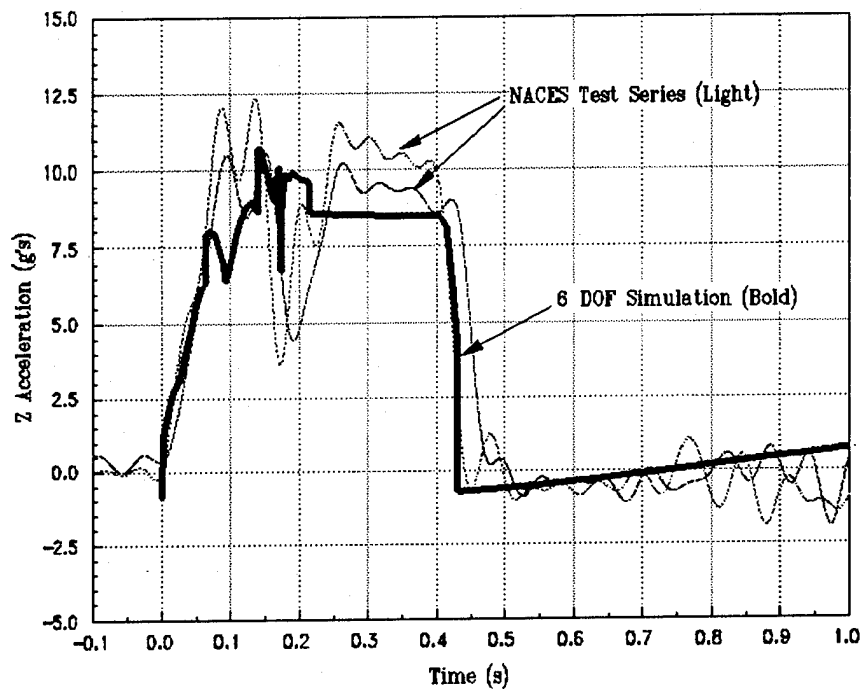


Y Acceleration vs. Time
212 lb Aircrew, 0 KEAS

NACES ESCAPE SYSTEM VALIDATION VERTICAL (Z) ACCELERATION, 0 KEAS EJECTION

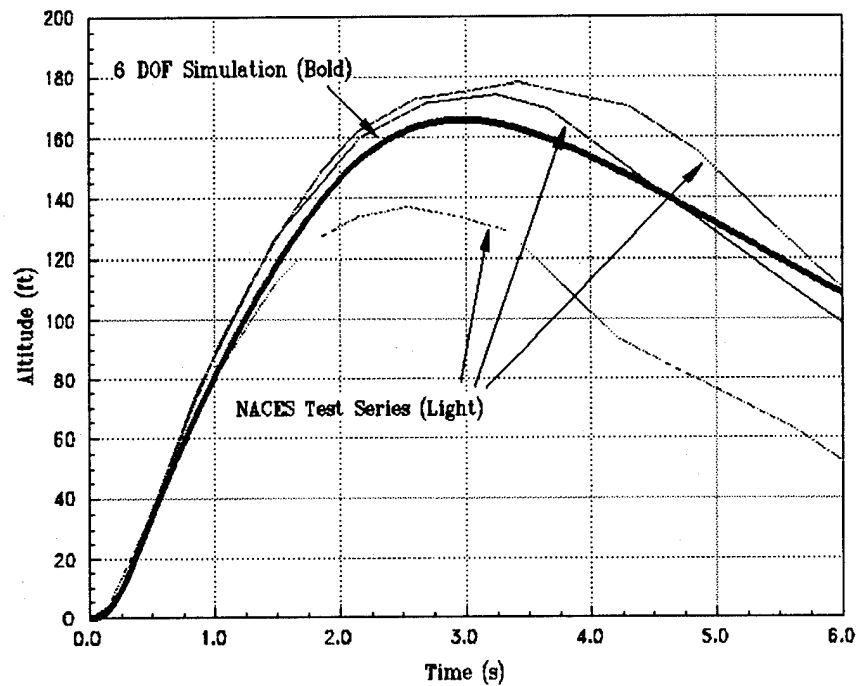


Z Acceleration vs. Time
135 lb Aircrew, 0 KEAS

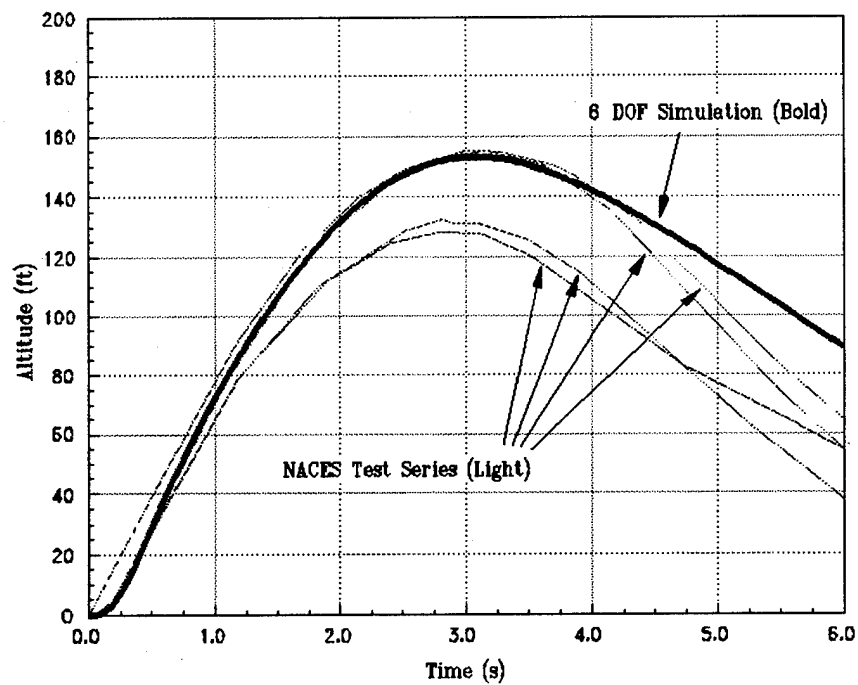


Z Acceleration vs. Time
212 lb Aircrew, 0 KEAS

NACES ESCAPE SYSTEM VALIDATION TRAJECTORY, 0 KEAS EJECTION

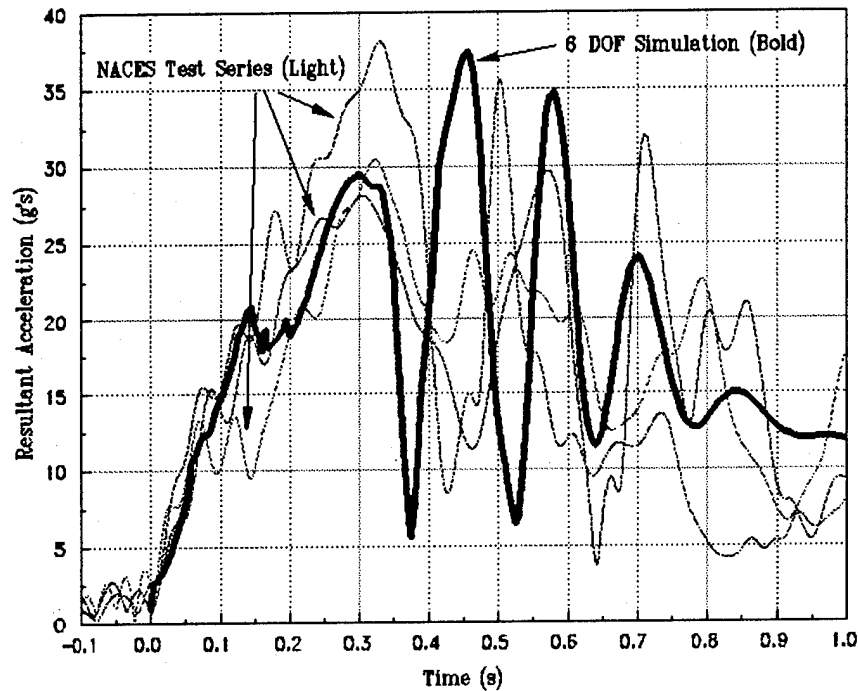


Altitude vs. Time
135 lb Aircrew, 0 KEAS

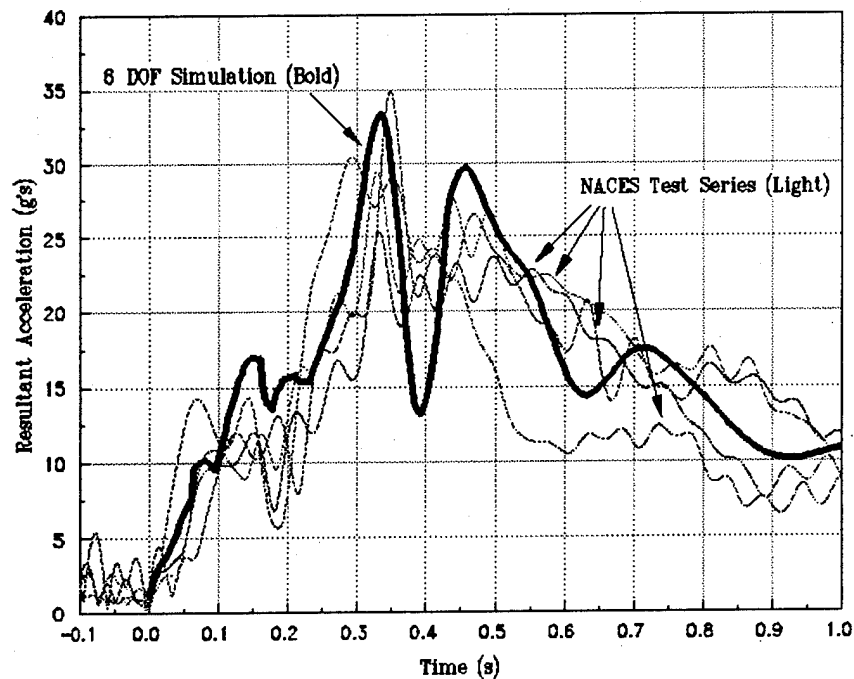


Altitude vs. Time
212 lb Aircrew, 0 KEAS

NACES ESCAPE SYSTEM VALIDATION RESULTANT ACCELERATION, 600 KEAS EJECTION

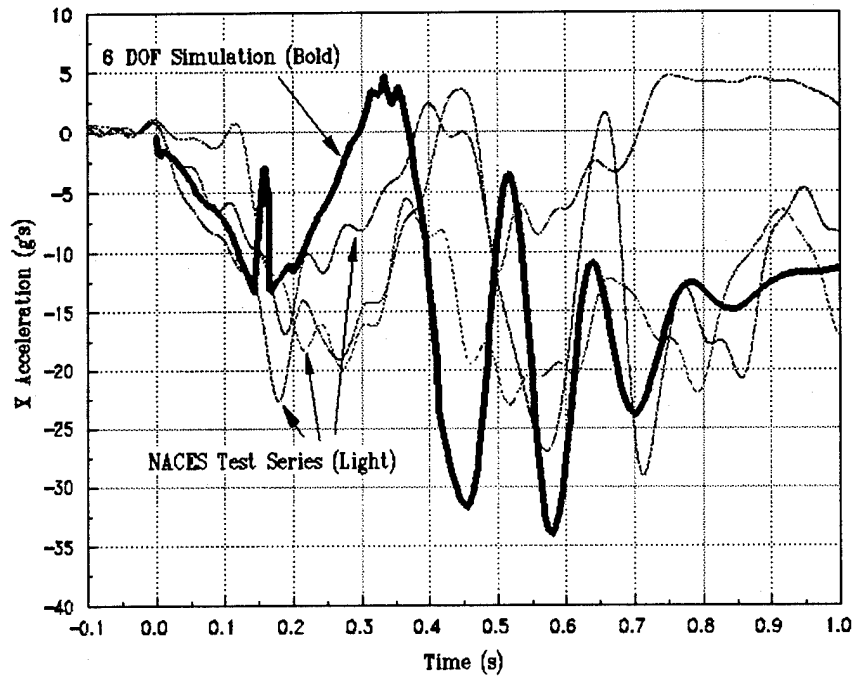


Resultant Acceleration vs. Time
135 lb Aircrew, 600 KEAS

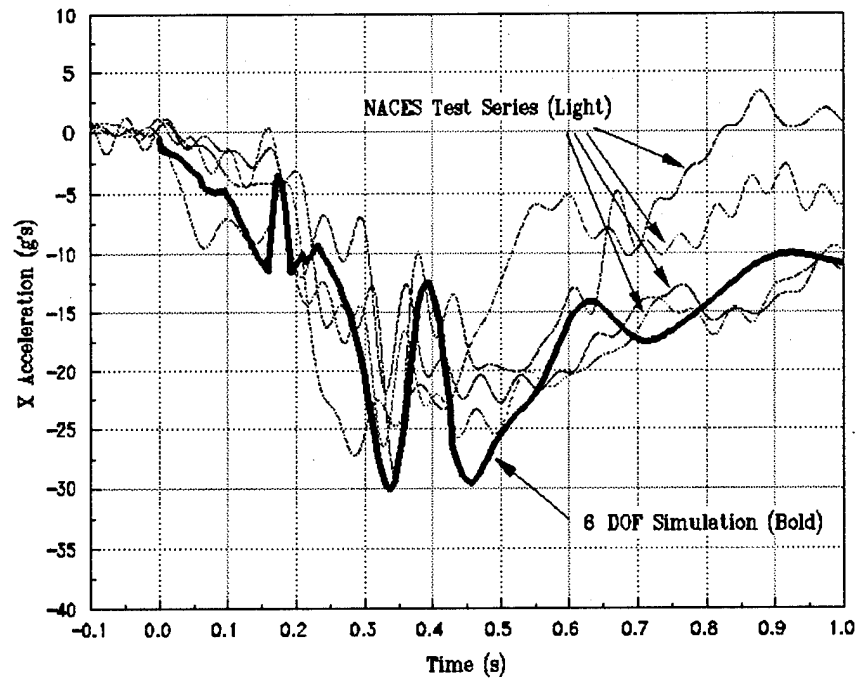


Resultant Acceleration vs. Time
212 lb Aircrew, 600 KEAS

NACES ESCAPE SYSTEM VALIDATION DOWN RANGE (X) ACCELERATION, 600 KEAS EJECTION

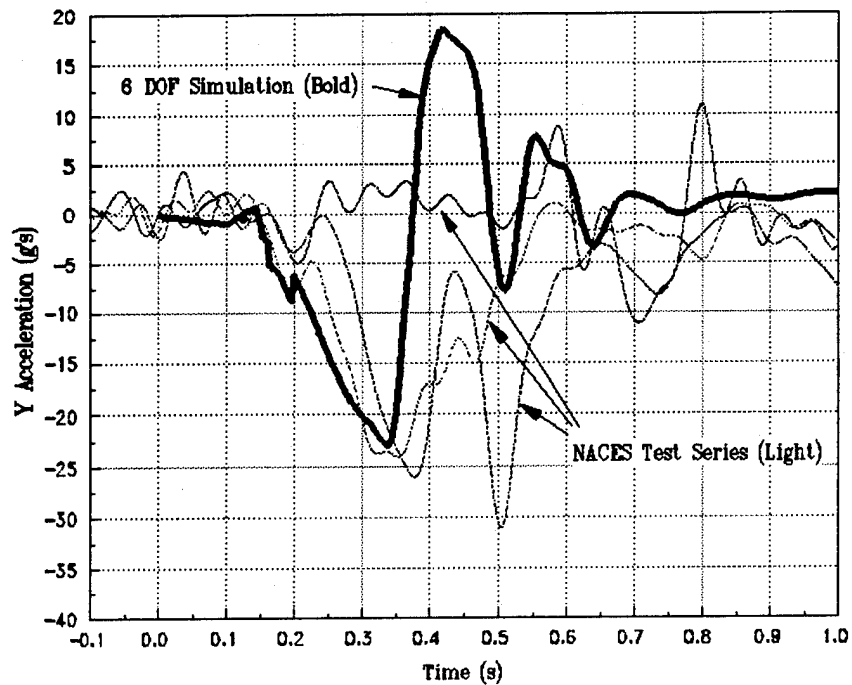


X Acceleration vs. Time
135 lb Aircrew, 600 KEAS

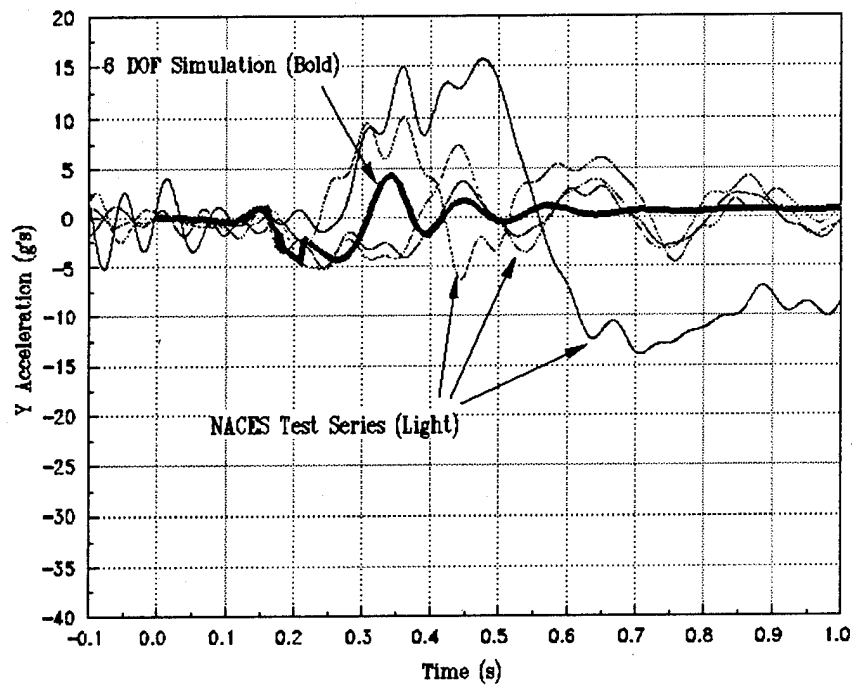


X Acceleration vs. Time
212 lb Aircrew, 600 KEAS

NACES ESCAPE SYSTEM VALIDATION LATERAL (Y) ACCELERATION, 600 KEAS EJECTION

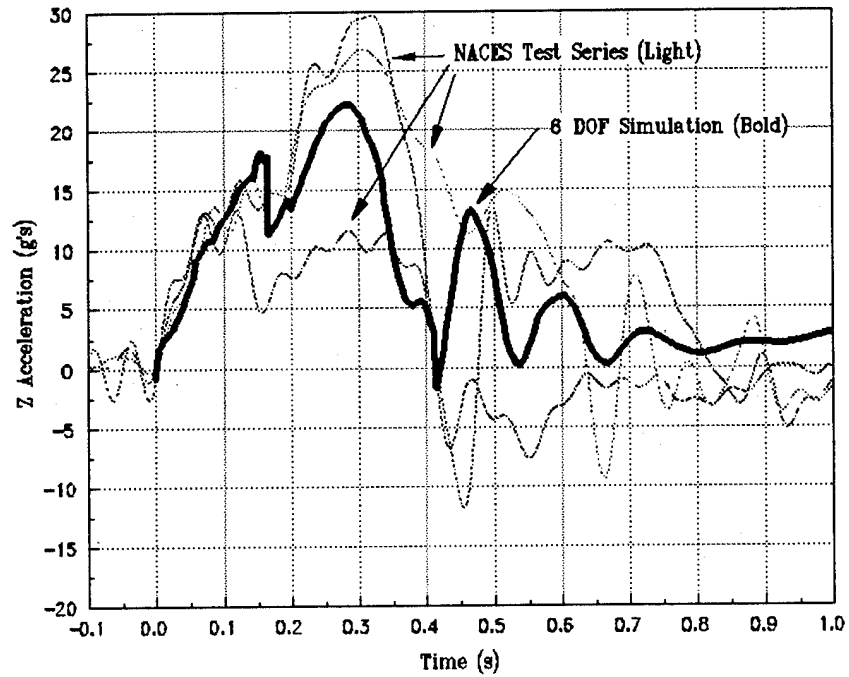


Y Acceleration vs. Time
135 lb Aircrew, 600 KEAS

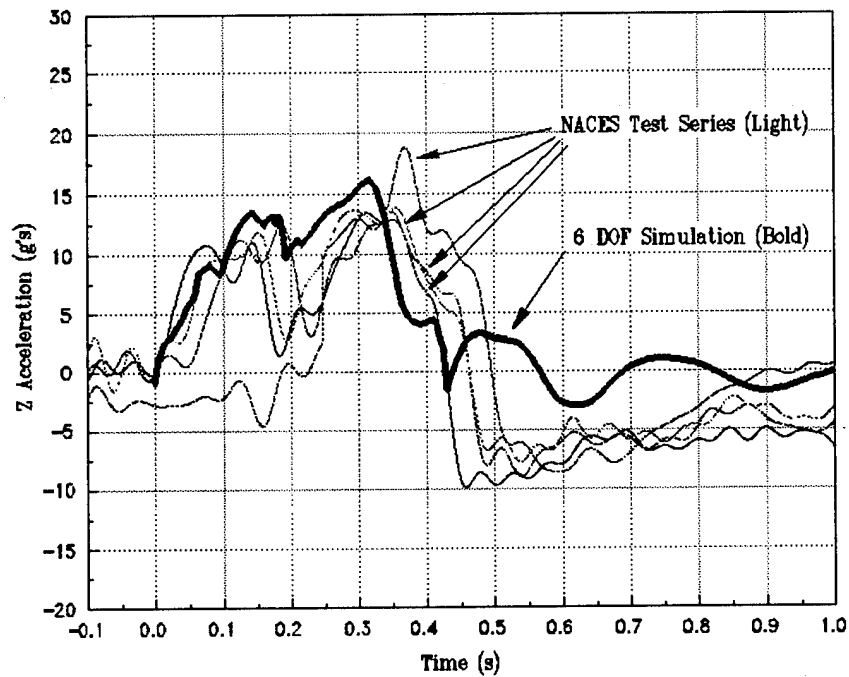


Y Acceleration vs. Time
212 lb Aircrew, 600 KEAS

NACES ESCAPE SYSTEM VALIDATION VERTICAL (Z) ACCELERATION, 600 KEAS EJECTION

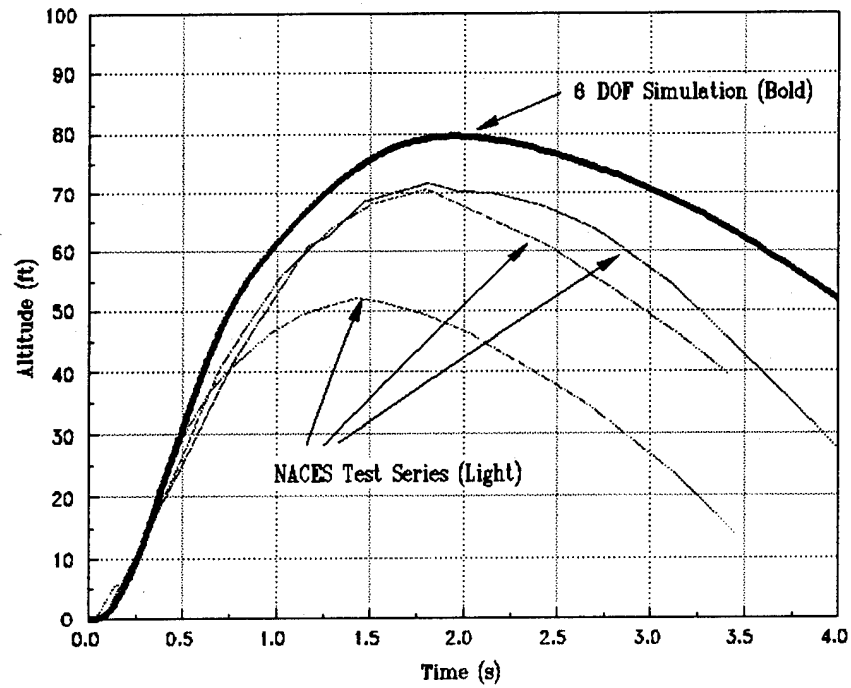


Z Acceleration vs. Time
135 lb Aircrew, 600 KEAS

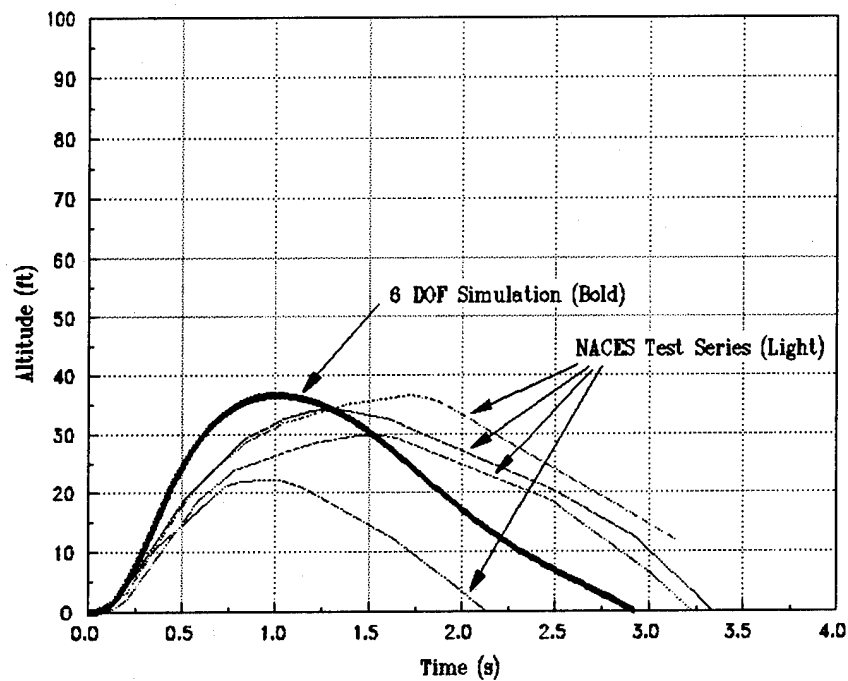


Z Acceleration vs. Time
212 lb Aircrew, 600 KEAS

NACES ESCAPE SYSTEM VALIDATION TRAJECTORY, 600 KEAS EJECTION

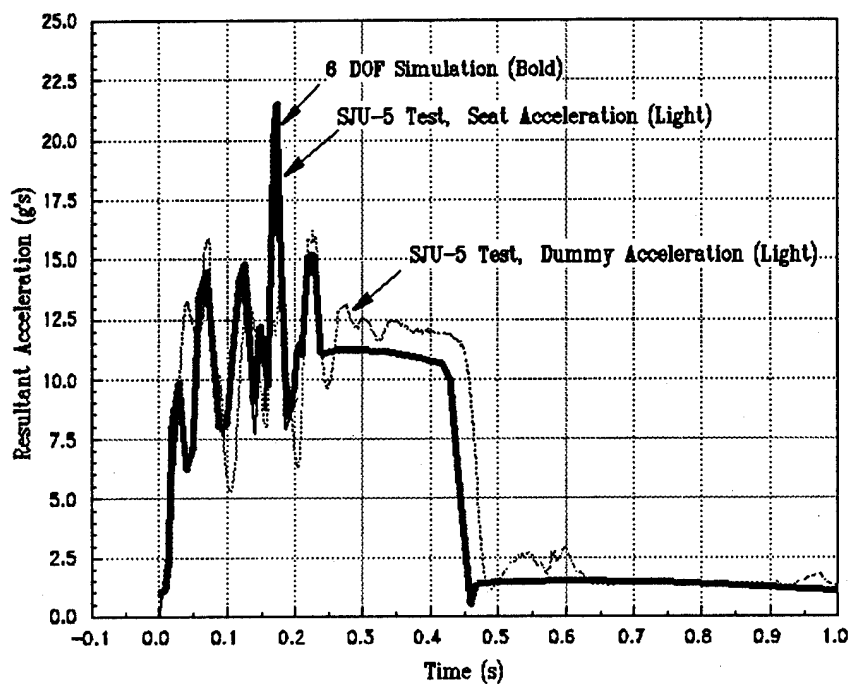


Altitude vs. Time
135 lb Aircrew, 600 KEAS

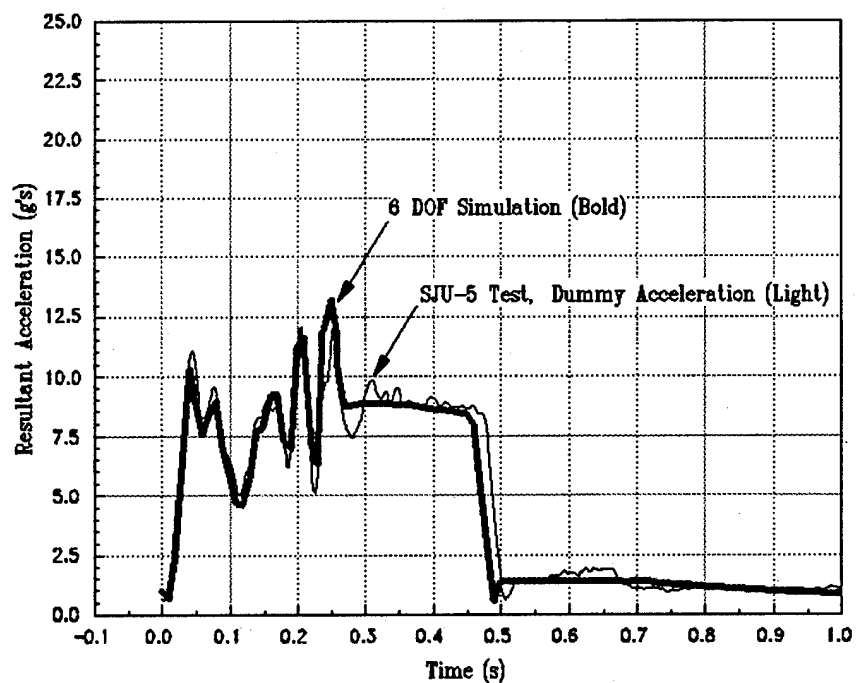


Altitude vs. Time
212 lb Aircrew, 600 KEAS

SJU-5 ESCAPE SYSTEM VALIDATION RESULTANT ACCELERATION, 0 KEAS EJECTION

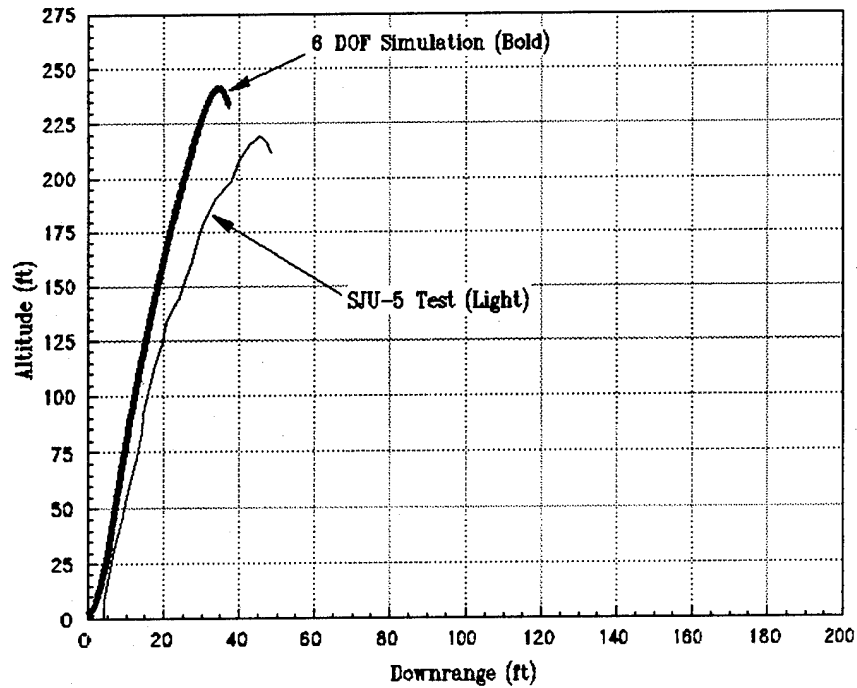


Resultant Acceleration vs. Time
135 lb Aircrew, 0 KEAS

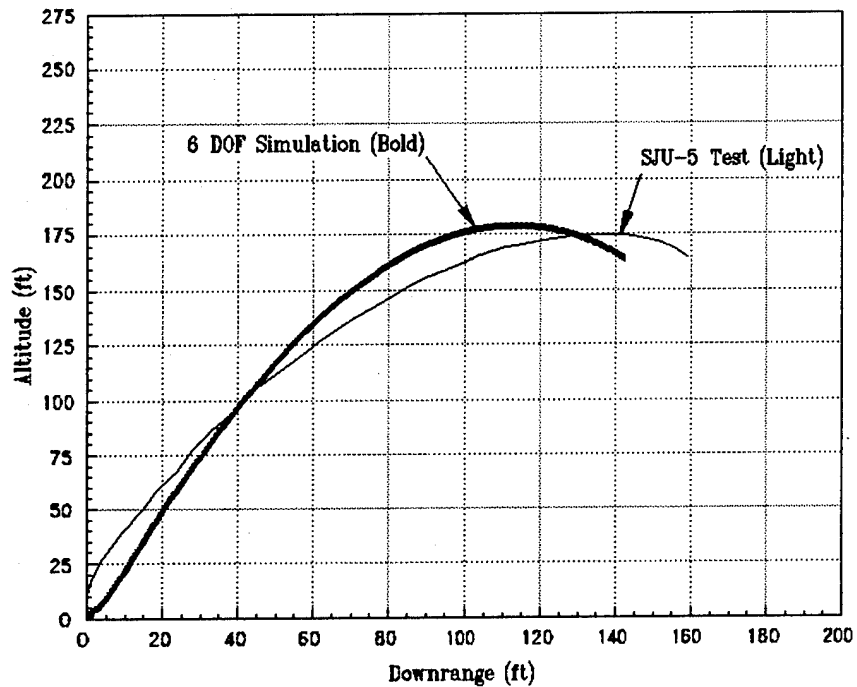


Resultant Acceleration vs. Time
212 lb Aircrew, 0 KEAS

SJU-5 ESCAPE SYSTEM VALIDATION TRAJECTORY, 0 KEAS EJECTION

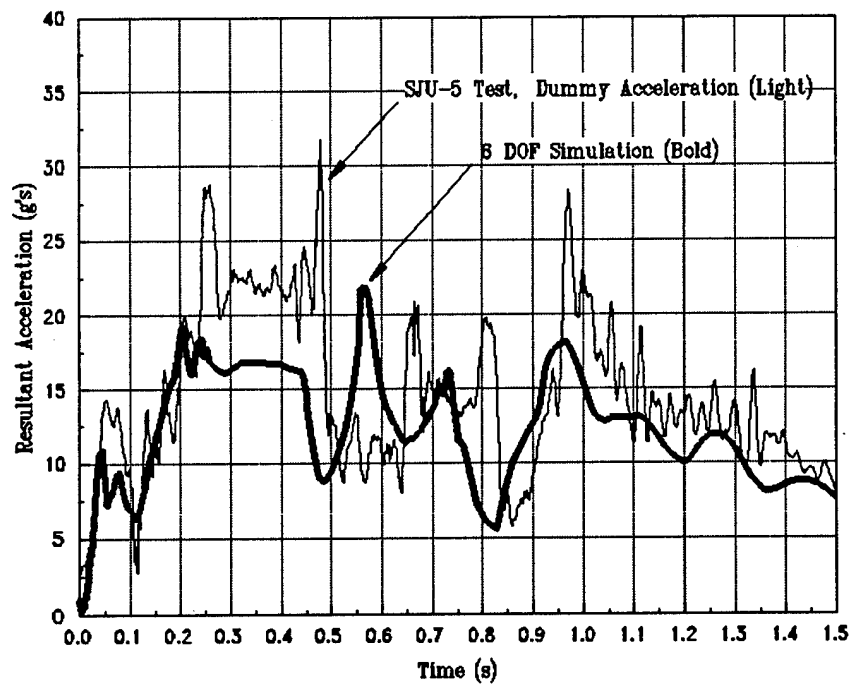
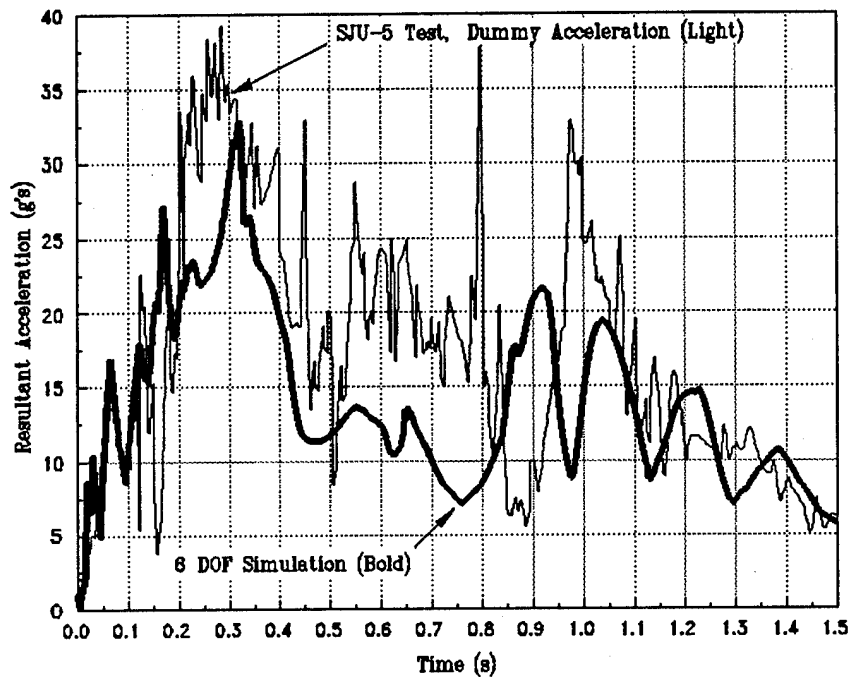


Altitude vs. Downrange Distance
135 lb Aircrew, 0 KEAS

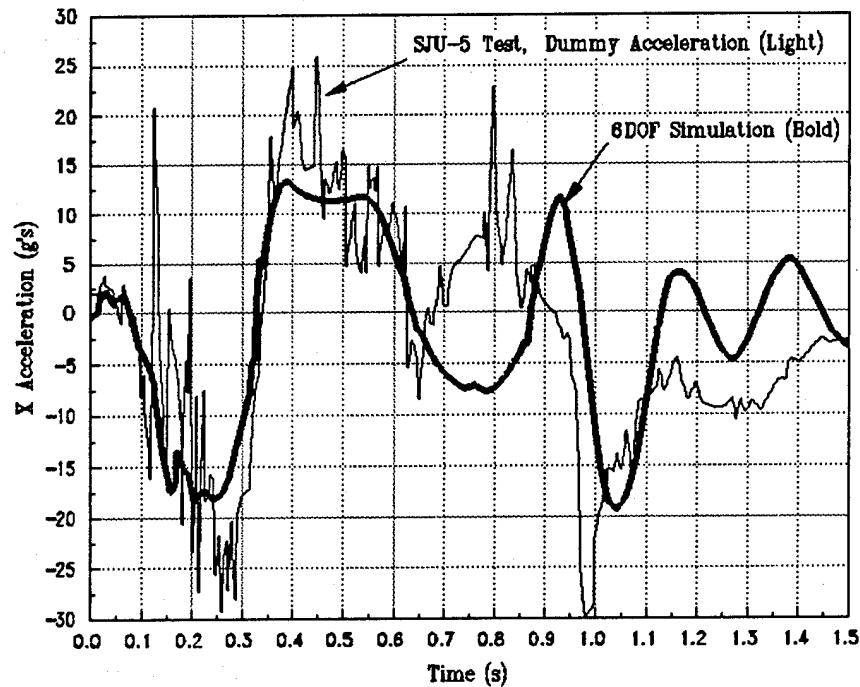


Altitude vs. Downrange Distance
212 lb Aircrew, 0 KEAS

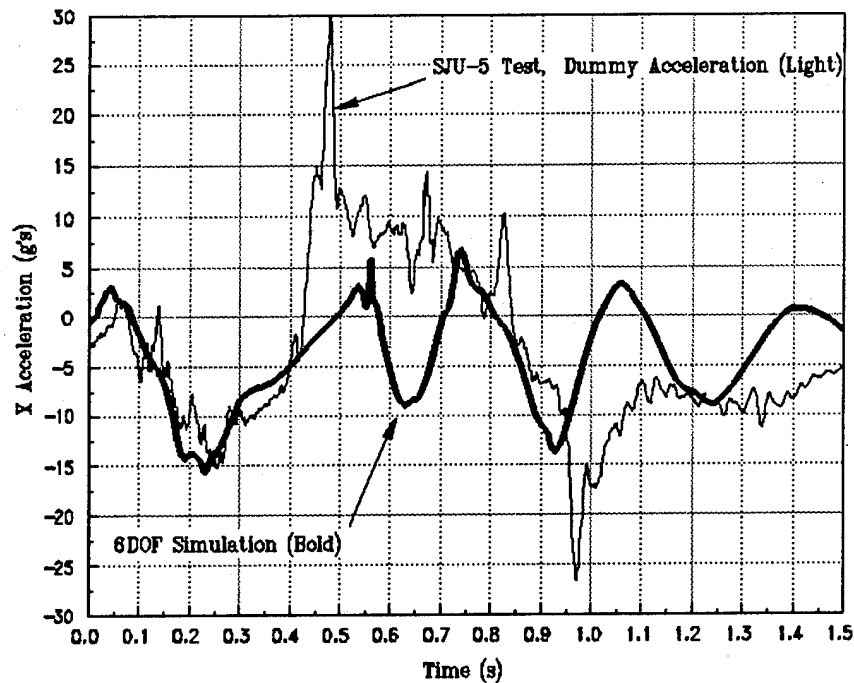
SJU-5 ESCAPE SYSTEM VALIDATION RESULTANT ACCELERATION, 600 KEAS EJECTION



SJU-5 ESCAPE SYSTEM VALIDATION DOWN RANGE (X) ACCELERATION, 600 KEAS EJECTION

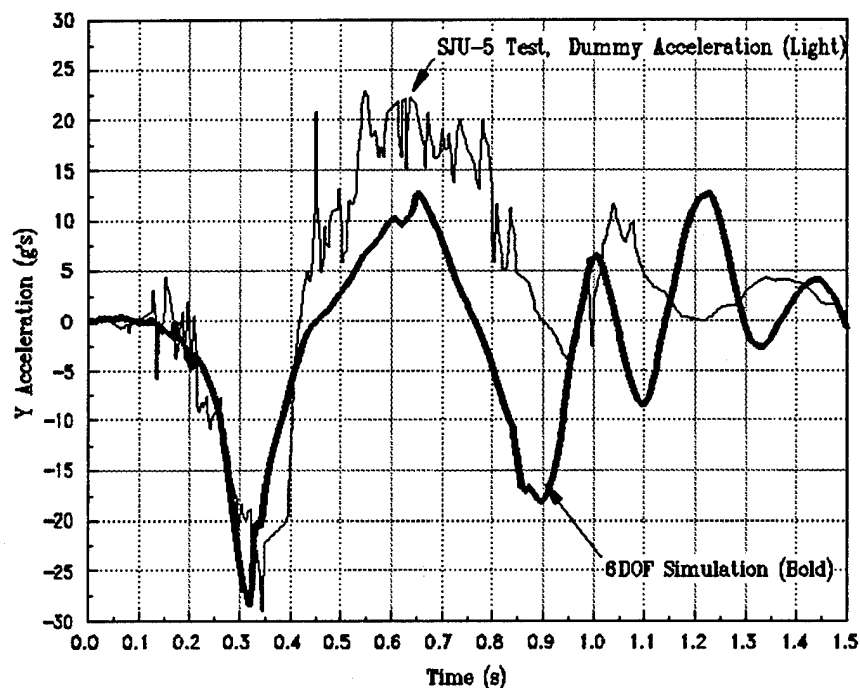


X Acceleration vs. Time
135 lb Aircrew, 600 KEAS

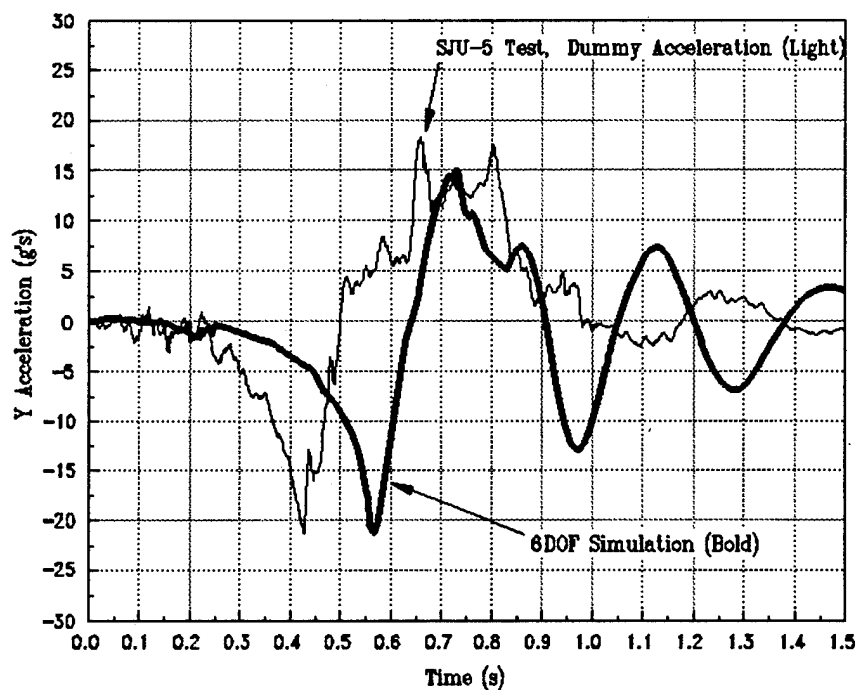


X Acceleration vs. Time
212 lb Aircrew, 600 KEAS

SJU-5 ESCAPE SYSTEM VALIDATION LATERAL (Y) ACCELERATION, 600 KEAS EJECTION

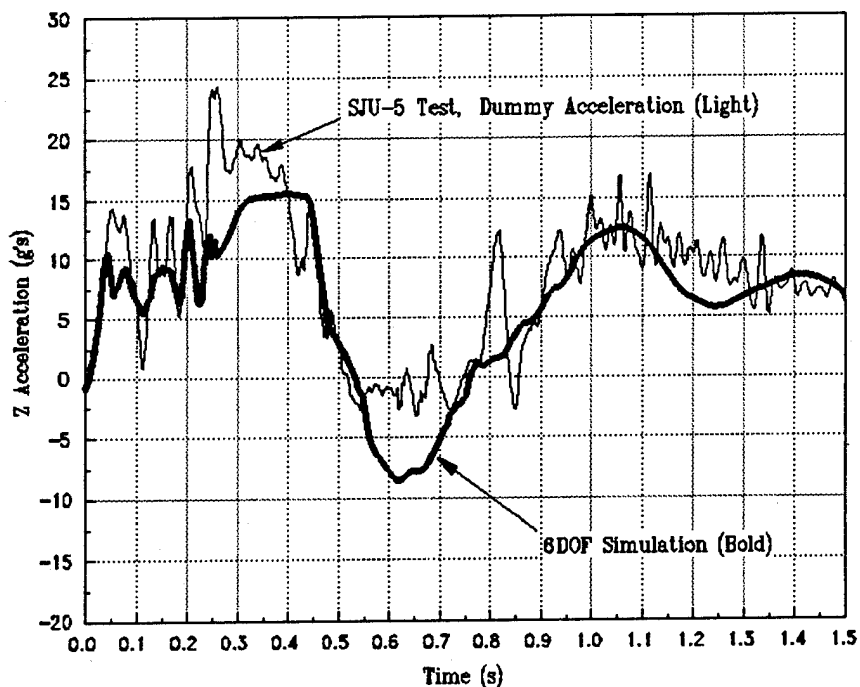
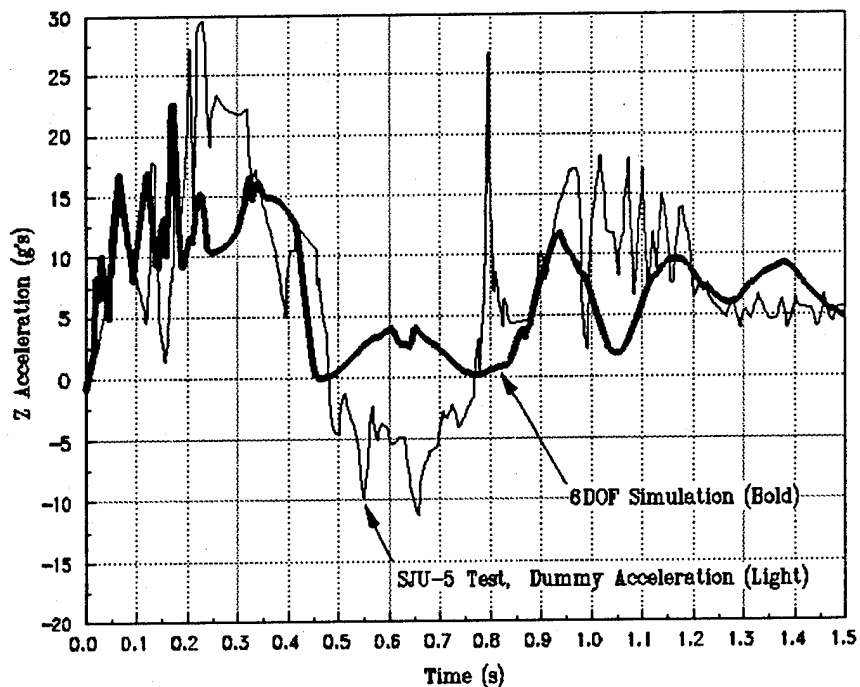


Y Acceleration vs. Time
135 lb Aircrew, 600 KEAS

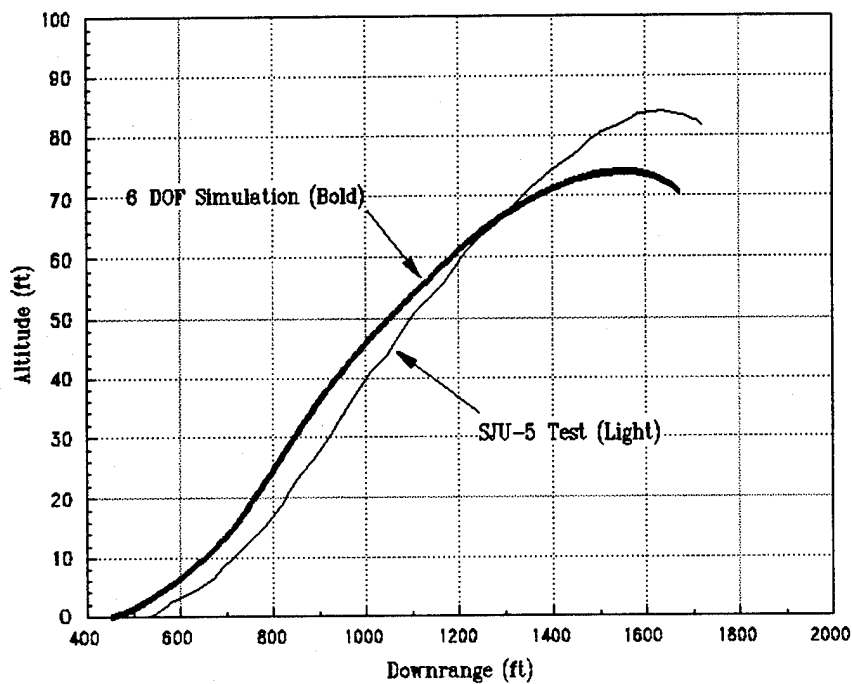


Y Acceleration vs. Time
212 lb Aircrew, 600 KEAS

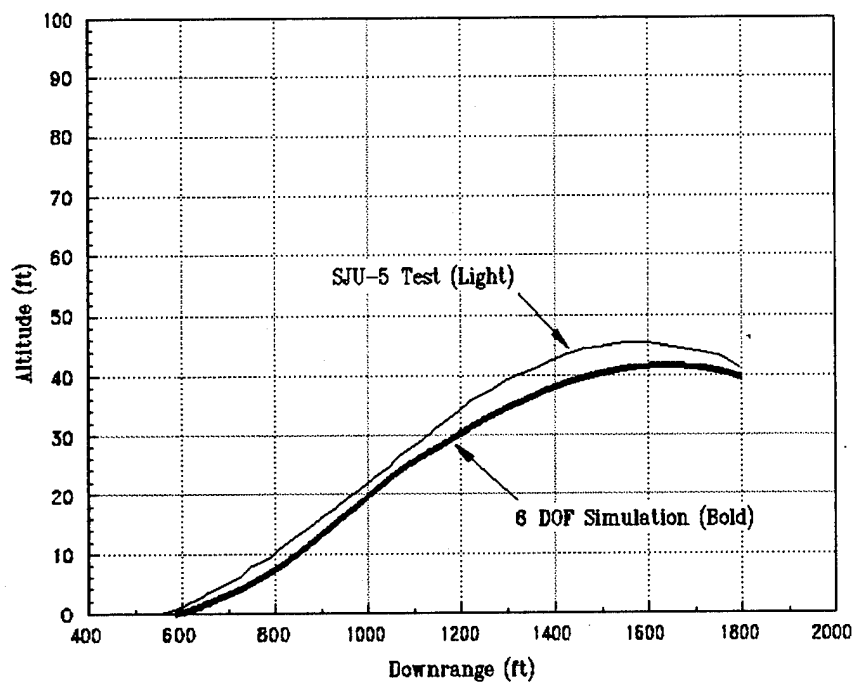
SJU-5 ESCAPE SYSTEM VALIDATION VERTICAL (Z) ACCELERATION, 600 KEAS EJECTION



SJU-5 ESCAPE SYSTEM VALIDATION TRAJECTORY, 600 KEAS EJECTION

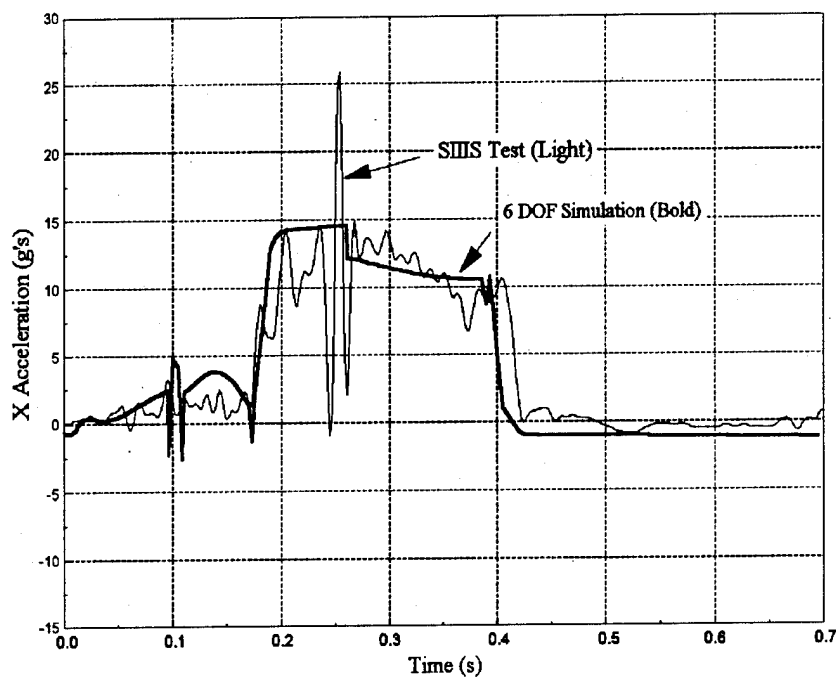


Altitude vs. Downrange Distance
135 lb Aircrew, 600 KEAS

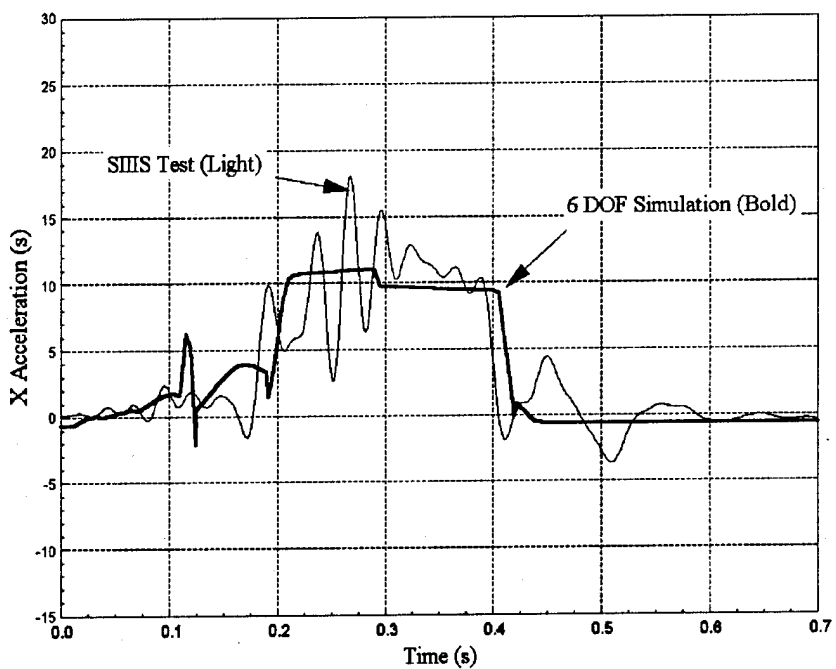


Altitude vs. Downrange Distance
212 lb Aircrew, 600 KEAS

SIIS ESCAPE SYSTEM VALIDATION **DOWN RANGE (X) ACCELERATION, 0 KEAS EJECTION**

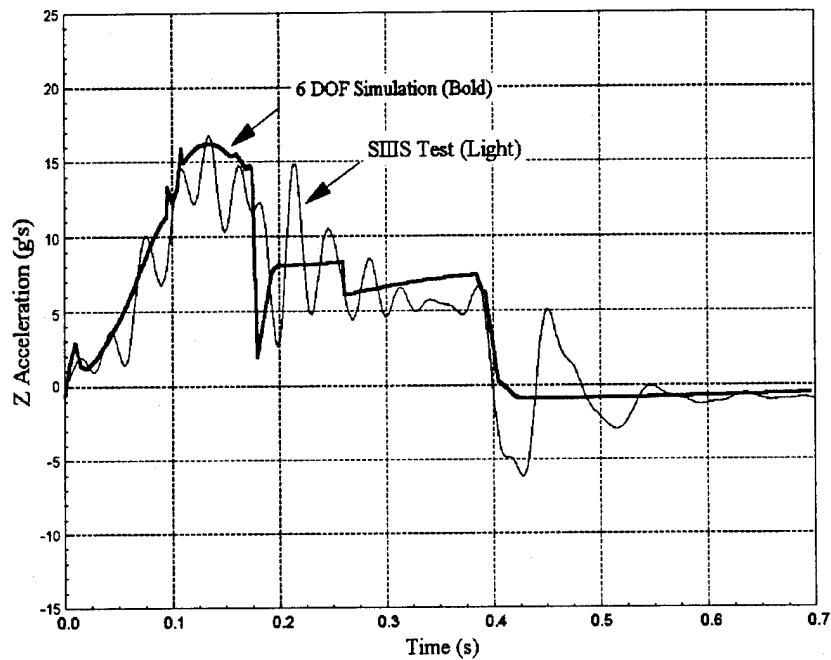


X Acceleration vs. Time
 135 lb Aircrew, 0 KEAS

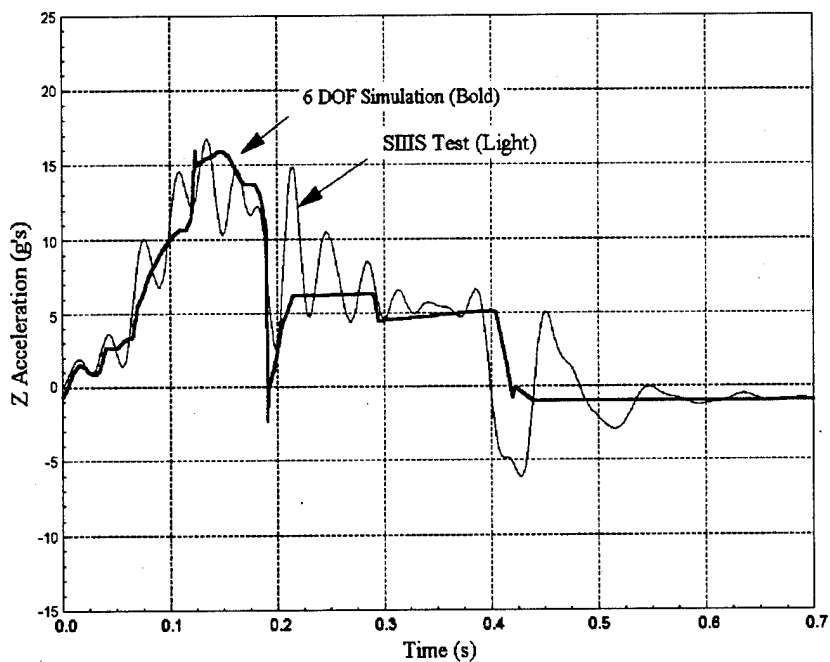


X Acceleration vs. Time
 212 lb Aircrew, 0 KEAS

SIIS ESCAPE SYSTEM VALIDATION VERTICAL (Z) ACCELERATION, 0 KEAS EJECTION

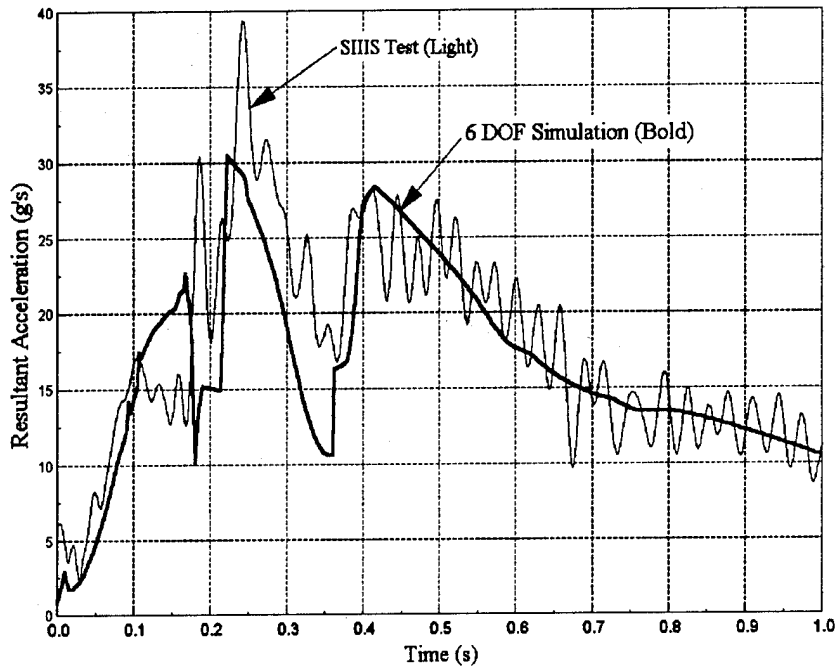


Z Acceleration vs. Time
135 lb Aircrew, 0 KEAS

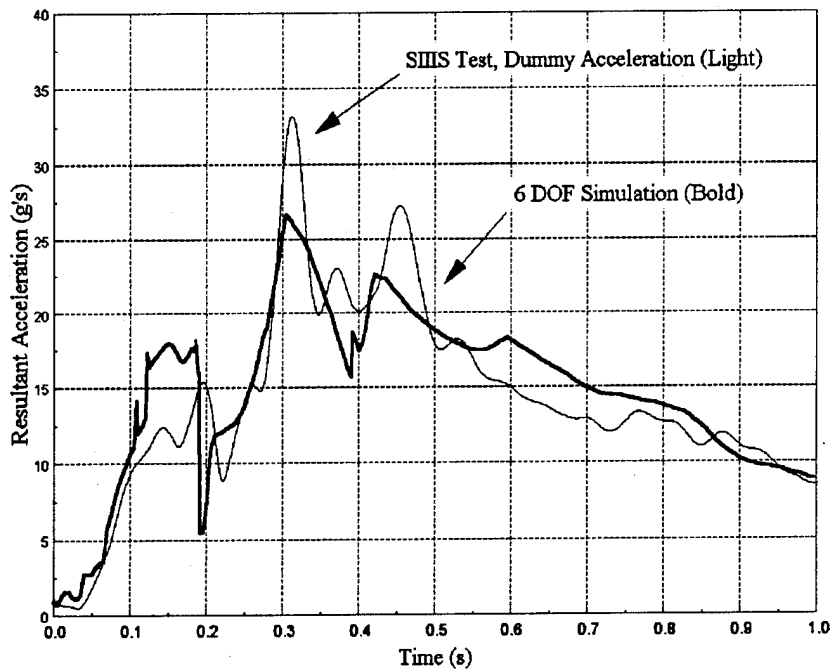


Z Acceleration vs. Time
212 lb Aircrew, 0 KEAS

SIIS ESCAPE SYSTEM VALIDATION **RESULTANT ACCELERATION, 600 KEAS E JECTION**

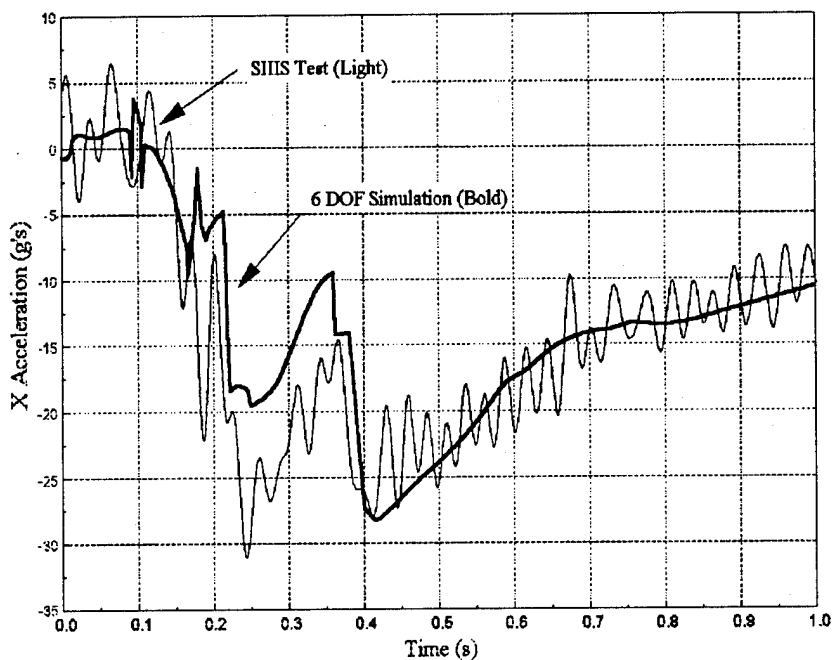


Resultant Acceleration vs. Time
 135 lb Aircrew, 600 KEAS

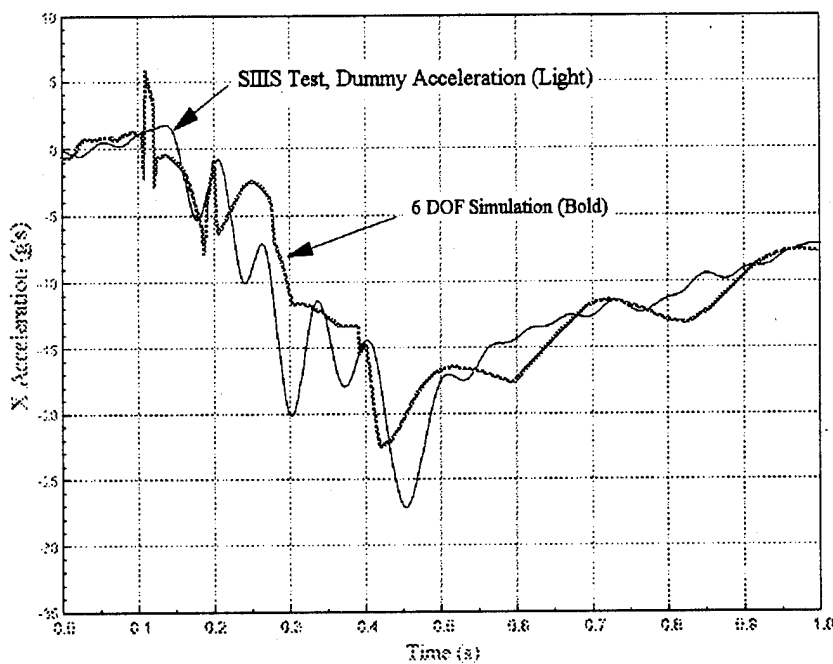


Resultant Acceleration vs. Time
 212 lb Aircrew, 600 KEAS

SIHS ESCAPE SYSTEM VALIDATION DOWN RANGE (X) ACCELERATION, 600 KEAS EJECTION

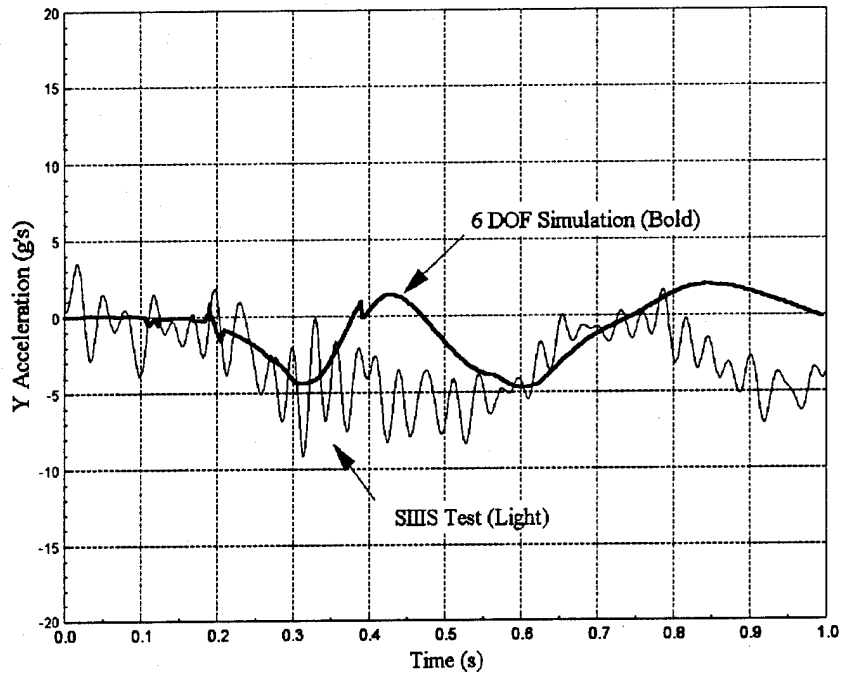


**X Acceleration vs. Time
135 lb Aircrew, 600 KEAS**

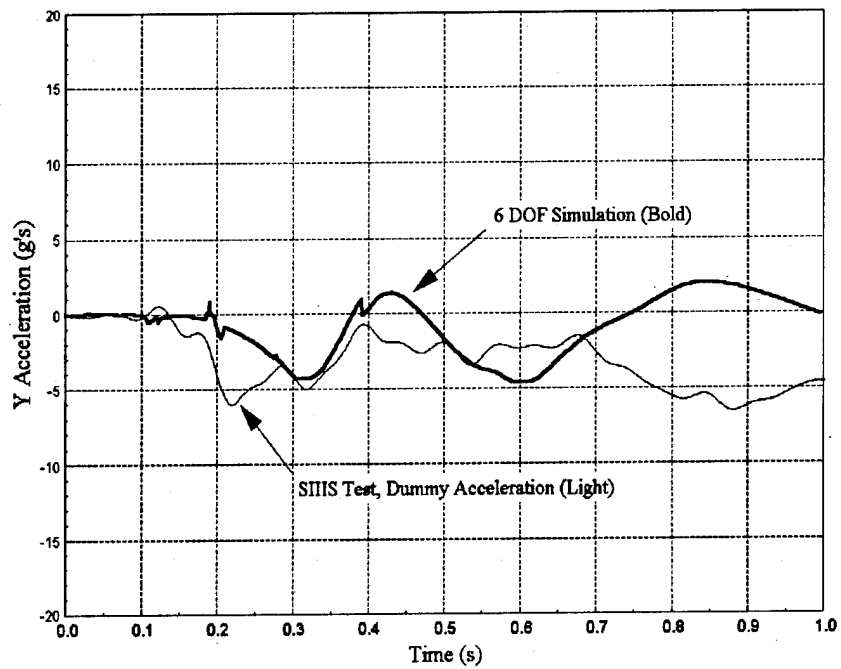


**X Acceleration vs. Time
212 lb Aircrew, 600 KEAS**

SIHS ESCAPE SYSTEM VALIDATION **LATERAL (Y) ACCELERATION, 600 KEAS EJECTION**

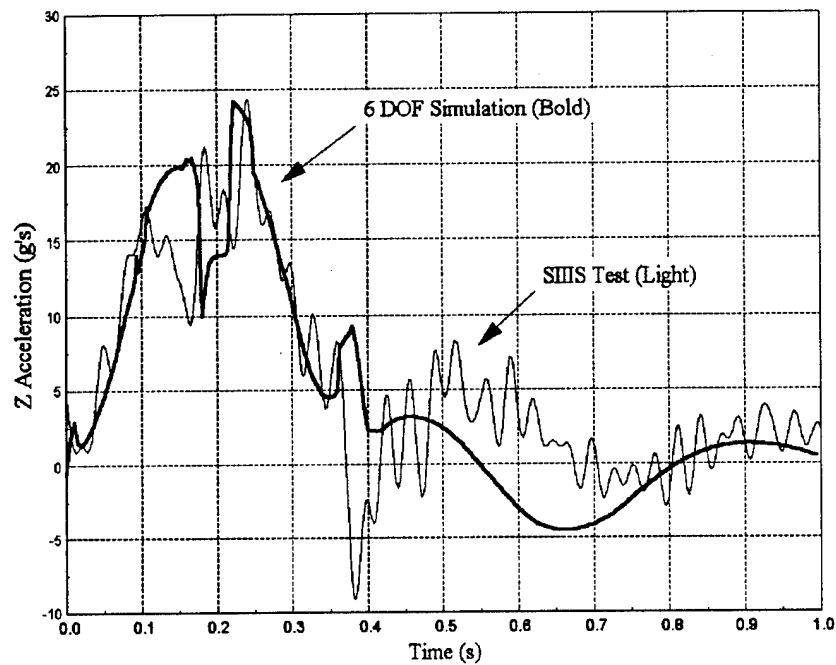


Y Acceleration vs. Time
 135 lb Aircrew, 600 KEAS

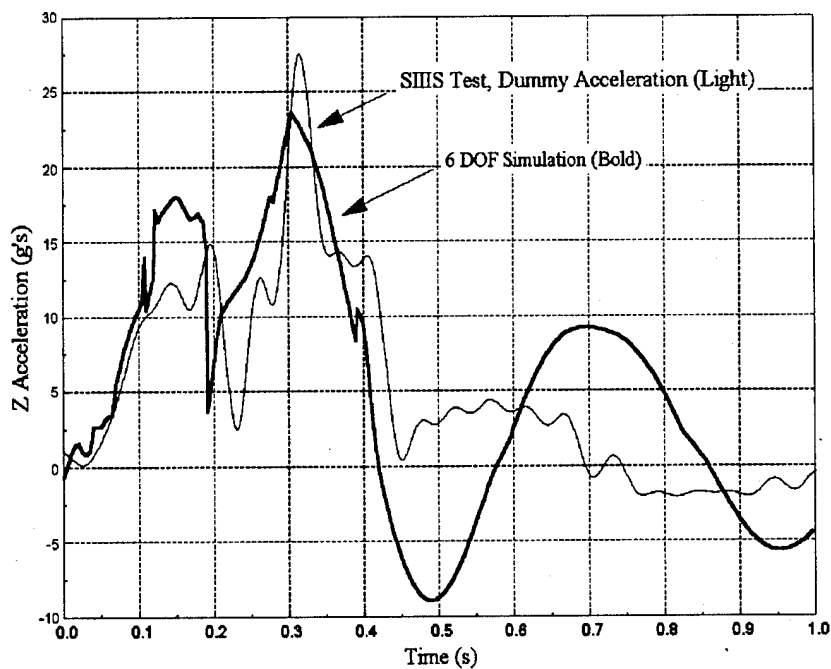


Y Acceleration vs. Time
 212 lb Aircrew, 600 KEAS

SIIS ESCAPE SYSTEM VALIDATION **VERTICAL (Z) ACCELERATION, 600 KEAS EJECTION**

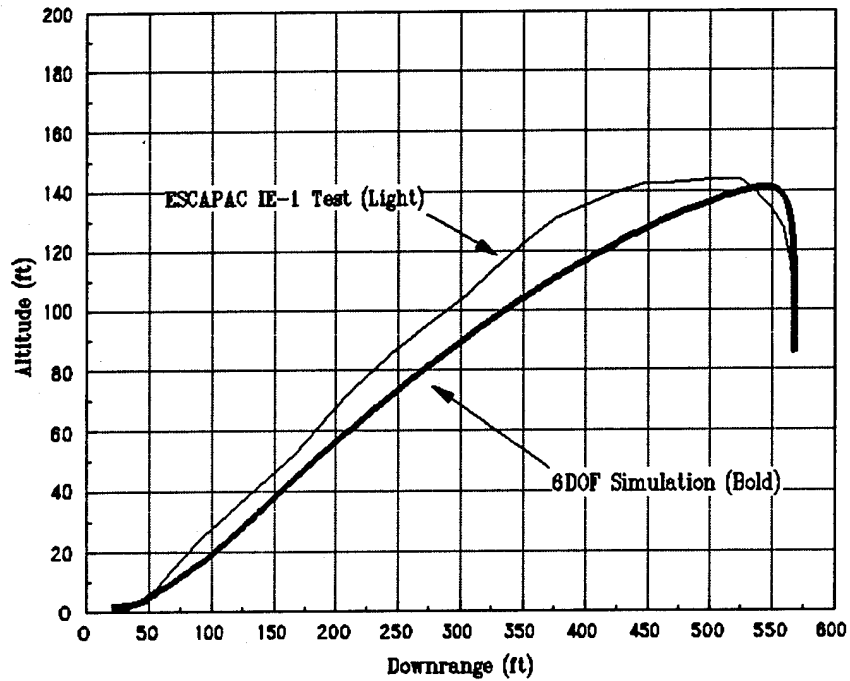


Z Acceleration vs. Time
 135 lb Aircrew, 600 KEAS

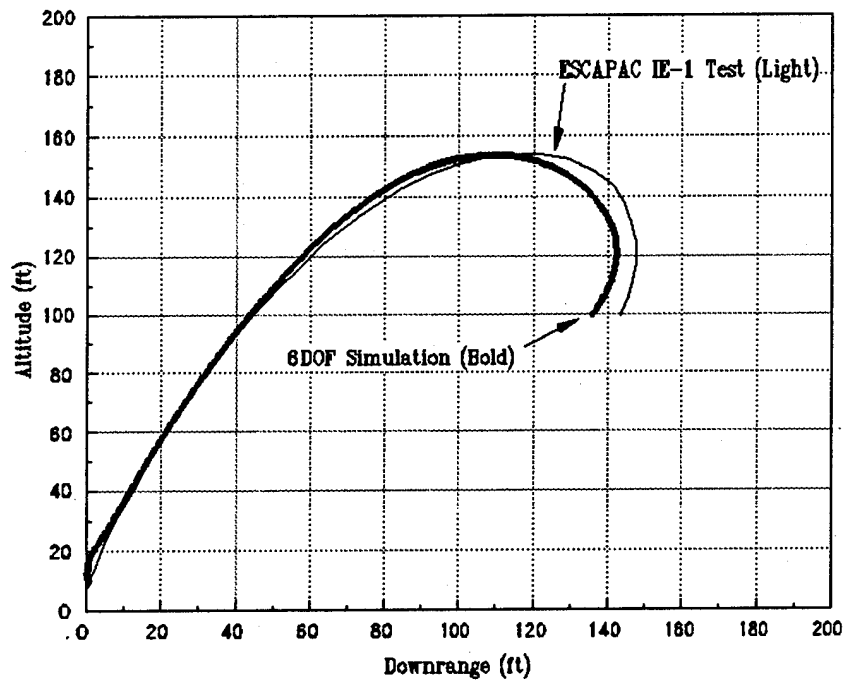


Z Acceleration vs. Time
 212 lb Aircrew, 600 KEAS

ESCAPAC IE-1 ESCAPE SYSTEM VALIDATION TRAJECTORY

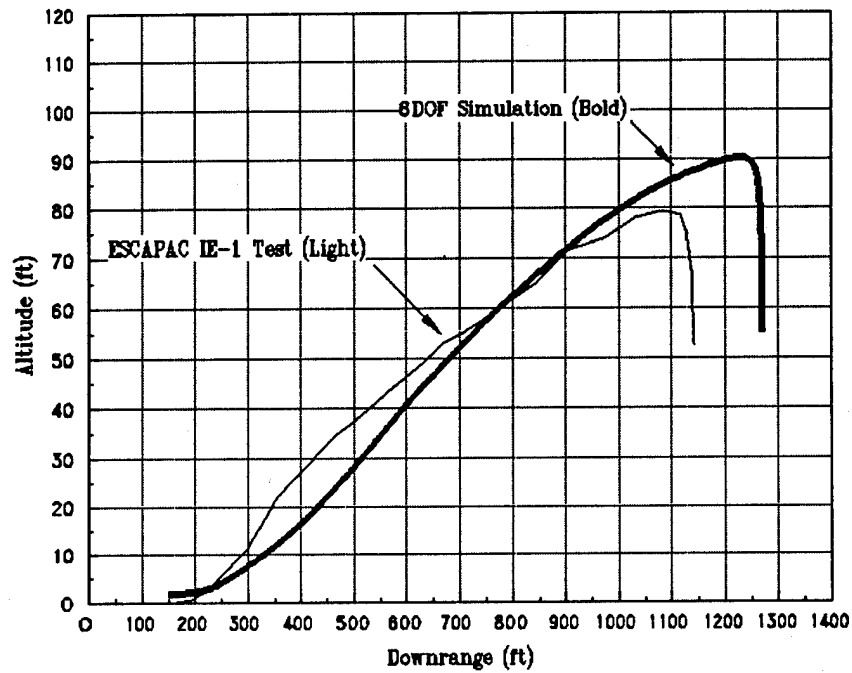


Altitude vs. Downrange Distance
135 lb Aircrew, 120 KEAS

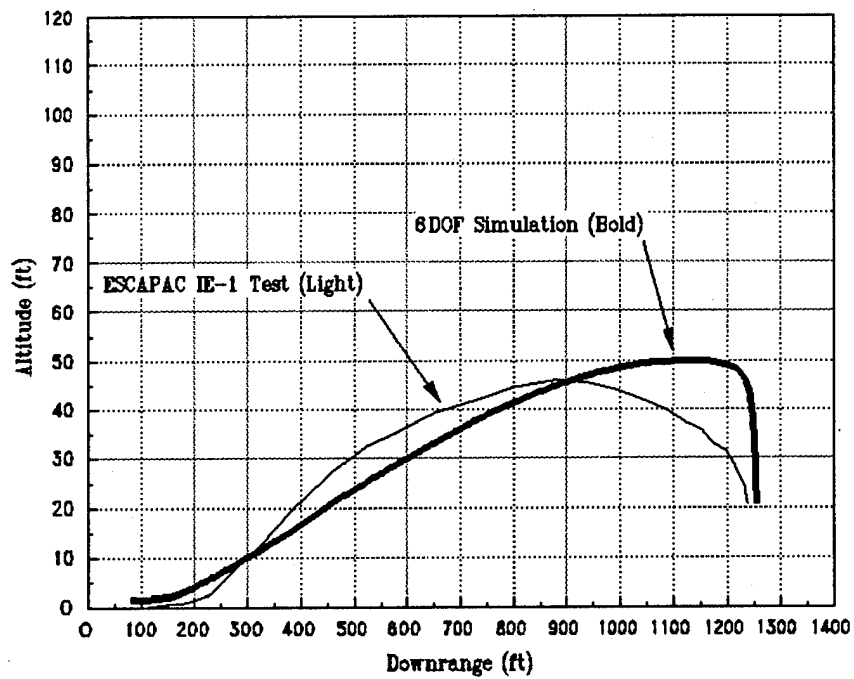


Altitude vs. Downrange Distance
212 lb Aircrew, 0 KEAS

ESCAPAC IE-1 ESCAPE SYSTEM VALIDATION TRAJECTORY, 450 KEAS



Altitude vs. Downrange Distance
135 lb Aircrew, 450 KEAS



Altitude vs. Downrange Distance
212 lb Aircrew, 450 KEAS

GRU-7 & LS-1A ESCAPE SYSTEM VALIDATION ACCELERATION

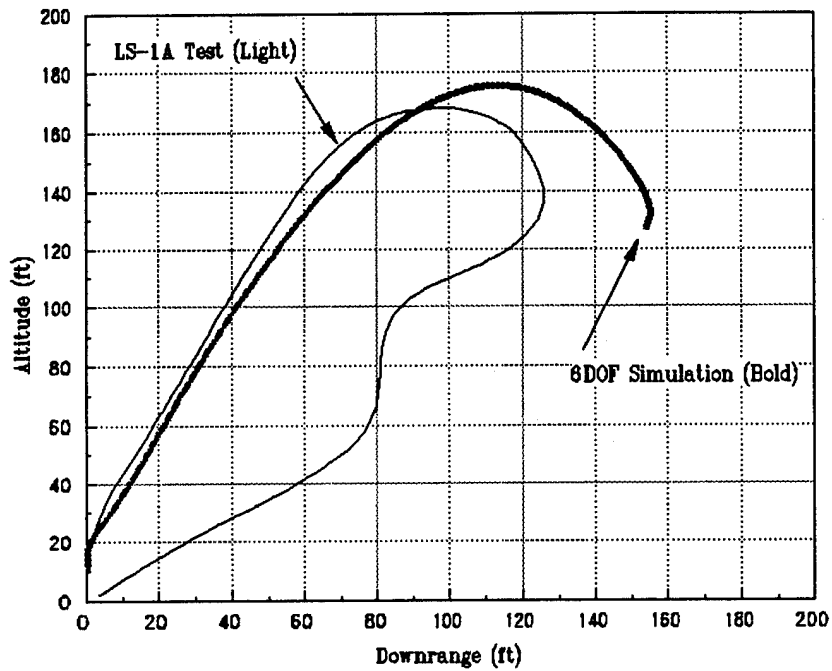
GRU-7 Propulsion Validation				
	140 lb Occupant		204 lb Occupant	
	Test	Simulation	Test	Simulation
Rocket Ave. Gz	8.7	9.7	7.2	7.8

GRU-7 Drogue Validation				
	140 lb Occupant		204 lb Occupant	
Airspeed	Test	Simulation	Test	Simulation
(KEAS)	Peak gs	Peak gs	Peak gs	Peak gs
265	10.4	8.1	7.8	7.2
435	16.8	17.3	16.3	14.8
600	>25 *	25.0	24.8	23.4

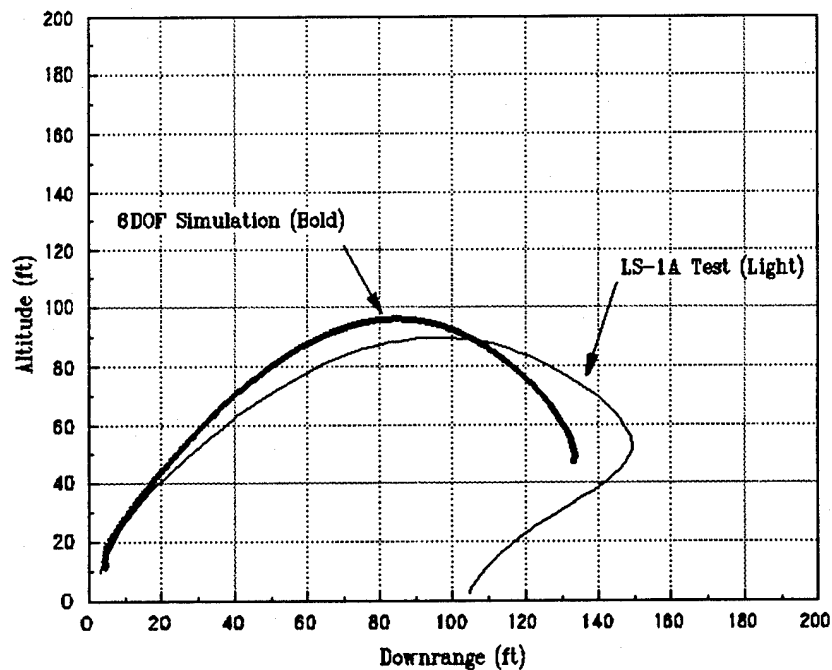
* Measured acceleration level greater than 25 g accelerometer limit.

LS-1A Acceleration Validation				
	140 lb Occupant		204 lb Occupant	
Speed	Test	Simulation	Test	Simulation
(KEAS)	Peak gs	Peak gs	Peak gs	Peak gs
0	13.0	13.5	11.0	12.1
30	13.5	13.5	12.5	12.1

LS-1A ESCAPE SYSTEM VALIDATION TRAJECTORY, 0 KEAS

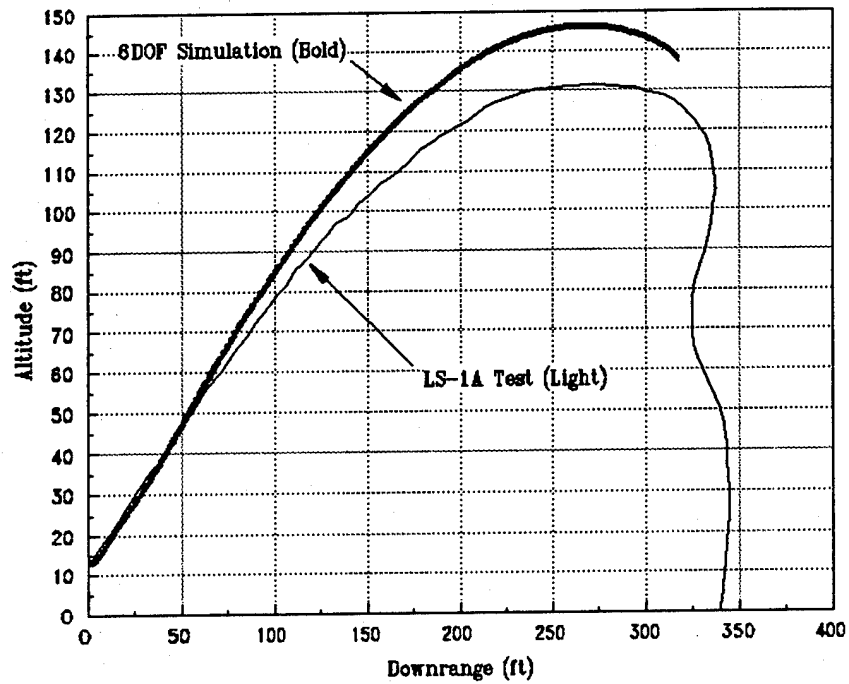


Altitude vs. Downrange Distance
140 lb Aircrew, 0 KEAS

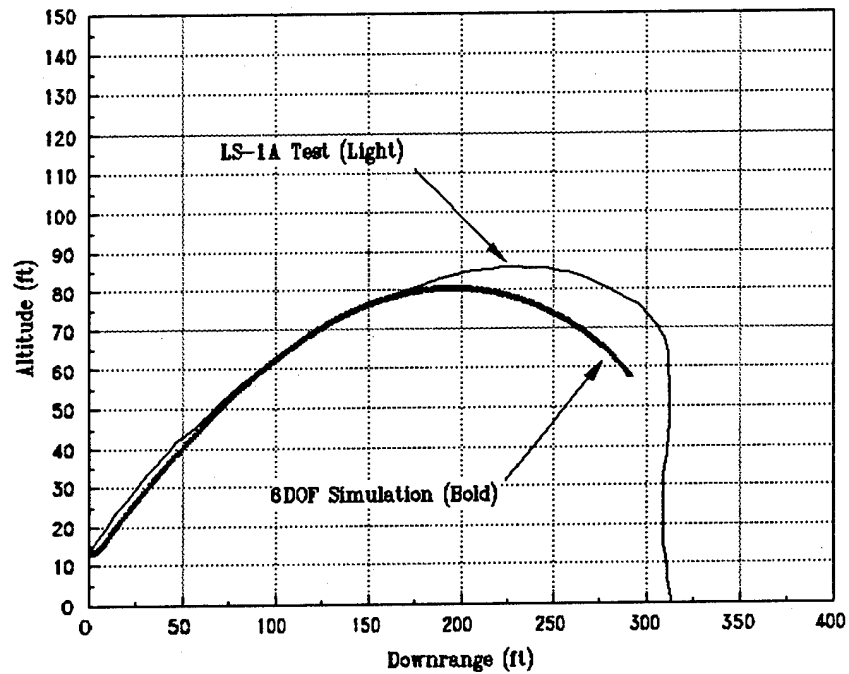


Altitude vs. Downrange Distance
204 lb Aircrew, 0 KEAS

LS-1A ESCAPE SYSTEM VALIDATION TRAJECTORY, 30 KEAS



Altitude vs. Downrange Distance
140 lb Aircrew, 30 KEAS



Altitude vs. Downrange Distance
204 lb Aircrew, 30 KEAS

APPENDIX B:
Occupant Inertial Properties Analysis

APPROACH

To determine the seat/occupant cg and MOI for the 100 lb and 116 lb occupants the empirically measured 135 lb and 140 lb inertial properties were as follows. The inertial properties for 135 lb and 140 lb occupant body segments were derived from a male data base. The occupants were considered in an approximate seated position, and the occupant cg were determined using the body segment positions, masses, and cg. The body segment moments of inertia were then rotated and translated to the occupant cg using the parallel axis theorem.

Knowing the properties for the 135 lb and 140 lb occupants alone in an ejection position, the effects of the occupants on the seat/occupant cg and MOI were removed leaving the cg and MOI of the ejection seats alone. The seat alone inertial properties are representative of the seats at full ejection weight combined with flight gear and clothing.

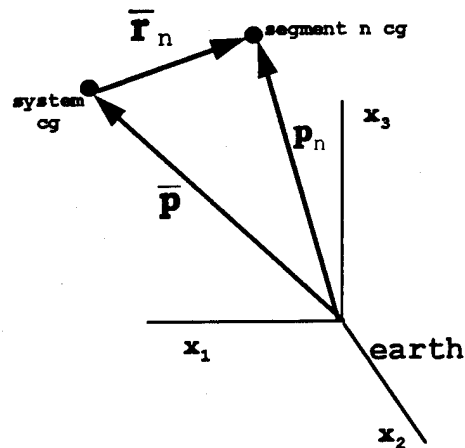
The inertial properties of the 100 lb and 116 lb occupant body segments were then calculated using regression formulas. The cg and MOI for these occupants in an ejection position were calculated as described above for the 135 lb and 140 lb occupants. The effect of the 100 lb and 116 lb occupants' cg and MOI were then added to the seat alone cg and MOI giving the seat/occupant properties for these aircrew weights.

Occupant gender was a factor in the determination of mass distribution. The mass distribution for the 100 lb and 116 lb occupants is representative of that of a female. The mass distribution for the 135 lb, 140 lb, 204 lb, and 212 lb occupants is representative of that of a male.

The relations are as follows:

Center of Gravity

$$\bar{p}_i = \sum_n (m_n (p_i)_n) / \sum_n m_n$$

Translation of Moments of Inertia - Parallel Axis Theorem:

Shown above are the vectors defining the translation of body segment moments of inertia

$$\bar{\mathbf{r}}_n = \mathbf{p}_n - \bar{\mathbf{p}}$$

$$\bar{\mathbf{r}}_n = x_n \mathbf{i} + y_n \mathbf{j} + z_n \mathbf{k}$$

$$(I_{xx})_n = (\bar{I}'_{xx})_n + (m(y^2 + z^2))_n$$

$$(I_{yy})_n = (\bar{I}'_{yy})_n + (m(x^2 + z^2))_n$$

$$(I_{zz})_n = (\bar{I}'_{zz})_n + (m(x^2 + y^2))_n$$

$$(I_{xy})_n = (\bar{I}'_{xy})_n - (mxy)_n$$

$$(I_{xz})_n = (\bar{I}'_{xz})_n - (mzx)_n$$

$$(I_{yz})_n = (\bar{I}'_{yz})_n - (myz)_n$$

where:

n	number of body segments plus the seat
\mathbf{p}_n	position vector of the center of gravity of each body segment and the seat
$\bar{\mathbf{p}}$	position vector of the center of gravity the seat and body system
$\bar{\mathbf{r}}_n$	position vector from the system center of gravity to each body segment and the seat
$(\bar{I}'_{ij})_n$	component of the moment of inertia tensor of the body segment about the local segment coordinate system
$(I_{ij})_n$	component of the moment of inertia tensor of the body segment about the system center of gravity

Since $\bar{r}^2 = x^2 + y^2 + z^2$, the parallel axis theorem applied to each body segment can be summarized by the following:

$$(I_{ij})_n = (\bar{I}'_{ij})_n - (m (\bar{r}_i \bar{r}_j - \bar{r}^2 \delta_{ij}))_n \text{ (no sum)}$$

In order to add the individual moments of inertia of each body segment, the moments of inertia must be rotated to a common coordinate system.

Rotation of Moments of Inertia:

For the rotated coordinate system defined by the following direction cosine matrix:

$$\{s\}_n = [dcm]_n \{s'\}_n$$

then,

$$[I]_n = [dcm]_n [I']_n [dcm]_n^T$$

where:

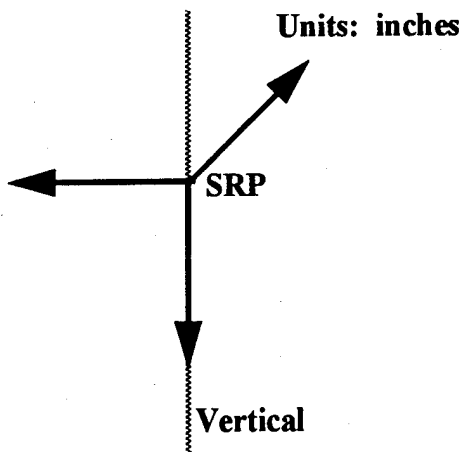
$\{s'\}$	position vector for a point with respect to the body segment coordinate system
$\{s\}$	position vector for that point with respect to the rotated coordinate system (the seat)
$[dcm]_n$	direction cosine matrix relating the rotation of the coordinate systems
$[I']_n$	moment of inertia tensor of each body segment and the seat, about the system center of gravity
$[I]_n$	moment of inertia tensor of each body segment and the seat, about the system center of gravity, and rotated into the seat coordinate system

And so the total system moment of inertia was obtained by simply adding each element of the moment of inertia tensor as follows:

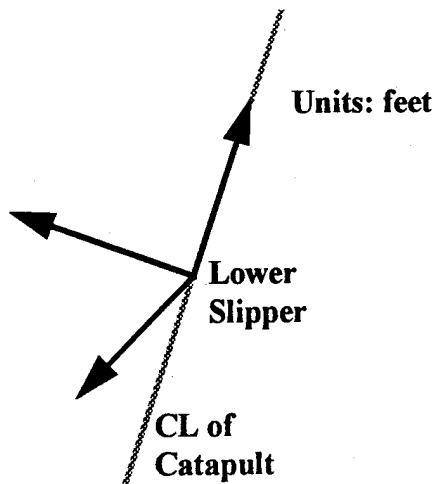
$$(I_{ij})_{Total} = \sum_n (I_{ij})_n$$

$$\mathbf{I} = [(I_{ij})_{Total}]$$

The results of the calculations for the NACES seat system have been included in this appendix as an example. The relevant coordinate systems used in the NACES calculations are illustrated below.



Sear Reference Point (SRP)



Seat Coordinate System (SCS)
Rail angle of 22 degrees was used (F-18)

The inertial properties used for each of the occupant in the NACES calculations are shown below. Body segment definitions are shown on the final page.

212 LB MALE

Mass Properties of 212 lb Male

Occupant Alone

seg	weight (lb)	x (in)	y (in)	z (in)	Ixx (inlbs ²)	Iyy (inlbs ²)	Izz (inlbs ²)	Ixy (inlbs ²)	Iyz (inlbs ²)	Ixz (inlbs ²)
LT	34.960	3.791	0.000	-3.381	1.648	1.028	1.851	0.000	0.000	0.049
CT	13.610	2.592	0.000	-8.575	0.457	0.252	0.629	0.000	0.000	0.042
UT	55.080	0.799	0.000	-16.340	3.500	2.860	2.562	0.000	0.000	-0.229
N	3.250	-1.032	0.000	-24.782	0.027	0.027	0.022	0.000	0.000	0.000
H	11.820	-1.032	0.000	-31.112	0.267	0.304	0.157	0.000	0.000	0.000
RUL	23.170	12.069	3.370	-3.868	0.272	2.014	2.014	0.000	0.000	0.000
RLL	9.840	23.427	3.370	2.709	0.464	0.485	0.087	0.000	0.000	-0.092
RF	2.070	28.310	3.370	12.609	0.007	0.040	0.039	0.000	0.000	0.007
LUL	23.170	12.069	-3.370	-3.868	0.272	2.014	2.014	0.000	0.000	0.000
LLL	9.840	23.427	-3.370	2.709	0.464	0.485	0.087	0.000	0.000	-0.092
LF	2.070	28.310	-3.370	12.609	0.007	0.040	0.039	0.000	0.000	0.007
RUA	5.670	-0.377	6.150	-16.296	0.171	0.171	0.028	0.000	0.000	0.000
RLA	5.880	5.237	0.536	-10.362	0.171	0.171	0.316	0.147	0.018	-0.018
LUA	5.670	-0.377	-6.150	-16.296	0.171	0.171	0.028	0.000	0.000	0.000
LLA	5.880	5.237	-0.536	-10.362	0.171	0.171	0.316	-0.147	-0.018	-0.018
Total	211.980	6.562	0.000	-9.263	55.608	87.503	46.287	0.000	0.000	-31.097

cg(SRP):=> 9.555 0.000 6.130 (in) Parallel to the catapult, origin at SRP

cg(SCS):=> 1.112 0.000 0.814 (ft) Parallel to catapult, origin at lower slipper

Moments:=> 6.325 0.000 1.594 (slug-ft^2)

of :=> 0.000 7.292 0.000

Inertia:=> 1.594 0.000 2.166

Occupant and NACES, seat full down

seg	weight (lb)	x (in)	y (in)	z (in)	Ixx (inlbs ²)	Iyy (inlbs ²)	Izz (inlbs ²)	Ixy (inlbs ²)	Iyz (inlbs ²)	Ixz (inlbs ²)
LT	34.960	3.791	0.000	-3.381	1.648	1.028	1.851	0.000	0.000	0.049
CT	13.610	2.592	0.000	-8.575	0.457	0.252	0.629	0.000	0.000	0.042
UT	55.080	0.799	0.000	-16.340	3.500	2.860	2.562	0.000	0.000	-0.229
N	3.250	-1.032	0.000	-24.782	0.027	0.027	0.022	0.000	0.000	0.000
H	11.820	-1.032	0.000	-31.112	0.267	0.304	0.157	0.000	0.000	0.000
RUL	23.170	12.069	3.370	-3.868	0.272	2.014	2.014	0.000	0.000	0.000
RLL	9.840	23.427	3.370	2.709	0.464	0.485	0.087	0.000	0.000	-0.092
RF	2.070	28.310	3.370	12.609	0.007	0.040	0.039	0.000	0.000	0.007
LUL	23.170	12.069	-3.370	-3.868	0.272	2.014	2.014	0.000	0.000	0.000
LLL	9.840	23.427	-3.370	2.709	0.464	0.485	0.087	0.000	0.000	-0.092
LF	2.070	28.310	-3.370	12.609	0.007	0.040	0.039	0.000	0.000	0.007
RUA	5.670	-0.377	6.150	-16.296	0.171	0.171	0.028	0.000	0.000	0.000
RLA	5.880	5.237	0.536	-10.362	0.171	0.171	0.316	0.147	0.018	-0.018
LUA	5.670	-0.377	-6.150	-16.296	0.171	0.171	0.028	0.000	0.000	0.000
LLA	5.880	5.237	-0.536	-10.362	0.171	0.171	0.316	-0.147	-0.018	-0.018
VEH	262.000	-0.888	0.000	-13.955	193.420	290.160	130.940	0.000	0.000	-87.634
Total	473.980	2.444	0.000	-11.857	255.709	401.193	194.075	0.000	0.000	-129.341

cg(SRP):=> 6.707 0.000 10.078 (in) Parallel to the catapult, origin at SRP

cg(SCS):=> 0.875 0.000 1.143 (ft) Parallel to catapult, origin at lower slipper

Moments:=> 28.076 0.000 5.969 (slug-ft^2)

of :=> 0.000 33.433 0.000

Inertia:=> 5.969 0.000 9.406

135 LB MALE

Mass Properties of 135 lb Male

Occupant Alone

seg	weight (lb)	x (in)	y (in)	z (in)	Ixx (inlbs ²)	Iyy (inlbs ²)	Izz (inlbs ²)	Ixy (inlbs ²)	Iyz (inlbs ²)	Ixz (inlbs ²)
LT	22.470	3.791	0.000	-3.381	0.805	0.484	0.803	0.000	0.000	-0.001
CT	7.540	2.639	0.000	-8.370	0.162	0.086	0.215	0.000	0.000	0.013
UT	33.150	1.006	0.000	-15.444	1.569	1.287	1.035	0.000	0.000	-0.130
N	2.550	-0.602	0.000	-23.191	0.019	0.019	0.013	0.000	0.000	0.000
H	10.680	-0.602	0.000	-29.521	0.221	0.252	0.132	0.000	0.000	0.000
RUL	13.670	11.550	3.150	-3.167	0.106	0.905	0.905	0.000	0.000	0.000
RLL	6.440	21.673	3.150	2.952	0.247	0.258	0.042	0.000	0.000	-0.050
RF	1.480	26.290	3.150	12.040	0.004	0.024	0.024	0.000	0.000	0.004
LUL	13.670	11.550	-3.150	-3.167	0.106	0.905	0.905	0.000	0.000	0.000
LLL	6.440	21.673	-3.150	2.952	0.247	0.258	0.042	0.000	0.000	-0.050
LF	1.480	26.290	-3.150	12.040	0.004	0.024	0.024	0.000	0.000	0.004
RUA	3.550	-0.004	5.940	-14.759	0.092	0.092	0.011	0.000	0.000	0.000
RLA	4.170	5.321	0.615	-9.110	0.105	0.105	0.195	0.092	0.011	-0.011
LUA	3.550	-0.004	-5.940	-14.759	0.092	0.092	0.011	0.000	0.000	0.000
LLA	4.170	5.321	-0.615	-9.110	0.105	0.105	0.195	-0.092	-0.011	-0.011
Total	135.010	6.278	0.000	-9.030	35.217	52.780	24.638	0.000	0.000	-19.053

cg(SRP):=>	9.203	0.000	6.021	(in)	Parallel to the catapult, origin at SRP					
cg(SCS):=>	1.083	0.000	1.353	(ft)	Parallel to catapult, origin at lower slipper					
Moments:=>	3.914	0.000	0.836	(slug-ft ²)						
of :=>	0.000	4.398	0.000							
Inertia:=>	0.836	0.000	1.074							

Occupant and NACES, seat full up

seg	weight (lb)	x (in)	y (in)	z (in)	Ixx (inlbs ²)	Iyy (inlbs ²)	Izz (inlbs ²)	Ixy (inlbs ²)	Iyz (inlbs ²)	Ixz (inlbs ²)
LT	22.470	3.791	0.000	-3.381	0.805	0.484	0.803	0.000	0.000	-0.001
CT	7.540	2.639	0.000	-8.370	0.162	0.086	0.215	0.000	0.000	0.013
UT	33.150	1.006	0.000	-15.444	1.569	1.287	1.035	0.000	0.000	-0.130
N	2.550	-0.602	0.000	-23.191	0.019	0.019	0.013	0.000	0.000	0.000
H	10.680	-0.602	0.000	-29.521	0.221	0.252	0.132	0.000	0.000	0.000
RUL	13.670	11.550	3.150	-3.167	0.106	0.905	0.905	0.000	0.000	0.000
RLL	6.440	21.673	3.150	2.952	0.247	0.258	0.042	0.000	0.000	-0.050
RF	1.480	26.290	3.150	12.040	0.004	0.024	0.024	0.000	0.000	0.004
LUL	13.670	11.550	-3.150	-3.167	0.106	0.905	0.905	0.000	0.000	0.000
LLL	6.440	21.673	-3.150	2.952	0.247	0.258	0.042	0.000	0.000	-0.050
LF	1.480	26.290	-3.150	12.040	0.004	0.024	0.024	0.000	0.000	0.004
RUA	3.550	-0.004	5.940	-14.759	0.092	0.092	0.011	0.000	0.000	0.000
RLA	4.170	5.321	0.615	-9.110	0.105	0.105	0.195	0.092	0.011	-0.011
LUA	3.550	-0.004	-5.940	-14.759	0.092	0.092	0.011	0.000	0.000	0.000
LLA	4.170	5.321	-0.615	-9.110	0.105	0.105	0.195	-0.092	-0.011	-0.011
VEH	251.100	0.441	0.000	-8.293	139.809	196.536	105.687	0.000	0.000	-66.312
Total	386.110	2.482	0.000	-8.551	175.149	257.187	138.072	0.000	0.000	-84.387

cg(SRP):=>	5.505	0.000	6.998	(in)	Parallel to the catapult, origin at SRP					
cg(SCS):=>	0.775	0.000	1.434	(ft)	Parallel to catapult, origin at lower slipper					
Moments:=>	19.047	0.000	3.985	(slug-ft ²)						
of :=>	0.000	21.432	0.000							
Inertia:=>	3.985	0.000	7.055							

116 LB FEMALE

Mass Properties of 116 lb Female

Occupant Alone

seg	weight (lb)	x (in)	y (in)	z (in)	Ixx (inlbs ²)	Iyy (inlbs ²)	Izz (inlbs ²)	Ixy (inlbs ²)	Iyz (inlbs ²)	Ixz (inlbs ²)
LT	22.050	3.791	0.000	-3.381	0.843	0.495	0.773	0.000	0.000	-0.017
CT	4.420	2.554	0.000	-8.740	0.070	0.037	0.093	0.000	0.000	0.005
UT	23.440	1.116	0.000	-14.966	0.831	0.713	0.622	0.000	0.000	-0.051
N	1.820	-0.197	0.000	-21.277	0.011	0.011	0.008	0.000	0.000	0.000
H	8.480	-0.197	0.000	-27.207	0.159	0.181	0.092	0.000	0.000	0.000
RUL	16.150	11.674	3.330	-3.021	0.155	1.113	1.113	0.000	0.000	0.000
RLL	5.740	22.037	3.330	3.186	0.220	0.231	0.036	0.000	0.000	-0.045
RF	1.240	26.058	3.330	11.102	0.003	0.017	0.017	0.000	0.000	0.003
LUL	16.150	11.674	-3.330	-3.021	0.155	1.113	1.113	0.000	0.000	0.000
LLL	5.740	22.037	-3.330	3.186	0.220	0.231	0.036	0.000	0.000	-0.045
LF	1.240	26.058	-3.330	11.102	0.003	0.017	0.017	0.000	0.000	0.003
RUA	2.190	0.372	5.420	-13.712	0.044	0.044	0.005	0.000	0.000	0.000
RLA	2.580	4.922	0.869	-8.789	0.048	0.048	0.090	0.042	0.005	-0.005
LUA	2.190	0.372	-5.420	-13.712	0.044	0.044	0.005	0.000	0.000	0.000
LLA	2.580	4.922	-0.869	-8.789	0.048	0.048	0.090	-0.042	-0.005	-0.005
Total	116.010	7.247	0.000	-7.519	26.078	41.613	21.502	0.000	0.000	-15.026

cg(SRP):=> 9.536 0.000 4.257 (in) Parallel to the catapult, origin at SRP

cg(SCS):=> 1.111 0.000 1.206 (ft) Parallel to catapult, origin at lower slipper

Moments:=> 2.989 0.000 0.768 (slug-ft²)
of :=> 0.000 3.468 0.000
Inertia:=> 0.768 0.000 0.976

Occupant and NACES, seat full up

seg	weight (lb)	x (in)	y (in)	z (in)	Ixx (inlbs ²)	Iyy (inlbs ²)	Izz (inlbs ²)	Ixy (inlbs ²)	Iyz (inlbs ²)	Ixz (inlbs ²)
LT	22.050	3.791	0.000	-3.381	0.843	0.495	0.773	0.000	0.000	-0.017
CT	4.420	2.554	0.000	-8.740	0.070	0.037	0.093	0.000	0.000	0.005
UT	23.440	1.116	0.000	-14.966	0.831	0.713	0.622	0.000	0.000	-0.051
N	1.820	-0.197	0.000	-21.277	0.011	0.011	0.008	0.000	0.000	0.000
H	8.480	-0.197	0.000	-27.207	0.159	0.181	0.092	0.000	0.000	0.000
RUL	16.150	11.674	3.330	-3.021	0.155	1.113	1.113	0.000	0.000	0.000
RLL	5.740	22.037	3.330	3.186	0.220	0.231	0.036	0.000	0.000	-0.045
RF	1.240	26.058	3.330	11.102	0.003	0.017	0.017	0.000	0.000	0.003
LUL	16.150	11.674	-3.330	-3.021	0.155	1.113	1.113	0.000	0.000	0.000
LLL	5.740	22.037	-3.330	3.186	0.220	0.231	0.036	0.000	0.000	-0.045
LF	1.240	26.058	-3.330	11.102	0.003	0.017	0.017	0.000	0.000	0.003
RUA	2.190	0.372	5.420	-13.712	0.044	0.044	0.005	0.000	0.000	0.000
RLA	2.580	4.922	0.869	-8.789	0.048	0.048	0.090	0.042	0.005	-0.005
LUA	2.190	0.372	-5.420	-13.712	0.044	0.044	0.005	0.000	0.000	0.000
LLA	2.580	4.922	-0.869	-8.789	0.048	0.048	0.090	-0.042	-0.005	-0.005
VEH	251.100	0.441	0.000	-8.293	139.809	196.536	105.687	0.000	0.000	-66.312
Total	367.110	2.592	0.000	-8.049	166.010	247.791	136.708	0.000	0.000	-82.421

cg(SRP):=> 5.418 0.000 6.492 (in) Parallel to the catapult, origin at SRP

cg(SCS):=> 0.768 0.000 1.392 (ft) Parallel to catapult, origin at lower slipper

Moments:=> 18.263 0.000 4.093 (slug-ft²)
of :=> 0.000 20.649 0.000
Inertia:=> 4.093 0.000 6.964

100 LB FEMALE

Mass Properties of 100 lb Female

Occupant Alone

Occupant Alone										
seg	weight (lb)	x (in)	y (in)	z (in)	Ixx (inlbs ²)	Iyy (inlbs ²)	Izz (inlbs ²)	Ixy (inlbs ²)	Iyz (inlbs ²)	Ixz (inlbs ²)
LT	18.770	3.791	0.000	-3.381	0.657	0.386	0.586	0.000	0.000	-0.017
CT	3.720	2.579	0.000	-8.633	0.052	0.027	0.068	0.000	0.000	0.004
UT	20.170	1.168	0.000	-14.742	0.664	0.569	0.479	0.000	0.000	-0.045
N	1.700	-0.105	0.000	-20.937	0.010	0.010	0.007	0.000	0.000	0.000
H	8.080	-0.105	0.000	-26.837	0.147	0.167	0.086	0.000	0.000	0.000
RUL	13.570	11.509	3.220	-2.913	0.115	0.866	0.866	0.000	0.000	0.000
RLL	5.000	21.553	3.220	3.167	0.181	0.189	0.029	0.000	0.000	-0.037
RF	1.110	25.497	3.220	10.884	0.003	0.015	0.015	0.000	0.000	0.003
LUL	13.570	11.509	-3.220	-2.913	0.115	0.866	0.866	0.000	0.000	0.000
LLL	5.000	21.553	-3.220	3.167	0.181	0.189	0.029	0.000	0.000	-0.037
LF	1.110	25.497	-3.220	10.884	0.003	0.015	0.015	0.000	0.000	0.003
RUA	1.830	0.457	5.380	-13.361	0.035	0.035	0.004	0.000	0.000	0.000
RLA	2.270	4.930	0.907	-8.518	0.041	0.041	0.076	0.036	0.004	-0.004
LUA	1.830	0.457	-5.380	-13.361	0.035	0.035	0.004	0.000	0.000	0.000
LLA	2.270	4.930	-0.907	-8.518	0.041	0.041	0.076	-0.036	-0.004	-0.004
Total	100.000	7.118	0.000	-7.562	22.521	35.431	17.622	0.000	0.000	-12.864

cg(SRP):=>		9.433	0.000	4.345	(in)	Parallel to the catapult, origin at SRP				

cg(SCS):=>		1.102	0.000	1.213	(ft)	Parallel to catapult, origin at lower slipper				

Moments:=>		2.564	0.000	0.629	(slug-ft^2)					
of :=>		0.000	2.953	0.000						
Inertia:=>		0.629	0.000	0.781						

Occupant and NACES, seat full up

seg	weight (lb)	x (in)	y (in)	z (in)	Ixx (inlbs ²)	Iyy (inlbs ²)	Izz (inlbs ²)	Ixy (inlbs ²)	Iyz (inlbs ²)	Ixz (inlbs ²)
LT	18.770	3.791	0.000	-3.381	0.657	0.386	0.586	0.000	0.000	-0.017
CT	3.720	2.579	0.000	-8.633	0.052	0.027	0.068	0.000	0.000	0.004
UT	20.170	1.168	0.000	-14.742	0.664	0.569	0.479	0.000	0.000	-0.045
N	1.700	-0.105	0.000	-20.937	0.010	0.010	0.007	0.000	0.000	0.000
H	8.080	-0.105	0.000	-26.837	0.147	0.167	0.086	0.000	0.000	0.000
RUL	13.570	11.509	3.220	-2.913	0.115	0.866	0.866	0.000	0.000	0.000
RLL	5.000	21.553	3.220	3.167	0.181	0.189	0.029	0.000	0.000	-0.037
RF	1.110	25.497	3.220	10.884	0.003	0.015	0.015	0.000	0.000	0.003
LUL	13.570	11.509	-3.220	-2.913	0.115	0.866	0.866	0.000	0.000	0.000
LLL	5.000	21.553	-3.220	3.167	0.181	0.189	0.029	0.000	0.000	-0.037
LF	1.110	25.497	-3.220	10.884	0.003	0.015	0.015	0.000	0.000	0.003
RUA	1.830	0.457	5.380	-13.361	0.035	0.035	0.004	0.000	0.000	0.000
RLA	2.270	4.930	0.907	-8.518	0.041	0.041	0.076	0.036	0.004	-0.004
LUA	1.830	0.457	-5.380	-13.361	0.035	0.035	0.004	0.000	0.000	0.000
LLA	2.270	4.930	-0.907	-8.518	0.041	0.041	0.076	-0.036	-0.004	-0.004
VEH	251.100	0.441	0.000	-8.293	139.809	196.536	105.687	0.000	0.000	-66.312
Total	351.100	2.343	0.000	-8.085	162.429	240.324	131.567	0.000	0.000	-80.081

cg(SRP) ==>		5.201	0.000	6.618	(in)	Parallel to the catapult, origin at SRP				

cg(SCS) ==>		0.749	0.000	1.403	(ft)	Parallel to catapult, origin at lower slipper				

Moments ==>		17.811	0.000	3.907	(slug-ft^2)					
of ==>		0.000	20.027	0.000						
Inertia ==>		3.907	0.000	6.689						

BODY SEGMENT DEFINITIONS

Designation	Description
LT	Lower Torso
CT	Center Torso
UT	Upper Torso
N	Neck
H	Head
RUL	Right Upper Leg
RLL	Right Lower Leg
RF	Right Foot
LUL	Left Upper Leg
LLL	Left Lower Leg
LF	Left Foot
RUA	Right Upper Arm
RLA	Right Lower Arm
LUA	Left Upper Arm
LLA	Left Lower Arm
VEH	Vehicle (Seat)

REFERENCES

Hawkins, K., "NACES Motor Nozzle Co-Ordinates & Vectors, C of G Positions & Moments of Inertia," Martin Baker Technical Note 1981, 15 Jan 1990.

Greenwood, D., *Principles of Dynamics*, Prentice Hall, 1988

DISTRIBUTION LIST
Report No. NAWCADWAR-96-17-TR

Naval Air Systems Command.....	6
Systems Engineering Department	
1421 Jefferson Davis Highway	
Attn: S. Price, Code 4.6.1	
Arlington, VA 22243-5120	
Naval Air Systems Command.....	1
Systems Engineering Department	
1421 Jefferson Davis Highway	
Attn: T. Pavlik, Code 4.6.1	
Arlington, VA 22243-5120	
Naval Air Systems Command.....	2
1421 Jefferson Davis Highway	
Attn: B. Giblin, Code 4.6	
Arlington, VA 22243-5120	
Naval Air Warfare Center, Aircraft Division.....	30
Attn: J. Nichols, Code 4.6.2.1	
P.O. Box 5152	
Warminster, PA 18974-0591	
AL/CFBV.....	2
Attn: Dr. I. Kaleps	
Building 441	
2610 Seventh St.	
Wright Patterson AFB, OH 45433-7901	
Defense Technical Information Center.....	2
Attn: DTIC-FDAB	
Cameron Station BG5	
Alexandria, VA 22304-6145	
Center for Naval Analysis.....	1
4401 Fort Avenue	
P.O. Box 16268	
Alexandria, VA 22302-0268	
Commander, Naval Air Warfare Center.....	2
Code 7.2.4.3A, MS 2	
Building 405	
Patuxent River, MD 20670-5304	